

DYNAMIC BRIDGES

An Unconventional Rice Kinesin Links Actin and Microtubules

Zur Erlangung des akademischen Grades eines

Doktors der Naturwissenschaften

(Dr. rer. nat.)

der Fakultät für Chemie und Biowissenschaften
des Karlsruher Instituts für Technologie (KIT)
vorgelegte

Dissertation

von

Nicole Frey

aus Darmstadt

Die vorliegende Dissertation wurde am Botanischen Institut des Karlsruher Instituts für Technologie (KIT), Lehrstuhl 1 für Molekulare Zellbiologie, im Zeitraum von April 2007 bis März 2010 angefertigt.

Dekan: Prof. Dr. Stefan Bräse

Referent: Prof. Dr. Peter Nick

Korreferent: Prof. Dr. Martin Bastmeyer

Tag der mündlichen Prüfung: 22.04.2010

Hiermit erkläre ich, dass ich die vorliegende Dissertation, abgesehen von der Benutzung der angegebenen Hilfsmittel, selbständig verfasst habe.

Alle Stellen, die gemäß Wortlaut oder Inhalt aus anderen Arbeiten entnommen sind, wurden durch Angabe der Quelle als Entlehnungen kenntlich gemacht.

Diese Dissertation liegt in gleicher oder ähnlicher Form keiner anderen Prüfungsbehörde vor.

Karlsruhe, den 01. März 2010

Nicole Frey

Mein besonderer Dank gilt Herrn Prof. Dr. Peter Nick, der die vorliegende Doktorarbeit in seiner Arbeitsgruppe ermöglichte, mir große Freiheit in der Bearbeitung dieses interessanten und abwechslungsreichen Themas gewährte und stete Unterstützung zukommen ließ.

Herrn Prof. Dr. Martin Bastmeyer danke ich für die Übernahme des Korreferats.

Für die kompetente Einführung in die "Welt der Reispflanzen", sowie die geduldige und ausführliche Beantwortung vieler Fragen im Lauf dieser Arbeit danke ich Dr. Michael Riemann. Aleksandra Jovanović, Kai Eggenberger und Dr. Jan Maisch hatten immer offene Ohren für meine zahlreichen Fragen zu Zellkulturen, Färbetechniken, sowie dem Apotom und ermöglichten mir den reibungslosen Einstieg in das zellbiologische Arbeiten. Der gesamten AG Lamparter danke ich für viele gute Ratschläge zur Proteinexpression- und analyse.

Jan Siebenbrock und Tobias Schunck aus der AG Fischer danke ich für die gute und immer wieder schöne Zusammenarbeit bei der Reinigung von und der Arbeit mit unserem Lieblingsprotein aus Schwein.

Jan Klotz und Kerstin Schwarz trugen durch Diplomarbeit und F3-Praktikum zu Teilen dieser Dissertation bei. Danke für eure tolle Arbeit!

Für exzellente technische Unterstützung, die mir in vielerlei Hinsicht die Arbeit sehr erleichterte, bedanke ich mich bei unseren ehemaligen und aktuellen Azubis Markus Riese, Sarah Rocke, Franziska Bühler, Juliane Draksler, Olivia Huber und Anna Görnhardt. Die Mitarbeiter des Botanischen Gartens des KIT unterstützten mich auf hervorragende Weise bei der Aufzucht meiner Reispflanzen.

Thank you to all colleagues at the Institute of Botany I for the really nice working atmosphere during the last three years. Insbesondere die "Bewohner des Dachgeschosses" trugen zum Gelingen dieser Arbeit durch stetige Diskussionsbereitschaft, viele Ratschläge und gute Laune bei. Danke euch allen für die schöne Zeit!

Für die kompetente Diskussion zahlreicher statistischer und mathematischer Fragestellungen während der letzten drei Jahre, den erfrischenden Blick von Außen auf biologische Ergebnisse, detailgenaues Korrekturlesen dieser Arbeit und alle erdenkliche Unterstützung danke ich Christian. Schließlich geht ein großes Dankeschön an meine Eltern, die mir mein Studium und somit diese Dissertation erst ermöglichten.

CONTENT

<i>Abbreviations</i>	V
<i>Zusammenfassung</i>	1
<i>Introduction</i>	3
1 The sensitive nature of the plant cytoskeleton	3
1.1 Microtubules and actin filaments as dynamic cellular players	4
1.2 Cytoskeletal organization during plant cell growth and development.....	5
1.2.1 Cell expansion.....	6
1.2.2 Cell division.....	7
2 Interaction and cross-talk between microtubules and microfilaments in plants	9
3 The superfamily of kinesins	10
3.1 Structural characteristics of kinesin motors.....	11
3.2 Plants possess a most peculiar set of kinesins.....	13
3.3 Plant kinesin-14 – a class of its own.....	15
4 Might KCHs act as dynamic linkers of microtubules and actin filaments?	17
5 The scope of this work	18
<i>Materials and Methods</i>	19
1 Materials	19
1.1 Standard reagents.....	19
1.2 Organisms.....	19
1.2.1 Bacteria.....	19
1.2.2 Tobacco cell cultures.....	19
1.2.3 Rice material.....	20
1.3 Media.....	20
1.4 Primers.....	21
1.4.1 Primers for genotyping.....	21
1.4.2 Primers for gene expression analysis.....	21
1.4.3 Cloning primers.....	22
1.4.4 Sequencing primers.....	22

1.5 Plasmids.....	23
1.5.1 Cloning plasmids.....	23
1.5.2 Constructs for recombinant protein expression.....	23
1.5.3 Constructs for plant transformation.....	24
1.6 Antibodies.....	24
2 Methods	25
2.1 <i>In silico</i> analysis.....	25
2.1.1 Phylogenetic analysis of KCHs.....	25
2.1.2 Sequence analysis of <i>OsKCHI</i>	26
2.1.3 Database search for cDNA clones and knock-out mutants	26
2.2 Cultivation techniques.....	26
2.2.1 Cultivation of bacteria.....	26
2.2.2 Cultivation of rice plants.....	27
2.2.3 Maintenance of tobacco BY-2 cell cultures.....	27
2.3 Molecular biological methods.....	28
2.3.1 General methods.....	28
2.3.2 Purification of nucleic acids.....	30
2.3.3 Molecular analytics.....	31
2.3.4 Cloning and manipulation of plasmids.....	33
2.4 Cell biological methods.....	35
2.4.1 Plant transformations.....	35
2.4.2 Visualization of actin filaments and microtubules in fixed cells.....	36
2.4.3 Treatments of tobacco BY-2 cells with microtubule and actin drugs.....	37
2.4.4 Microscopy and image analysis.....	37
2.5 Phenotyping methods.....	38
2.5.1 Phenotyping of tobacco BY-2 cell lines.....	38
2.5.2 Phenotyping of rice <i>kchl</i> mutants	38
2.6 Biochemical methods.....	39
2.6.1 Standard methods.....	39
2.6.2 Protein expression and purification.....	41
2.6.3 Preparation of pig brain tubulin.....	43
2.6.4 <i>In vitro</i> polymerization of microtubules and actin filaments.....	45
2.6.5 Protein analysis.....	46

Results	49
1 <i>In silico</i> analysis of KCHs	49
1.1 KCHs form a highly conserved, plant-specific subgroup within the Kin-14 family	49
1.2 <i>OsKCH1</i> is a KCH member from rice	51
2 Investigation of OsKCH1 bifunctionality	52
2.1 OsKCH1 colocalizes <i>in vivo</i> with microtubules and actin	53
2.1.1 OsKCH1-800 is expressed in punctate, filamentous structures	53
2.1.2 OsKCH1-800 and OsKCH1-mot colocalize with cortical microtubules	55
2.1.3 OsKCH1-800 colocalizes with longitudinally oriented actin filaments	57
2.2 Recombinant KCH1 cosediments <i>in vitro</i> with microtubules and actin	60
2.2.1 OsKCH1 can be recombinantly expressed and purified	60
2.2.2 OsKCH1 cosedimentation is domain-dependent	61
3 Characterization of the biological role of OsKCH1	63
3.1 <i>OsKCH1</i> gene expression is regulated during development	63
3.2 <i>kch1</i> insertion mutants show impaired cell expansion	64
3.3 <i>KCH1</i> overexpressors show impaired cell division	68
3.4 <i>KCH1</i> overexpressors show delayed but morphologically normal mitosis	70
3.5 OsKCH1 is dynamically repartitioned during the cell cycle	71
3.6 <i>KCH1</i> overexpressors show delayed nuclear positioning	73
4 Analysis of the cytoskeletal binding of OsKCH1	75
4.1 OsKCH1 shows high affinity to actin and lower affinity to microtubules	75
4.2 OsKCH1 oligomerization is required for microtubule and actin bundling	78
4.2.1 OsKCH1 forms oligomers <i>in vitro</i> and <i>in vivo</i>	78
4.2.2 OsKCH1 bundles and cross-links microtubules and actin filaments <i>in vitro</i>	80
4.3 OsKCH1 harbors certain dynamic properties	82
4.3.1 OsKCH1 does not induce microtubule depolymerization	82
4.3.2 OsKCH1 shows slow motility <i>in vivo</i>	83
5 Summary of results	85

Discussion	87
1 KCHs are plant-specific and evolutionary conserved	87
2 OsKCH1 is a bifunctional protein	88
2.1 OsKCH1 associates with actin and microtubules <i>in vivo</i> and <i>in vitro</i>	88
2.2 In addition to KCHs a variety of other players are involved in cytoskeletal coordination in plants.....	89
3 OsKCH1 influences cell division, cell elongation and premitotic nuclear migration	91
3.1 Changes in <i>OsKCH1</i> expression levels alter cell division and elongation.....	91
3.2 OsKCH1 influences nuclear positioning.....	93
3.3 KCHs could represent functional homologues of dyneins in nuclear positioning.....	96
4 OsKCH1 is a dynamic structural linker of the cytoskeleton	97
4.1 KCH family members are unusual in their cytoskeletal binding affinities.....	98
4.2 OsKCH1 oligomers bind and bundle actin and microtubules.....	99
4.3 KCHs contribute to a dynamic cytoskeletal reorganization.....	101
Conclusion	104
Outlook	106
References	108
Appendix	122
1 Overview of KCHs in different plants	122
2 Sequence information	123
2.1 Coding sequence of <i>OsKCH1</i>	123
2.2 Sequence of the BY-2 PCR amplification product.....	124
Curriculum Vitae	125

ABBREVIATIONS

2,4-D	2,4-dichlorophenoxyacetic acid
A	Ampere
aa	amino acids
ABP	actin-binding protein
ADP	adenosine-5'-diphosphate
APS	ammonium peroxydisulfate
ATP	adenosine-5'-triphosphate
Amp	Ampicilin
AMP-PNP	adenylyl imidodiphosphate
AtKatD	<i>Arabidopsis thaliana</i> kinesin with calponin-homology domain
bp	base pair
BiFC	Bimolecular Fluorescence Complementation
BLAST	Basic Local Alignment Search Tool
BSA	bovine serum albumin
BY-2	tobacco cell line <i>Nicotiana tabacum</i> L. cv. Bright Yellow 2
CaMV	Cauliflower mosaic virus
CFP	cyan fluorescent protein
CH	calponin-homology
cm	centimeter
CPRF2	common plant regulatory factor 2
cv.	cultivar
d	day
Da	Dalton
DIC	differential interference contrast
DMSO	dimethyl sulfoxide
DsRed	<i>Discosoma sp.</i> red fluorescent protein
DTT	Dithiothreitol
ϵ	element of
EDTA	ethylene diamine tetraacetic acid
EGTA	ethylene glycol tetraacetic acid
ERM	ezrin, radixin, moesin protein family
FABD2	fimbrin actin-binding domain 2
FITC	fluorescein isothiocyanate
fl	full length
FPLC	fast protein liquid chromatography

fw	forward
g	acceleration of gravity
g	gram
GDP	guanosine-5'-diphosphate
GFP	green fluorescent protein
GhKCH1	<i>Gossypium hirsutum</i> kinesin with calponin-homology domain 1
GhKCH2	<i>Gossypium hirsutum</i> kinesin with calponin-homology domain 2
GTP	guanosine-5'-triphosphate
h	hour
His	histidine
Htz	heterozygote
Hyg	Hygromycin
kb	kilo base pairs
kDa	kilo Dalton
Kan	Kanamycin
KatA	<i>Arabidopsis thaliana</i> kinesin-14 A family member
KatD	<i>Arabidopsis thaliana</i> kinesin with calponin-homology domain
KCBP	kinesin-like calmodulin-binding protein
KCH	kinesin with calponin-homology domain
K_d	dissociation constant
KIF	kinesin family like protein
Kin	kinesin
l	liter
LB	Luria broth medium
μ	micro
m	milli
M	Molar (mole/liter)
MBP	microtubule-binding protein
MBD-MAP4	microtubule-binding domain of microtubule-associated protein 4
MI	mitotic index
min	minutes
MS	Murashige and Skoog medium
Mt	mutant
MW	molecular weight
n	nano
NCBI	National Center for Bioinformation
Ncd	Non-claret disjunctional
nm	nanometer

NP	nuclear position
OD ₆₀₀	optical density, measured at 600 nm
OsKCH1	<i>Oryza sativa</i> kinesin with calponin-homology domain 1
PAGE	polyacrylamide gel electrophoresis
PBS	phosphate buffered saline
PCR	Polymerase chain reaction
PPB	preprophase band
psi	pound-force per square inch
qPCR	quantitative Polymerase chain reaction
RFP	red fluorescent protein
rpm	rounds per minute
RT	room temperature
RT PCR	reverse transcription Polymerase chain reaction
rv	reverse
SDS	Sodium dodecyl sulfate
SE	standard error
sec	second
SEC	size-exclusion chromatography
ssp.	subspecies
TAMRA	5'-carboxytetramethylrhodamine
TE	Tris-EDTA buffer
TEMED	N',N',N',N',-tetramethyl-ethane.1,2-diamine
T _A	annealing temperature
Tris	tris(hydroxymethyl)-aminomethane
TRITC	tetramethyl rhodamine isothiocyanate
U	unit
V	Volt
v/v	volume per volume
w/v	weight per volume
Wt	wildtype
YC	C-terminal halve of yellow fluorescent protein
YFP	yellow fluorescent protein
YN	N-terminal halve of yellow fluorescent protein

ZUSAMMENFASSUNG

Wachstum und Entwicklung pflanzlicher Zellen erfordern eine enge räumliche und zeitliche Koordinierung von Mikrotubuli und Aktinfilamenten, den Hauptkomponenten des Zytoskeletts. Dazu notwendige Vermittlerproteine sind – im Unterschied zu tierischen und pilzlichen Systemen – in der Pflanze bisher weitergehend unbekannt. Die kürzlich identifizierten Kinesine mit Calponin-homologer Domäne (KCHs) könnten aufgrund ihrer hochkonservierten Aktin- und Mikrotubuli-Bindemotive in diesem Kontext eine zentrale Rolle spielen. Die vorliegende Dissertation beschäftigt sich daher mit der Frage, inwiefern KCHs direkte Vermittler zwischen beiden Zytoskelettkomponenten darstellen und in welche biologischen Prozesse diese Proteine involviert sind.

KCHs konnten in allen bisher sequenzierten Landpflanzen identifiziert werden, nicht jedoch in Tieren, Pilzen und Algen. Sie bilden eine phylogentisch eng verwandte Gruppe innerhalb der Kinesin-14 Familie. Zu ihrer funktionellen Charakterisierung wurde in dieser Arbeit das Reisprotein OsKCH1 ausgewählt und *in vivo* sowie *in vitro* auf Bindung an Mikrotubuli und Aktin untersucht. Mikroskopische Studien zeigten eine Colokalisation von OsKCH1 mit beiden Elementen des Zytoskeletts *in vivo* – sowohl in Zellen mit ausgeprägtem Streckungswachstum als auch in meristematischen Zellen. Wirkstoffbehandlungen zeigten die Sensitivität der Lokalisationsmuster von OsKCH1 gegenüber Mikrotubuli- und Aktininhibitoren. Die direkte Bindung von OsKCH1 an beide Elemente des Zytoskeletts wurde zudem *in vitro* über Cosedimentation nachgewiesen.

Ein erster Einblick in die biologische Funktion der KCHs konnte durch Genexpressionsstudien gewonnen werden. Die Transkription von *OsKCH1* unterlag in verschiedenen Stadien der Reisentwicklung einer deutlichen Regulierung. Höchste Expressionsniveaus existierten hierbei in Geweben mit starker Teilungsaktivität. Anschließende phänotypische Untersuchungen von Knock-down- und Überexpressionsmutanten zeigten eine Beeinflussung des Zusammenspiels von Zellstreckung und Zellteilung durch veränderte *KCH1*-Expressionslevel. Weiterführende mikroskopische Studien gaben schließlich Hinweise auf eine Funktion von KCH1 in der prämitotischen Positionierung des Zellkerns, einem Prozess der in pflanzlichen Zellen einer engen Interaktion von Aktinfilamenten und Mikrotubuli bedarf. Eine quantitative Untersuchung der Kernpositionierung bestärkte diese Vermutung: Tabakzellen mit erhöhten *KCH1*-Expressionsniveaus zeigten signifikante Verzögerungen in der Kernwanderung im Vergleich zu Wildtypzellen.

In Anlehnung an bekannte Kernpositionierungsmechanismen in tierischen und pilzlichen Systemen wurden Arbeitsmodelle entwickelt, die KCHs als dynamische und strukturelle Koordinatoren von Mikrotubuli- und Aktinnetzwerken während der Kernwanderung in Pflanzenzellen beschreiben. Weiterführende biochemische Analysen konnten diese Modelle zusätzlich stützen. Eine Oligomerisierung von OsKCH1 wurde sowohl *in vitro* als auch *in vivo* beobachtet – sie bildet die Voraussetzung für eine simultane Bindung des Proteins an beide Elemente des Zytoskeletts. Die Fähigkeit von OsKCH1 als direktes Bindeglied zwischen Aktin und Mikrotubuli zu fungieren wurde schließlich *in vitro* durch Bündelungstests bestätigt. *In vivo*-Zeitserien gaben zudem erste Hinweise auf dynamische Eigenschaften von OsKCH1 als Kinesinmotor.

INTRODUCTION

1 The sensitive nature of the plant cytoskeleton

The photosynthetic lifestyle of plants relies on a surface increase in outward direction. The plant architecture must, as a consequence, be able to cope with a substantial degree of mechanic load. While aquatic plants can maintain considerable body sizes even on the base of fairly simple architectures due to the presence of water buoyancy, the transition to terrestrial habitats required the development of a flexible and simultaneously robust mechanical lattice. On the organ level, this is represented by the load-bearing elements of the vessel system (Zimmermann, 1965). On the cellular level, plants have developed rigid cell walls that confer stability.

These changes in architecture not only fundamentally influence the basic processes of plant cell division and cell expansion. They as well determine the sessile lifestyle of plants, which in turn leads to the special dependence of plants on their habitat. During animal development, body shape is mostly independent of the environment. Plants, by contrast, have to cope with altering environmental conditions by changes in their *Bauplan* – which results in a high degree of morphogenetic plasticity. A challenge with mechanical load, for instance, will lead to a reallocation of load-bearing elements on the different levels of organization such that mechanical tensions are equilibrated in an optimal way. With respect to whole-plant physiology, this can lead to thigmomorphogenesis – alterations of growth that result in adaptive changes of shape (Jaffe, 1973).

On a cellular level, the continuous adaption to changing conditions requires an efficient sensing and a subsequent integration of forces and tensions. The main structure involved in this processes is the plant cytoskeleton. It consists of two elements – microtubules and actin filaments – which will be introduced in molecular detail in the following chapter. Both components act in concert as efficient tensegrity system – a structure that stabilizes itself by balancing the counteracting forces of compression and tension (Ingber, 1998, 2003a, 2003b). Actin microfilaments that are not only contractile, but mechanically comparable to silk fibers, represent the tensile elements; the rigid, glass-fiber like microtubules act as compression-resistant components (Gittes et al., 1993). Mechanic stimulation is typically followed by an appropriate reorganization of these tensegrial elements. The plant cytoskeleton is, thus, not only a structure that provides additional mechanic stability – as necessary in animal cells – but must as well directly participate in the sensing of stress and strain patterns. In plant cells that possess rigid cell walls and are thus already endowed with stability, the role of the cytoskeleton is optimized towards sensing and integration of such mechanic stimuli during cell growth and development (for review see Nick, 2010).

The following sections will first introduce microtubules and actin filaments as molecular components of the cytoskeleton in more detail. As subsequently summarized, the spatial organization of these elements is highly dynamic and undergoes fundamental reorganizations during the cell cycle. These include both functional and probably also structural interconnections between microtubules and actin filaments (Wasteneys and Galway, 2003, Collings, 2008).

1.1 Microtubules and actin filaments as dynamic cellular players

The plant cytoskeleton is comprised of two different types of linear, proteinaceous polymers: actin filaments and microtubules. Intermediary filaments – known to constitute a third cytoskeletal component in animal cells – are absent in plants. Microtubules and actin filaments establish dynamic filamentous networks within the cell. These are tightly associated with various developmental and cellular functions, such as cell division, intracellular transport, cell morphogenesis and the maintenance of cell growth and stability.

Microtubules are rigid, hollow rods with a diameter of 25 nm and varying lengths between 200 nm and 25 μm . They are dynamic structures that undergo continual assembly and disassembly within the cell and are involved in various processes, including for example the determination of cell shape, intracellular transport and the separation of chromosomes during mitosis. Microtubules are constructed of dimers of two closely related 50 kDa proteins, α - and β -tubulin, polymerizing end-to-end into protofilaments. The hollow cylindrical filament shape is formed by parallel self-arrangement of these filaments into a helix. One turn of the helix contains 13 tubulin dimers, each from a different protofilament (Fig. 1 A). Consequently, the resulting microtubules are polar structures with two distinct plus- and minus-ends (for review see Mandelkow and Mandelkow, 1989).

Microtubules can undergo rapid cycles of assembly and disassembly due to polymerization and depolymerization of tubulin dimers, regulated by GTP binding and hydrolysis. Characteristic dynamic variations of the microtubule cytoskeleton within the cell include treadmilling and dynamic instability. Treadmilling is a process in which tubulin dimers bound to GDP are continually lost from the minus-end and replaced by the addition of GTP-bound dimers to the plus-end of the same microtubule. Dynamic instability results in an alternation between cycles of growth and shrinkage, depending on the equilibrium between rates of polymerization and GTP hydrolysis. Due to dynamic instability, most microtubules undergo continuous and rapid turnover within the cell – with typical microtubule half-lives of only several minutes (for review see Desai and Mitchison, 1997).

Actin, on the other side, is a globular, highly conserved 42 kDa protein which polymerizes head-to-tail into polar actin protofilaments. Two parallel protofilaments twist around each other in a right-handed helix to form actin filaments: thin, flexible fibers of approximately 7 nm in diameter and up to several micrometers in length (Fig. 1 B). Within the cell, actin filaments (or microfilaments) are organized into higher-order structures and forming bundles or three-dimensional networks with the properties of semi-solid gels (for review see Insall and Machesky, 2009). The assembly and disassembly of actin filaments, their cross-linking into bundles and networks, and their association with other cell structures such as the plasma membrane or the nucleus, are regulated by a variety of actin-binding proteins, thus creating a highly dynamic and tunable structure (for review see Hussey et al., 2006).

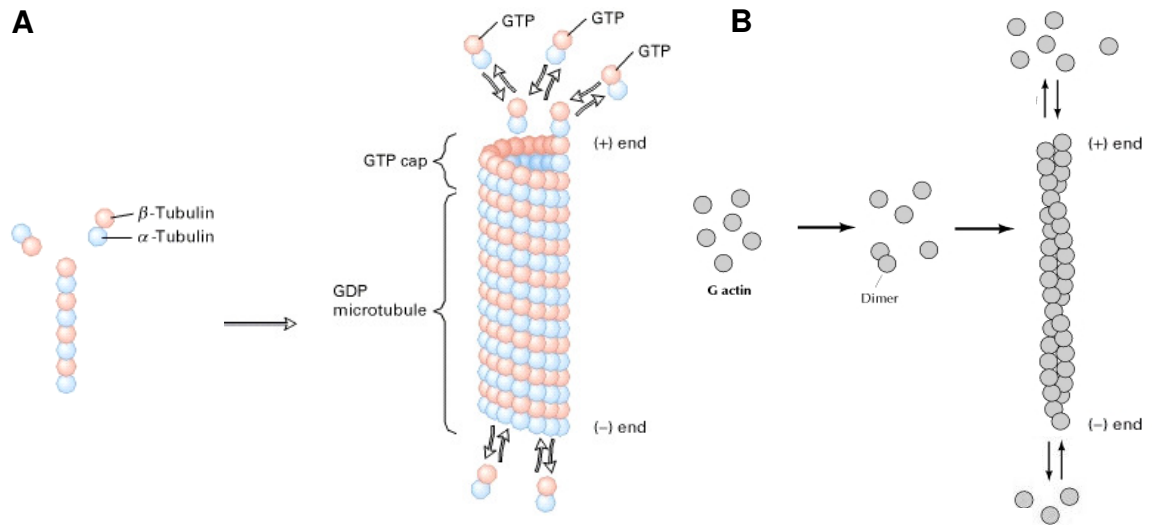


Fig. 1: Reversible polymerization of microtubules and actin microfilaments

[A] Assembly of microtubules (schematic: Lodish et al., 2007; modified). Free α/β -tubulin dimers associate longitudinally to form short protofilaments. These associate laterally into a microtubule with 13 protofilaments. The microtubule then grows by the addition of subunits to the ends of protofilaments. GTP is bound in the free tubulin dimers to the exchangeable nucleotide-binding site on the β -tubulin monomer. After incorporation of a dimeric subunit into a microtubule, the GTP on the β -tubulin is hydrolyzed to GDP. When the rate of polymerization is higher than the rate of GTP hydrolysis, a cap of GTP-bound subunits is generated at the plus-end. [B] Assembly of actin microfilaments (schematic: Cooper and Hausman, 2003; modified). Globular actin monomers associate to dimers and trimers, which then reversibly grow by addition of monomers to both ends to form actin filaments.

Similar to microtubules, actin polymerization is reversible. Filaments can depolymerize by dissociation of actin subunits, allowing actin filaments to be rapidly broken down or to show treadmilling behavior. The rate at which actin monomers are incorporated into filaments is depending on their concentration and the rate of ATP hydrolysis (Korn et al., 1987).

1.2 Cytoskeletal organization during plant cell growth and development

Cell division, expansion, differentiation and cell-to-cell communication are fundamental processes during the development of multicellular organisms. Especially plants as sessile organisms have to integrate external stimuli in these processes in order to cope with altering environmental conditions. The orientation of cell division planes and the direction of cell expansion is thus strictly controlled during plant morphogenesis. As described in the following sections, the cytoskeleton plays important roles in these processes.

1.2.1 Cell expansion

While growth in animal cells is mainly pursued via cell division, plant cell growth mainly relies on cell expansion, and division is rather limited to meristematic tissues (for review see Steeves and Sussex, 1989). Plant cells are enclosed in cell walls and their directed expansion is thus an essentially irreversible process that plays a key role during organ morphogenesis. Cytoskeletal elements mainly determine the directionality of cell expansion and thus represent important components during plant cell growth.

Most plant cells expand by diffuse growth driven through turgor pressure. The growth direction along one main axis is established by the rigid cell wall, consisting of cross-linked cellulose microfibrils that are arranged in parallel to one another and transversely to the direction of cell elongation. This microfibrillar network resists radial expansion much more than longitudinal expansion and thus promotes cells elongation perpendicular to the microfibril orientation as reaction to the turgor pressure. Cellulose microfibrils are synthesized by a multi-subunit enzymatic complex, the cellulose synthase, which is integrated into the plasma membrane. A widely accepted model predicts that cellulose synthase moves along cortical microtubules. In interphasic cells, these are organized in arrays of parallel bundles perpendicular to the axis of preferential cell expansion and represent the template for an oriented deposition of microfibrils in the cell wall. According to this hypothesis, the main axis of cell expansion is ultimately determined by the orientation of the cortical microtubules (for review see Giddings and Staehelin, 1991; Nick, 2008). In response to various external and internal stimuli the arrays of cortical microtubules can undergo reorientation that, in turn, will as well shift the preferential direction of cellulose deposition and, as consequence, the mechanical anisotropy of the yielding cell wall. The proportionality of cell expansion can thus be adapted in response to external signals (for review see Nick, 2008).

In interphasic plant cells, actin is organized into several distinct arrays that presumably exert different functions. Actin filaments form randomly arranged networks in the cell cortex and around the nucleus, and extend through cytoplasmic strands (reviewed by Staiger and Lloyd, 1991; Kost and Chua, 2002; see Fig. 2 A). In contrast to animal cells where intracellular organization and membrane trafficking is maintained essentially by microtubules, in plant cells actin filaments are mainly responsible for the positioning and the dynamic behavior of cell organelles either by myosin-dependent movement (Jedd and Chua, 2002) or actin dynamics (Gossot and Geitmann, 2007; Cárdenas et al., 2008). This is especially important for cells with pronounced tip growth, such as pollen tubes or root hairs, where actin functions as track for the transport of vesicles with cell wall material that are inserted into to tip (Hepler et al., 2001; Vidali et al., 2009). In cells that expand by diffuse growth in a tissue context as described above, the role of actin is, however, different and not as obvious as for tip growth. In these cells, actin is predominantly present as longitudinal filament bundles that form transvacuolar strands. Their rigidity and their degree of bundling is regulated by various signals that include plant hormones (Grabski and Schindler, 1996; Maisch and Nick, 2007), kinase cascades (Grabski et al., 1998), and light (Waller and Nick, 1997), and is directly associated with changes in growth rate. In

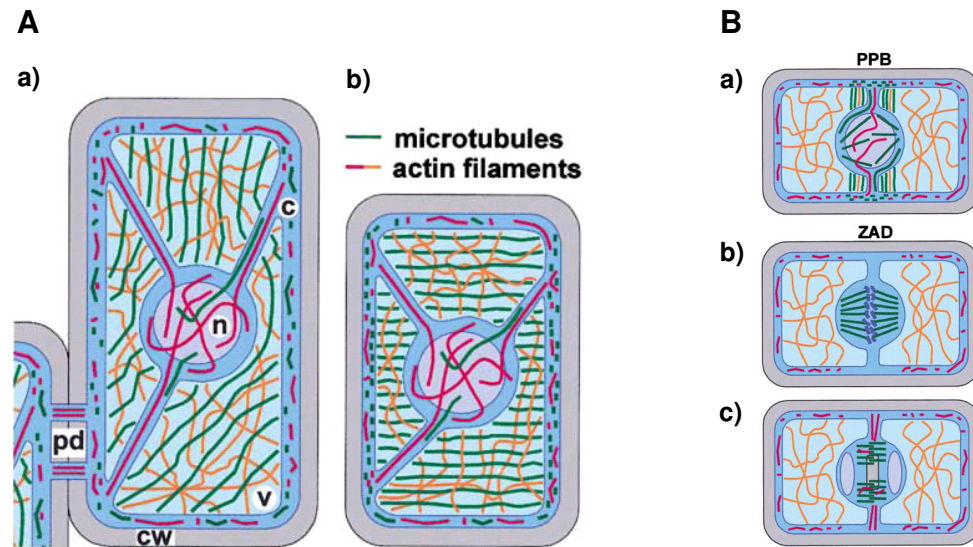


Fig. 2: The plant cytoskeleton during cell growth and division

[A] Cytoskeletal structures in non-growing cells (a) and in cells that elongate by diffuse growth (b). Cytoplasmic strands are indicated in dark blue, the nucleus is shown in purple. [B] Cytoskeletal structures during preprophase (a), metaphase (b), and cytokinesis (c). Chromosomes are represented in dark blue and attached to microtubules in (b). Abbreviations: pd, plasmodesmata; c, cytoplasm; n, nucleus; v, vacuole; cw, cell wall; PPB, preprophase band; ZAD, zone of actin depletion. Image source: Kost and Chua, 2002.

addition to the transvacuolar bundles, a fine network of highly dynamic microfilaments can be detected in the cortical cytoplasm of elongating cells, often accompanying cortical microtubules (for review see Collings, 2008). Interestingly, the pharmacological disruption of actin causes a partially abnormal deposition of microfibrils (Seagull, 1990), pointing towards a direct interconnection with cortical microtubules. This is in accordance with the observation that actin filaments are required for the reorganization of microtubular structures in different cell types (Kobayashi et al., 1988; Schmit and Lambert, 1988; Eun and Lee, 1997). Actin within a tissue context is thus not directly controlling cell growth by direct mechanical constriction. It rather controls the proper localization and activity of the machinery that regulates cell expansion.

1.2.2 Cell division

Cells in developing plant tissues generally divide anticlinally – with the division plane perpendicular to the organ surface. Daughter cells then elongate perpendicularly to the plane of cell division. This results in the controlled and directed expansion of developing organs. Rare periclinal or asymmetrical cell divisions in meristems and embryos result in the establishment of new cell layers and the formation of daughter cells with distinct developmental fates. Stringent control of the positioning of cell division planes is thus of crucial importance for plant morphogenesis and development, and is under tight cytoskeletal control. Both microtubules and actin

filaments are essential components of the basic machineries that are required for nuclear division and cytokinesis (reviewed by Staehlin and Hepler, 1996; Jürgens, 2005; Nick, 2008).

In plant cells that prepare for division, typically a migration of the nucleus occurs towards the site where the prospective cell plate will form. This migration was found to be highly sensitive to inhibitors of both microtubules and microfilaments (Katsuta and Shibaoka, 1988; Katsuta et al., 1990) indicating a tight interplay between the two types of cytoskeletal elements in this process. Katsuta et al. (1990) proposed that the premitotic network of microtubules might serve as scaffold for the positioning of actin filaments that establish and maintain the position of the nucleus and the mitotic apparatus.

The spatial control of cell division employs specialized populations of microtubules that are unique to plant cells: the cortical microtubules, the preprophase band (PPB) and the phragmoplast (reviewed by Nick, 2008). At the onset of mitosis, cortical microtubules typically condense into a narrow ring around the nucleus, the PPB, which determines the future cell division plane (see Fig. 2 B). When the spindle is formed, the PPB disappears completely but leaves landmarks in the cell cortex that later target the extending cell plate to the correct fusion site. Such landmarks have been proposed to involve local differentiations at the cell wall (Mineyuki and Gunning, 1990), and a cortical region largely devoid of filamentous actin (zone of actin depletion) that remains at the position of the PPB after disappearance of the PPB (Cleary et al., 1992). The suggestion that the actin cytoskeleton may have a function in cell plate guidance is supported by the observation of actin filaments that extend from the expanding cell plate to the cortical fusion site (Traas et al., 1987; Valster et al., 1997) and the demonstration of actin assembly at the edge of growing cell plates (Endle et al., 1998). This is supported by reports, where treatment with actin-depolymerizing drugs resulted in abnormal cell plate positioning (Mineyuki and Palevitz, 1990; Eleftheriou and Palevitz, 1992).

The mitotic spindle, which poles lack centrosomes and astral microtubules and are in consequence less focused as compared to animal cells, mediates karyokinesis and disintegrates after anaphase. Subsequently, the phragmoplast develops – a microtubular structure that participates in the production of the cell plate between the two newly generated daughter nuclei during cytokinesis (reviewed by Kost and Chua, 2002; Nick, 2008; see Fig. 2 B, c). The major components of the phragmoplast are two opposing sets of parallel microtubules, aligned in a cylindrical shape and overlapping at the central plane. Golgi stacks accumulate around the phragmoplast during cytokinesis and cell wall materials are synthesized and delivered through secretory vesicles to the growing cell plate that eventually fuses with the parental cell wall (Nebenführ et al., 2000; Otegui et al., 2001).

2 Interaction and cross-talk between microtubules and microfilaments in plants

The plant cytoskeleton comprises, as described in detail in the previous chapters, two distinct and highly dynamic arrays of microtubules and actin microfilaments. For many processes during plant cell growth and development a tight temporal and spatial coordination of these two types of cytoskeletal elements is required. Thus, either a direct or an indirect interaction and cross-talk between microtubules and actin filaments is necessary (Wasteneys and Galway, 2003; Collings, 2008).

A variety of microscopic studies in fixed and living cells have reported that microfilaments co-align and cross-bridge to cortical microtubules (Franke et al., 1972; Ding et al., 1991a, 1991b; Collings and Wasteneys, 2005). These microtubule-associated microfilaments seem ubiquitous in plants, occurring in many different species and in diverse cell types (Franke et al., 1972; Ding et al., 1991a, 1991b; Tominaga et al., 1997). During the last decade, the microscopic observations were complemented by drug targeting experiments that as well pointed towards a direct interaction between microtubules and microfilaments. The disruption of actin microfilaments in cotton fibers, for example, causes parallel cortical microtubules to become randomly organized (Seagull, 1990). Similarly, microtubule depolymerization causes the loss of transverse cortical microfilaments in cultured carrot cells (Traas et al., 1987) and *Arabidopsis* roots (Collings and Wasteneys, 2005). The microtubule-stabilizing drug taxol, by contrast, enhances the presence of microtubule-associated microfilaments in maize roots (Chu et al., 1993; Blancaflor, 2000) and tobacco BY-2 cells (Collings et al., 1998). Pharmacological evidence furthermore suggests that

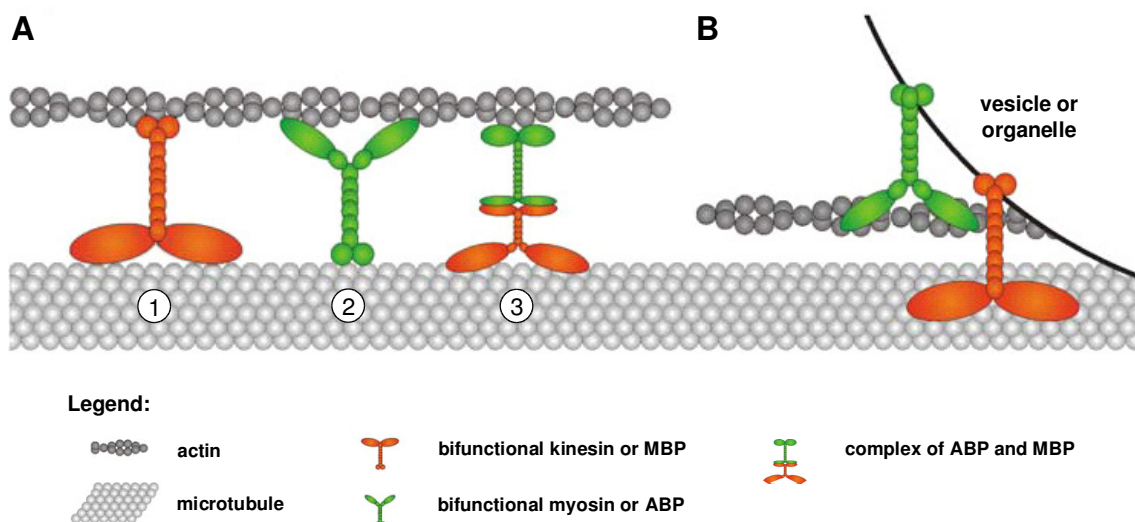


Fig. 3: Schematic depiction of possible ways of interaction between actin and microtubules

[A] Direct contact through motor proteins and other ABPs or MBPs can occur either via bifunctional interaction as displayed in examples (1) and (2), or by generation of complexes of monofunctional proteins that each are able to bind to one type of cytoskeletal element at a time (3). [B] Indirect contact can be generated by binding of motors and other ABPs or MBPs to the same structure within the cell, such as organelles, vesicles, or even the plasma membrane. Image source: Petrášek and Schwarzerová, 2009; modified.

an interaction between microfilaments and microtubules contributes to the control of cell elongation and tissue expansion (Seagull, 1990; Blancaflor, 2000; Collings et al., 2006).

Despite the extensive studies on microtubule-microfilament associations, relatively little research has been conducted on the proteins that might mediate them. Interactions between microtubules and actin microfilaments could either occur in a direct way, mediated through bifunctional proteins that are able to bind simultaneously to both cytoskeletal elements, or indirectly, by a connecting complex of two or more proteins that include a microtubule-binding and a different actin-binding protein. Indirect interaction could as well involve the coupling of microtubules and microfilaments via motors and other actin-binding proteins (ABPs) or microtubule-binding proteins (MBPs) that similarly bind to the same cellular structures at a time (for review see Rodriguez et al., 2003; Petrášek and Schwarzerová, 2009; Fig. 3).

In animals and fungi a number of proteins have been identified that mediate interaction between microtubules and microfilaments, either in a bifunctional way or as complexes of monofunctional proteins. These include the microtubule actin cross-linking factor MACF (Leung et al., 1999), the microtubule-associated proteins MAP1 and MAP2 (Dehmelt et al., 2003), formins, the microtubule motor dynein and related dynactin complexes, coronin, various complexes involving the microfilament-dependent motor protein myosin, and a class of actin-binding proteins referred to as ERM proteins (reviewed by Goode et al., 2000; Rodriguez et al., 2003).

Plants, however, lack homologues of MAP1 and MAP2, coronin, ERM proteins and dynein. Myosins and formins, which in animals can interact with both microtubules and microfilaments, have homologues in plants, however the evidence for a similar function in microtubule-microfilament cross-linking in plants have remained scarce (Deeks et al., 2002; Blanchoin and Staiger, 2008). Nevertheless, several other candidate plant proteins have been described, and recently first evidence accumulated in particular for a specific group of kinesins, the kinesins with calponin-homology domain (Tamura et al., 1999; Preuss et al., 2004).

The following section will thus first give a general introduction on kinesins and their characteristics as molecular motors, then focus on the diversity of kinesins in plants and finally specifically introduce the kinesins with calponin-homology domain.

3 The superfamily of kinesins

Kinesins belong to the perhaps most fascinating group of proteins associated with the cytoskeleton – the molecular motors. Such motor proteins are generally able to bind to a polarized cytoskeletal filament and use the energy derived from repeated cycles of ATP hydrolysis to move steadily and unidirectionally along to it (reviewed by Howard, 2001). In every eukaryotic cell dozens of motor proteins coexist, differing in the type of filament they bind to (either actin or microtubules), the direction in which they move along the filament, and the cargo they carry. Many motor proteins transport membrane-enclosed organelles such as mitochondria, Golgi stacks, or secretory vesicles towards their appropriate locations in the cell. Others cause cytoskeletal filaments to slide against each other, generating the force that drives such phenomena as

muscle contraction, ciliary beating, and cell division, or are implicated in morphogenesis, polarized growth and signal transduction.

In non-plant systems, three families of molecular motors, the kinesins, dyneins, and myosins, can be distinguished and have been well characterized during the last decade (reviewed by Krendel and Mooseker, 2005; Hook and Vallee, 2006; Hirokawa et al., 2009). While kinesins and dyneins are microtubule-associated proteins, myosins use actin filaments as their intracellular tracks. In the plant lineage, dynein and dynactin genes have to date only been identified in lower members, but are absent in the genomes of all so far sequenced flowering plants. This indicates that the dynein class of molecular motors might have been lost during evolution of angiosperms, maybe concomitantly with the loss of the flagellar apparatus (Lawrence et al., 2001).

Kinesins or kinesin superfamily proteins (KIFs) represent the most expanded class of molecular motors. Conventional kinesin, the first member of the kinesin superfamily, was identified in 1985 as the motile force underlying the movement of particles along microtubules of the giant axon of the squid (Vale et al., 1985). Since that time, a systematic molecular biological search has continuously found new kinesins and kinesin-related proteins in all eukaryotes, including the protists, fungi, invertebrates, animals, and plants. The number of kinesins identified to date in genomes that have been fully sequenced and at least partially annotated varies from 6 in budding yeast to 19 in *C. elegans*, 24 in *Drosophila*, 45 in humans, and 61 in *Arabidopsis*. Depending on their domain structure and organization, as well as the localization of their motor cores either at the N- or C-terminus or the center of the protein, kinesins can be classified into 14 subfamilies. These exhibit a great variety of cellular functions, ranging from the transport of organelles, vesicles, and mRNA, to spindle assembly and integrity, chromosome motility, microtubule dynamics, and trafficking of signaling modules (reviewed in Dagenbach and Endow, 2004; Miki et al., 2005; Hirokawa et al., 2009). The high degree of functional versatility is basically located in the non-motor regions of the protein and typically conserved within the different subfamilies. Recently, a new and generalized kinesin nomenclature has been proposed to resolve unspecific and redundant denominations, which is now widely accepted (Lawrence et al., 2004).

3.1 Structural characteristics of kinesin motors

Despite the high functional versatility found among kinesins from different subfamilies, several structural characteristics remain conserved. As common feature all kinesins share a globular, 360-residue motor domain that contains both the catalytic pocket for the hydrolysis of ATP and the binding sites for microtubules. The domain structure of conventional kinesin is exemplarily displayed in Fig. 4 A, where the characteristic protein structure with the globular motor domain (head), and the fan-shaped tail structure, is clearly visible. A long stalk region builds the connection between the head and the tail domains at the opposing ends of the molecule. It often includes one or several alpha-helical coiled-coil domains, associated with the oligomerization of kinesins to homo- or heterodimers or even tetramers (for review see Howard, 2001). While the

head domain is responsible for the movement empowered by hydrolysis of ATP (Schliwa, 2003; Cross, 2004; Ishii et al., 2004; Yildiz and Selvin, 2005), the highly diverse stalk and tail domains are important for the interaction with other subunits of the holoenzyme or with cargo molecules such as proteins, lipids or nucleic acids (reviewed in Miki et al., 2005; Hirokawa et al., 2009). A short region between head and stalk, the so called neck, contains further family-specific features and is essentially involved in the generation of intrinsic motor characteristics, such as processivity and the directionality of kinesin movement either towards the plus- or the minus-end of a microtubule.

Thus, the directionality of movement is highly dependent on the amino acid sequence of the neck-linker, as well as on the location of the motor domain either at the N- or C-terminus of the protein, and on the position of the neck upstream or downstream of the motor core (Wade and Kozielski, 2000; Woehlke and Schliwa, 2000). Plus-end directed motors, such as conventional kinesin, typically have their motor domain located at the N-terminus of the protein and a conserved neck-linker sequence is found directly downstream of this catalytic core. Minus-end directed motors such as Non-claret-disjunctional (Ncd), a kinesin-14 family member from *Drosophila* (Walker et al., 1990), by contrast, usually harbor C-terminally located motor domains, and conserved neck regions upstream of these motor cores (Endow, 1999). The importance of the neck-linker sequence for the determination of motor directionality was revealed through several experiments with motor chimeras, built from domains of intrinsically plus- and minus-end directed kinesins. In these assays, the neck sequence of the Ncd motor was found to be sufficient to confer minus-end motor directionality of the catalytic domain of conventional kinesin (Endow and Waligora, 1998) and *vice versa* (Case et al., 1997).

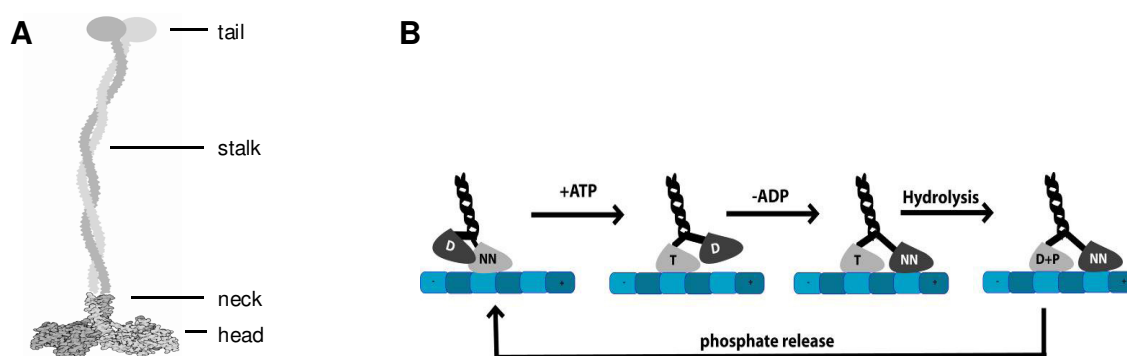


Fig. 4: Structural organization of kinesins

[A] Domain organization of conventional kinesin. Two identical heavy chains dimerize into the typical kinesin structure via coiled-coils within the stalk region. The globular motor domain and the adjacent neck mediate microtubule-binding. The tail region is involved in the binding of specific cargo or light chains. Image source: www.rcsb.org/pdb/. [B] Simplified 'hand-over-hand' model for kinesin movement. The sequence of events summarizes the chemo-mechanical cycle of one kinesin head during processive plus-end directed movement. Kinesin is shown in black/gray, microtubules in blue. Nucleotides bound to kinesin heads are abbreviated as follows: T, ATP; D, ADP; P, phosphate; NN, no nucleotide. Image source: Schliwa, 2003; modified.

Processivity is a second intrinsic motor characteristic and refers to the ability of a dimeric motor protein to bind to a filament and to take successive steps before detaching. Processive movement was first demonstrated for single molecules of conventional kinesin (Svoboda et al., 1993). It is thought to involve alternating filament binding and ATP hydrolysis by the two motor domains with one head always bound to the filament, and a transient state between the steps when two heads are bound (Higuchi and Endow, 2002; see Fig. 3 B). While conventional kinesin is able to move several microns along a microtubule before detaching (Svoboda et al., 1993), the microtubule minus-end directed *Drosophila* kinesin Ncd, by contrast, is a non-processive motor (Endow and Barker, 2003).

Not only conventional kinesin but the majority of the so far characterized kinesins are N-terminal motors that show microtubule plus-end-directed motility, and in many cases as well processive movement. Minus-end directed motility has to date only been found for certain members of the kinesin-14 subfamily that possess C-terminally located motor cores, and contain a characteristic and conserved 14-amino acid neck linker positioned upstream of this catalytic core. Kinesins with centrally located catalytic domains are found within the kinesin-13 subfamily, in parts of the plant kinesin-14 family, and among the unclassified orphan kinesins. Interestingly, several of these members have been associated with microtubule-end binding and ATP-dependent microtubule depolymerization activity, instead of showing unidirectional movement along microtubules (Desai and Mitchison, 1997; Hunter et al., 2003).

3.2 Plants possess a most peculiar set of kinesins

Only little is known about the specific functions of the different kinesins in plants. Recently, global database screenings of the fully sequenced plant genomes have led to the identification of a great number of kinesin candidate genes. To date their functional analysis is a wide subject of ongoing research.

With at least 61 different genes in *Arabidopsis thaliana*, 52 in *Populus trichocarpa*, and 41 in *Oryza sativa ssp. japonica*, the number of kinesins in plants is the highest among all the eukaryote genomes sequenced so far (Reddy and Day, 2001; Richardson et al., 2006). While several members, such as the mitotic kinesins of the kinesin-5 and the kinesin-6 families, are structurally and functionally highly conserved to fungi and animals (reviewed by Miki et al., 2005), many other plant kinesins are evolutionarily divergent.

A thorough phylogenetic analysis of kinesins from several photosynthetic organisms has revealed some striking differences in the composition of kinesins between plants and other organisms (Richardson et al., 2006). As displayed in Fig. 5, angiosperms, although having the largest total numbers of kinesins, possess only members in 10 of the 14 known subfamilies, and completely lack kinesins of class 2, 3, 9 and 11. Members of the kinesin-2 subfamily mediate intraflagellar transport of organelles within ciliates and flagellates. Interestingly, the flagellated unicellular photosynthetic eukaryote *Chlamydomonas reinhardtii* has one kinesin-2 which is as well involved in intraflagellar transport (Rosenbaum and Witman, 2002). The kinesin-3 subfam-

ily contains the highest number of members in animals. They are mainly involved in intracellular organelle transport. Not only class-3 kinesins but also other subclasses including the conventional kinesins that mainly act in vesicle transport processes in animal cells, are clearly under-represented in flowering plants (Richardson et al., 2006). The cargo-transport functions of these

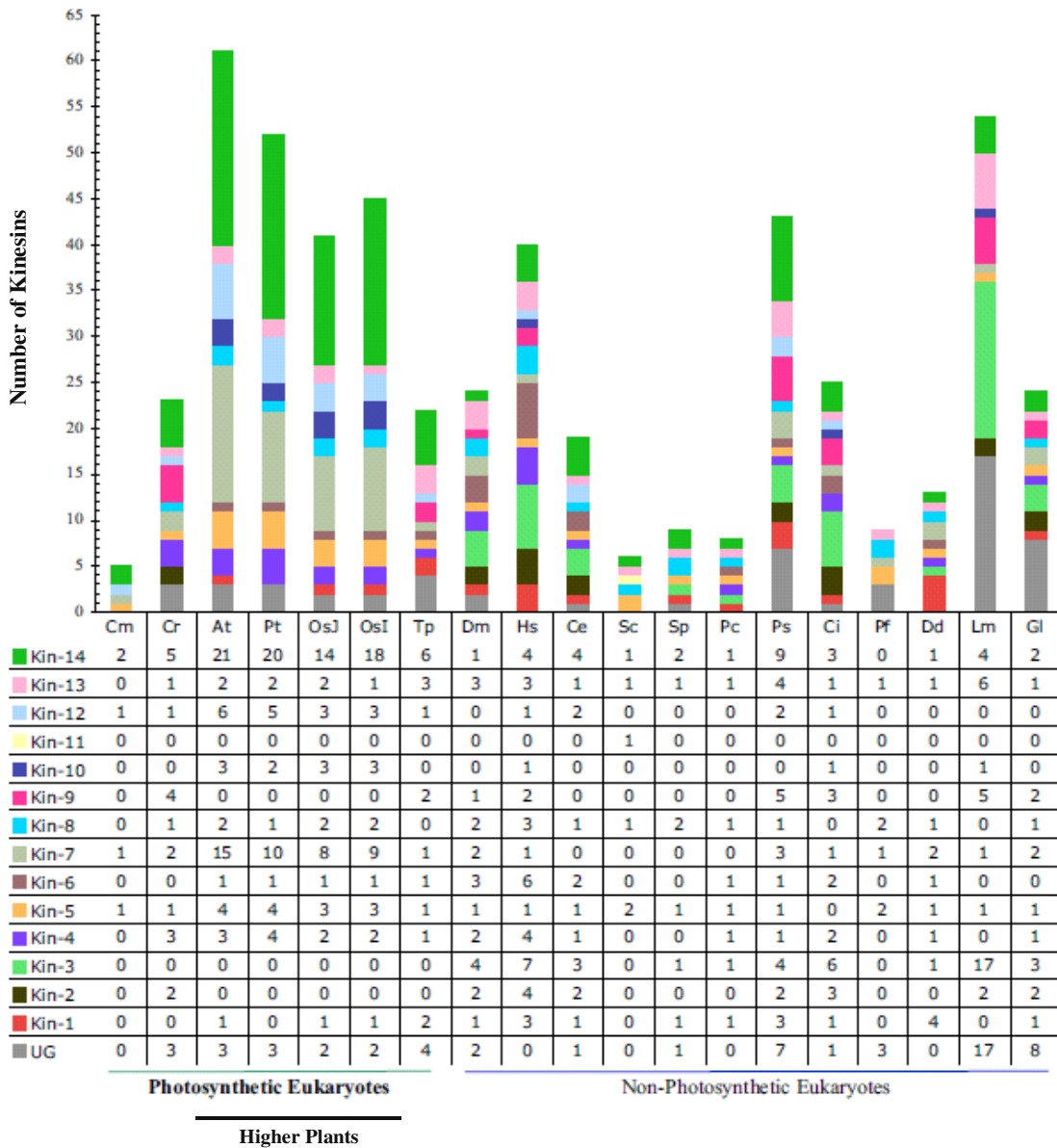


Fig. 5: Kinesin composition in different organisms

[A] Number and distribution of kinesins in photosynthetic and non-photosynthetic organisms. Tabular and graphical representation of the number of kinesins found in the completely sequenced genomes of 19 different species. The number of kinesins is shown on the y-axis. Different colors represent the distribution of kinesins into specific families together with details on the respective number of kinesins in each family per species. Abbreviations: Cm, *Cyanidoschyzon merolae*; Cr, *Chlamydomonas reinhardtii*; At, *Arabidopsis thaliana*; Pt, *Populus trichocarpa*; OsJ, *Oryza sativa ssp. japonica*; OsI, *Oryza sativa ssp. indica*; Tp, *Thalassiosira pseudonana*; Dm, *Drosophila melanogaster*; Hs, *Homo sapiens*; Ce, *Caenorhabditis elegans*; Sc, *Saccharomyces cerevisiae*; Sp, *Schizosaccharomyces pombe*; Pc, *Phaenerochaete chrysosporium*; Ps, *Phytophthora sojae*; Ci, *Ciona intestinalis*; Pf, *Plasmodium falciparum*; Dd, *Dictyostelium discoideum*; Lm, *Leishmania major*; Gl, *Giardia lamblia*. Image source: Richardson et al., 2006.

kinesins are thus either not needed in angiosperms, are performed by members of other subfamilies, or are even transferred to cargo-transporting myosins (Reddy and Day, 2001).

Other families such as kinesin-7 and kinesin-14, by contrast, are highly expanded in angiosperms and some members differ in domain organization greatly from their fungal and animal counterparts. Thus, 21 of the in total 61 kinesins from *Arabidopsis* belong to the kinesin-14 subfamily and 15 members can be attributed to class-7 (Fig. 5; Richardson et al., 2006). The exceptional distribution of plant kinesins has presumably originated in gene duplication and subsequent functional diversification. An inclusion of additional and unusual domains during further evolution indicate fundamental differences in functionality and might point to an involvement of some of these kinesins in several plant-specific features. The fact that plants have unique microtubule arrays, such as the PPB and the phragmoplast, and lack centrosomes to organize microtubules suggests that novel proteins would be required to perform plant-specific functions (Reddy and Day, 2001). Flowering plants, in addition, lack dyneins as well as dynein-complex proteins. Thus, the functions performed by these proteins in animals, including the establishment of spindle poles and the movement of nuclei and chromosomes, must be covered differently in plants (Koonce, 2000; Sharp et al., 2000). Besides their roles in transport processes, dyneins are important components of the flagellar apparatus and are still present in protists and lower plants that contain flagella during some stage of their life cycle (Lawrence et al., 2001; Wickstead and Gull, 2007). The striking absence of sequence homologues to cytoplasmic and flagellar dynein, and the lack of the flagellar kinesin-2 motors in flowering plants therefore suggest that these genes and their respective functions may have disappeared in angiosperms concomitantly with the loss of the flagellar apparatus (Lawrence et al., 2001; Miki et al., 2005; Wickstead and Gull, 2007). Hence, it is possible that the expansion of kinesins in plants accounts for the need for plant-specific as well as retrograde directed motors in angiosperms.

3.3 Plant kinesin-14 – a class of its own

Kinesin-14 is a diverse family, containing representatives from almost all major eukaryotic groups. In flowering plants, kinesin-14 represents the largest family and many of its members differ greatly with respect to structure and function from animal kinesin-14. They even contain additional plant-specific domains. Depending on their overall domain structure and the location of their motor core, either in the center of the protein or at the N- or C-terminus, the kinesin-14 family in plants can be further divided into three subgroups (Reddy and Day, 2001; Lee and Liu, 2004; see Fig. 6 for illustration).

Kinesins of the first group, such as the *Arabidopsis* members KatA, KatB and KatC, are closely related in structure and function to the animal and fungal kinesin-14 members *Drosophila melanogaster* Ncd and Kar3 from *Saccharomyces cerevisiae* (Richardson et al., 2006). Their motor domain is located at the C-terminus of the protein, together with the well-conserved, minus-end directing 14-amino acid neck linker which is found directly upstream of the motor core. KatA is a non-processive motor and plays a critical role in microtubule organization at the

spindle poles and the spindle midzone during meiosis and mitosis (Chen et al., 2002; Marcus et al., 2002, 2003).

Kinesins of the other two subgroups are clearly more divergent to animal and fungal kinesin-14 members. The kinesin-like calmodulin-binding protein (KCBP/Zwichel) occurs as single gene in most plant genomes and has a most unusual domain structure. In addition to their C-terminal motor, KCBPs contain a myosin-tail homology domain (MyTH4) and a talin-like region (ERM). The minus-end directed KCBP motor in *Arabidopsis* has a role in cell division and trichome morphogenesis and is regulated by calmodulin-binding in presence of micromolar concentrations of calcium ions (Reddy et al., 1996; Oppenheimer et al., 1997; Reddy and Day, 2001).

Members of the third group, the kinesins with calponin-homology domain (KCH), contain an internally located motor core and an N-terminally positioned calponin-homology (CH) domain. This domain of about 110 amino acids is very unusual for microtubule motor proteins, as it is widely known as actin-binding motif. The conserved CH domain was first identified at the N-terminus of calponin, an actin-binding protein abundantly present in muscle cells (Korenbaum and Rivero, 2002), but is as well found in other actin-binding proteins (Gimona et al., 2002). Typically, two CH domains in tandem are required to mediate actin-binding, such as in α -actinin or spectrin, or even four CH domains in the case of animal and plant fimbrins (Klein et al., 2004). Although one single CH domain is probably not sufficient to confer binding to actin microfilaments it may contribute indirectly to binding or it may be involved in signal transduction (Gimona and Mital, 1998). Members of the KCHs have so far only been identified in flowering plants and one hypothesis suggests, that this group of internal motors could have arisen by domain shuffling of a C-terminal motor (Richardson et al., 2006). Although many members of the kinesin-14 family have been shown to translocate towards the minus-end of microtubules (reviewed by Lee and Liu, 2004; Miki et al., 2005), it is not known whether KCHs show motility at all and, if so, moves towards the minus-end.

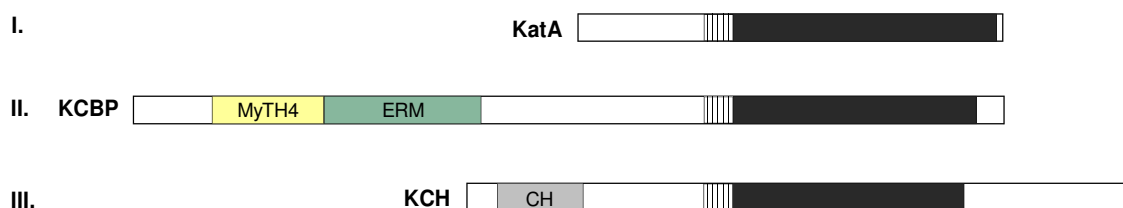


Fig. 6: Domain structure of representative members of the plant kinesin-14 family

The characteristic features of proteins that belong to the three subgroups of the plant kinesin-14 family, as deduced from a domain search using the SMART analysis tool (<http://smart.embl-heidelberg.de>). The C-terminally or centrally located kinesin motor cores are marked in dark gray. The typical minus-end directing neck linkers located upstream of the motor domain are shaded. Members of the KCBP and KCH subfamilies contain additional plant-specific domains. Schematic: Miki et al., 2005; modified.

4 Might KCHs act as dynamic linkers of microtubules and actin filaments?

As already described in detail in sections 1 and 2, many processes during plant cell growth and development require a tight spatiotemporal coordination between the highly dynamic arrays of actin filaments and microtubules. Either a direct or an indirect interaction between microtubules and actin filaments is thus necessary and has been shown by a variety of pharmacological and microscopic studies (reviewed by Collings, 2008). Despite these extensive studies on the microtubule-association of microfilaments, relatively little research has been conducted on the proteins that might mediate them. In animals and fungi numerous proteins have been identified that mediate such interaction, either in a bifunctional way or as complexes from monofunctional proteins (Goode et al., 2000; Rodriguez et al., 2003). In plants, however, the situation has remained unclear – and is even complicated by the fact that many of the linker proteins known from animals and fungi lack homologues in the plant system.

The recently identified kinesins with calponin-homology domain (KCH), however, represent interesting candidates in this context (Preuss et al., 2004). As already introduced in detail in section 3.3, KCH proteins constitute a subset of the kinesin-14 family in plants. With their conserved calponin-homology (CH) domain, a well known actin-binding motif, in combination with their kinesin-specific microtubule motor core, KCHs are the only plant proteins known to contain *de facto* both microtubule-interacting and microfilament-binding sites. In consequence they are strong candidates for a bifunctional mediation between the cytoskeletal elements.

The first KCH member, AtKatD from *Arabidopsis*, was identified in 1999 but not investigated for its microfilament- and microtubule-binding activity (Tamura et al., 1999). First experimental evidence on the involvement of KCHs in microtubule-microfilament interaction accumulated only recently through the investigation of the cotton KCH member GhKCH1 (Preuss et al., 2004). GhKCH1 decorated not only cortical microtubules in developing cotton fibers, as shown by immunofluorescence studies, but as well interacted *in vitro* with actin filaments in binding studies with recombinantly expressed GhKCH1 protein fragments. During the course of this project an additional member of KCH from cotton, GhKCH2, has been identified and similarly showed binding to microtubules and microfilaments *in vitro* (Xu et al., 2009).

The interaction of KCH proteins with both cytoskeletal elements is, however, still far from understood and it remains unclear, whether the observed microtubule- and microfilament-binding represents a general and conserved function of KCHs.

5 The scope of this work

A variety of pharmacological and microscopic studies points towards a direct or an indirect interaction between microtubules and actin filaments during many processes in plant cell growth and development. However, relatively little research has yet been conducted on the proteins that mediate such interplay in plant cells.

To fill this gap, the present work focuses on a recently identified group of candidate proteins, the kinesins with calponin-homology domain (KCHs), that might be involved in microtubule-microfilament interaction. KCHs are putative bifunctional proteins. They contain both a conserved calponin-homology domain, well known as actin-binding motif, and a kinesin-specific microtubule motor core. Members of the KCH family from cotton have already been linked with a putative role in microtubule-microfilament interaction in developing cotton fibers (Preuss et al., 2004; Xu et al., 2009). However, the developing cotton fiber is functionally specialized towards cellulose synthesis and has been widely used to study cortical microtubules that are particularly prominent in this cell type. These microtubule arrays become disoriented upon pharmacological elimination of actin filaments (Seagull, 1990), which is in contrast to other systems such as the *Arabidopsis* root (Collings et al., 2006). Thus, the interaction of microtubules and actin filaments in the cotton fiber system might have evolved as a characteristic feature along with the functional specification of this cell type.

This work therefore asks to what extent the presumed link between microtubules and actin represents a general and conserved function of KCHs. To address this question, a new kinesin should be identified from the monocotyledon plant rice. Its association with both microtubules and microfilaments will be analyzed through a combination of *in vivo* and *in vitro* investigations. Microscopic studies of etiolated rice coleoptiles as a model for cell expansion growth and of tobacco BY-2 cells as a model for cycling cells should answer the question of cell specificity of the putative association. *In vitro* binding assays will provide further molecular details on the protein interactions as well as on the domain-dependency of the association.

Dynamic bifunctional linkers of microtubules and microfilaments are important for the spatiotemporal coordination of both cytoskeletal elements during many cellular and developmental processes. Although KCH proteins represent interesting candidates for such bifunctional linkers, their direct implication in these cellular processes has remained elusive so far. Xu et al. (2009) proposed an involvement of GhKCH2 in cotton fiber elongation, but no further evidence has been provided.

Thus, a second scope of this work is thus to investigate the biological functions of the rice KCH member OsKCH1. For this purpose, a combined loss-of-function and gain-of-function approach will be chosen. *Tos17 kch1* knock-out mutants on the one hand, and a *KCH1* overexpression line generated in tobacco BY-2 cells on the other hand, should be investigated for specific phenotypes. The gene expression pattern of *OsKCH1* will furthermore be followed during plant development. A microscopic investigation of the localization pattern of OsKCH1 during the cell cycle should further help to understand the cellular functions of the protein.

MATERIALS AND METHODS

1 Materials

1.1 Standard reagents

Standard chemicals were purchased from Sigma-Aldrich (Steinheim, Germany) or Roth (Karlsruhe, Germany) unless otherwise stated. Reagents for molecular biology were obtained by New England Biolabs (NEB, Frankfurt, Germany), Qiagen (Hilden, Germany), Invitrogen (Karlsruhe, Germany), Macherey-Nagel (Düren, Germany) and Bio-Rad (München, Germany).

Bi-distilled water was produced in an Ultra Clear UVplus system (SG, Barsbüttel, Germany) and used for all experiments. Deionized water was made with a Seradest SD2800 filter device (ELGA LabWater, Celle, Germany) and used for rice cultivation. Fluid and solid materials and media were pressure sterilized in a type HA300 MIIC autoclave (Wolf Laboratories, York, UK). All materials for RNA extraction were heat sterilized in a drying oven (WTB Binder, Tuttlingen, Germany).

1.2 Organisms

1.2.1 Bacteria

Name	Genotype	Application	Source
<i>E. coli</i> XL1blue	RecA1, endA1, gyrA96, thi-1, hsdR17, supE44, relA1, lac, [F' proAB lacIqZΔM15 Tn10 (Tetr)]	Cloning	Stratagene, La Jolla, USA
<i>E. coli</i> DH5α	F, φ80dlacZΔM15, Δ(lacZYA-argF)U169, recA1, endA1, gyrA96, thi-1, hsdR17, supE44, relA1	Cloning	Invitrogen, Karlsruhe, Germany
<i>E. coli</i> BL21 (DE3)	F, ompT, gal, dcm, lon, hsdS _B (T _B m _B), λ(DE3 [lacI, lacUV5-T7 gene 1, ind1, sam7, nin5])	Protein expression	Invitrogen, Karlsruhe, Germany
<i>A. tumefaciens</i> LBA 4404	pAL4404, pIG121	BY-2 transformation	Invitrogen, Karlsruhe, Germany

Tab. 1: Overview of bacterial strains

1.2.2 Tobacco cell cultures

Name	Genotype	Application	Source
BY-2 Wt	<i>Nicotiana tabacum</i> L. cv. Bright Yellow 2, wild-type	Phenotyping, transient expression	Nagata et al., 1992
BY-2 KCH1	<i>Nicotiana tabacum</i> L. cv. Bright Yellow 2, CaMV-35s (EGFP, KCH1-fl), kan	Phenotyping, transient expression	This work, Klotz, 2008
BY-2 free GFP	<i>Nicotiana tabacum</i> L. cv. Bright Yellow 2, CaMV-35s (EGFP), kan	Phenotyping	K. Schwarzerová (Prague, Czech Republic)

Tab. 2: Overview of tobacco BY-2 cell cultures

1.2.3 Rice material

Name	Genotype	Application	Source
Nipponbare	<i>Oryza sativa</i> ssp. <i>japonica</i> cv. Nipponbare, wildtype	Phenotyping Transient expression	NIAS, Tsukuba, Japan
<i>kch1-1</i> (NF9840)	<i>Oryza sativa</i> ssp. <i>japonica</i> cv. Nipponbare, <i>kch1</i> ⁻ , <i>Tos17</i> insertion line	Phenotyping	Miyao et al., 2003; NIAS, Tsukuba, Japan
<i>kch1-2</i> (NG1558)	<i>Oryza sativa</i> ssp. <i>japonica</i> cv. Nipponbare, <i>kch1</i> ⁻ , <i>Tos17</i> insertion line	Phenotyping	Miyao et al., 2003; NIAS, Tsukuba, Japan

Tab. 3: Overview of rice lines

1.3 Media

Medium	Ingredient	Amount	Remark
Murashige and Skoog (MS) medium	Murashige-Skoog salts (Duchefa, Haarlem, Netherlands)	4.3 g/l	
	Sucrose	30 g/l	
	KH ₂ PO ₄	200 mg/l	
	Inositol	100 mg/l	
	Thiamine	1 mg/l	
	2,4-dichlorophenoxyacetic acid (2,4-D), pH 5.8	0.2 mg/l	
	*Agar-Agar, danish	0.8 % [w/v]	For solidification
	*Kanamycin	50 µg/ml	For selection
	*Cefotaxim	100 µg/ml	For selection
Water agar	Phyto Agar (Duchefa, Haarlem, Netherlands)	0.6 % [w/v]	
Luria broth (LB) medium	Yeast extract	5 g/l	
	Tryptone	10 g/l	
	NaCl	5 g/l	
	*Agar-Agar, Kobe I	1.5 % [w/v]	For solidification
	*Ampicillin / Spectinomycin	100 µg/ml	For selection
	*Zeocin	50 µg/ml	For selection
Super optimal broth (SOC) medium	Yeast extract	5 g/l	
	Tryptone	20 g/l	
	NaCl	10 mM	
	KCl	2.5 mM	
	MgCl ₂	10 mM	
	MgSO ₂	20 mM	
Yeast extract and beef (YEB) medium	Glucose	20 mM	
	Beef extract	5 g/l	
	Yeast extract	1 g/l	
	Pepton	1 g/l	
	Saccharose	5 g/l	
	MgCl ₂	2 mM	
	*Agar-Agar, Kobe I	1.5 % [w/v]	For solidification
	*Rifampicin / Spectinomycin	50 µg/ml	For selection
	*Streptomycin	300 µg/ml	For selection

Tab. 4: Composition of media

* Added optionally, depending on the respective media requirements.

1.4 Primers

All primers were ordered at MWG-Biotech (Ebersberg, Germany) and Sigma-Aldrich (Steinheim, Germany), or kindly provided by colleagues as cited.

1.4.1 Primers for genotyping

Name	Sequence	Application	T _A
LTRN6	ctgtatattggcccatgtccag	Genotyping of <i>Tos17</i> insertion lines, insert specific primer provided by M. Riemann (Karlsruhe, Germany)	60 °C
NF 13 fw	tttgtcagagtgaccgaaagt	Genotyping of <i>kch1-1</i> , upstream primer	60 °C
NF 14 rv	gcactagttccgggcttacgtg	Genotyping of <i>kch1-1</i> , downstream primer	60 °C
NF 15 fw	tacaatgagcaagtgaggatctc	Genotyping of <i>kch1-2</i> , upstream primer	60 °C
NF 16 rv	catctagttccgggcttacgtg	Genotyping of <i>kch1-2</i> , downstream primer	60 °C

Tab. 5: Overview of primers for genotyping

1.4.2 Primers for gene expression analysis

Name	Sequence	Application	T _A
Rubq 237 fw	gagcctctgttcgtaagta	qPCR detection of Ubiquitin, bp 237 fw (Riemann et al., 2008)	60 °C
Rubq 204 rv	actcgatggccattaaacc	qPCR detection of Ubiquitin, bp 304 rv (Riemann et al., 2008)	60 °C
NF 17 fw	cacgcagaagttacggttgt	qPCR detection of OsKCH1, bp 3287 fw	60 °C
NF 18 rv	ctttgttgaatggacatgg	qPCR detection of OsKCH1, bp 3360 rv	60 °C
NF 19 fw	acatagctcacgcagaa	qPCR detection of OsKCH1, bp 3277 fw	60 °C
NF 20 rv	taacatgatgaagcgtacaaac	qPCR detection of OsKCH1, bp 3389 rv	60 °C
NF 41 fw	attacagcaacgaagattcca	qPCR detection of OsKCH1, bp 2911 fw	60 °C
NF 42 rv	tctcaccttgcatagtgg	qPCR detection of OsKCH1, bp 3101 rv	60 °C
NF 73 fw	cacgtaagcccgaactagatgct	qPCR detection of KCH, degenerated primer fw	46 °C
NF 74 rv	gccttgagggtagcaatctgt	qPCR detection of KCH, degenerated primer rv	46 °C

Tab. 6: Overview of primers for quantification of gene expression levels

1.4.3 Cloning primers

Name	Sequence	Application	T _A
NF 43 fw	gggacaagttgtacaaaaagcaggtcg-atgaatatcacggaacaggtcaacctg	Gateway ENTR cloning, OsKCH1-mt, bp 831 fw	69 °C
NF 44 rv	gggacactttgtacaagaaagctggtag-gcattgtccggacctctaagt	Gateway ENTR cloning, OsKCH1-mt, bp 2330 rv	69 °C
NF 45 fw	ggggacaagttgtacaaaaagcag-gctcgtatggcccgcgctcgagga	Gateway ENTR cloning, OsKCH1-ch, bp 1 fw	69 °C
NF 46 rv	ggggaccactttgtacaagaaagctgg-gtacaaaacttcggtccactcatggtaa	Gateway ENTR cloning, OsKCH1-ch, bp 1419 rv	69 °C
NF 70 fw	ggggacaagttgtacaaaaagcag-gctcgtatggcccgcgctcgagga	Gateway ENTR cloning, OsKCH1-fl, bp 1 fw	69 °C
NF 71 rv	gggacactttgtacaagaaagctggtag-gcattgtccggacctctaagt	Gateway ENTR cloning, OsKCH1-fl, bp 2330 rv	69 °C
NF 57 fw	cgggatccgatgatggcccgcgctg	pET 21b cloning, KCH1-ch, sh, cc1, cc2, cc3 and fl, bp 1 fw	65 °C
NF 66 rv	ttagggccgcccactcaacaatcaatggg	pET 21b cloning, KCH1-sh, bp 750 rv	65 °C
NF 67 rv	ttagggccgcaactcaccatcaccatttac	pET 21b cloning, KCH1-cc1, bp 882 rv	65 °C
NF 68 rv	ttagggccgctccaggtaggaaagcct	pET 21b cloning, KCH1-cc2, bp 902 rv	65 °C
NF 69 rv	ttagggccgagggcttgactgtgtgctt	pET 21b cloning, KCH1-cc3, bp 2232 rv	65 °C
NF 55 fw	cgggatccgaatatcacggaacaggtcaa	pET 21b cloning, KCH1-mt, bp 831 fw	65 °C
NF 56 rv	ttagggccgcccattgtccggacct	pET 21b cloning, KCH1-mt and fl, bp 2330 rv	65 °C

Tab. 7: Overview of primers for cloning

1.4.4 Sequencing primers

Name	Sequence	Application	T _A
T7	taatacgaactactataggg	Standard sequencing primer, (GATC, Konstanz, Germany)	55° C
M13 FP	tgtaaacgacggccagt	Standard sequencing primer, (GATC, Konstanz, Germany)	55° C
pEGFP-FP	gatcacatggtcctgctg	Standard sequencing primer, (GATC, Konstanz, Germany)	55° C
Nos-r	gataatcatcgcaagaccggcaacagg	pMAV sequencing primer provided by K. Wanieck (Karlsruhe, Germany)	69 °C
35S-FP	cgcacaatcccactatccttcgcaa	pMAV sequencing primer provided by K. Wanieck (Karlsruhe, Germany)	66 °C

Tab. 8: Overview of primers for sequencing

1.5 Plasmids

All plasmids were either generated in the course of this work as described in 2.3.4, purchased, or kindly provided by colleagues as cited.

1.5.1 Cloning plasmids

Name	Annotations	Application	Source
pDONR/ZEO	Zeo ^R , pEM7, M13, T7, att1_Kan ^R ccdB_att2, SP6, T7	ENTR vector for Gateway-cloning	Invitrogen, Karlsruhe, Germany
p2YGW7	Amp ^R , p35S, EYFP, att1_ccdB_att2, SP6, T7	Destination vector for Gateway cloning	Karimi et al., 2005
pK7WGF2.0	RB-p35S EYFP, att1_ccdB_att2, Kan ^R -LB, Sm/Sp ^R	Binary destination vector for Gateway cloning	Karimi et al., 2002
pH7WGF2.0	RB-p35S EYFP, att1_ccdB_att2, Hyg ^R -LB, Sm/Sp ^R	Binary destination vector for Gateway cloning	Karimi et al., 2002
pMAV GW YC(YN)	Amp ^R , pMB1, p35S, att1_ccdB_att2, YC(YN), tNOS	Destination vector for Gateway cloning	Stolpe et al., 2005
pMAV YC(YN) GW	Amp ^R , pMB1, p35S, YC(YN), att1_ccdB_att2, tNOS	Destination vector for Gateway cloning	Stolpe et al., 2005
pET21b	Amp ^R , lacI, T7, MCS-6xHis, fl, ori	<i>E. coli</i> T7 protein expression vector	Novagen, San Diego, USA

Tab. 9: Overview of cloning plasmids

1.5.2 Constructs for recombinant protein expression

Name	Annotations	Application	Source
KCH1-sh	Residues 1-250 of OsKCH1 in pET21b	Recombinant expression of His-tagged KCH1-sh	This work
KCH1-cc1	Residues 1-294 of OsKCH1 in pET21b	Recombinant expression of His-tagged KCH1-cc1	This work
KCH1-cc2	Residues 1-373 of OsKCH1 in pET21b	Recombinant expression of His-tagged KCH1-cc2	This work
KCH1-ch	Residues 1-473 of OsKCH1 in pET21b	Recombinant expression of His-tagged KCH1-ch	This work
KCH1-mot	Residues 300-800 of OsKCH1 in pET21b	Recombinant expression of His-tagged KCH1-mot	This work
KCH1-cc3	Residues 1-744 of OsKCH1 in pET21b	Recombinant expression of His-tagged KCH1-cc3	This work
KCH1-fl	Residues 1-800 of OsKCH1 in pET21b	Recombinant expression of His-tagged KCH1-fl	This work

Tab. 10: Overview of constructs for recombinant protein expression

1.5.3 Constructs for plant transformation

Name	Annotations	Application	Source
OsKCH1-mot YFP	Residues 300-800 of OsKCH1 in p2YGW7	Transient transformation of rice and BY-2	This work
OsKCH1-ch YFP	Residues 1-473 of OsKCH1 in p2YGW7	Transient transformation of rice and BY-2	This work
OsKCH1-fl YFP	Residues 1-800 of OsKCH1 in p2YGW7	Transient transformation of rice and BY-2	This work; Klotz, 2008
OsKCH1-fl GFP	Residues 1-800 of OsKCH1 in p2K7WGF2.0	Transient and stable transformation of BY-2	This work; Klotz, 2008
OsKCH1-fl GFP	Residues 1-800 of OsKCH1 in p2H7WGF2.0	Transient transformation of BY-2, stable transformation of rice	This work
OsKCH1-fl YC(YN)	Residues 1-800 of OsKCH1 in pMAV YC(YN)	BiFC in rice and BY-2	This work, Klotz, 2008
YC(YN) OsKCH1-fl	Residues 1-800 of OsKCH1 in YC(YN) pMAV	BiFC in rice and BY-2	This work, Klotz, 2008
OsKCH1-ch YC(YN)	Residues 1-473 of OsKCH1 in pMAV YC(YN)	BiFC in rice and BY-2	This work, Klotz, 2008
FABD2 RFP	FABD2 (residues 325-687 of AtFim1) in p2RGW7	Transient transformation of rice and BY-2	Maisch et al., 2009
MAP4-MBD DsRED	Microtubule-binding domain of MAP4 in 35S-DsRed2-C1	Transient transformation of rice and BY-2	Marc et al., 1998
CPRF2 CFP	Transcription factor CPRF2 in pMAV4 CFP	Transient transformation of rice and BY-2	Kircher et al., 1999

Tab. 11: Overview of constructs for transient and stable transformation of rice and tobacco BY-2

1.6 Antibodies

All antibodies were purchased from Sigma-Aldrich (Steinheim, Germany).

Name	Description	Application	Dilution
Anti-penta His	Mouse monoclonal antibody targeting penta His-tagged proteins	Primary antibody for Western blotting	1:2000 in TBS
ATT	Mouse monoclonal antibody targeting tyrosinated α -tubulin	Primary antibody for Western blotting	1:300 in TBS
DM1A	Mouse monoclonal antibody targeting α -tubulin	Primary antibody for immunofluorescence	1:300 in TBS
Anti-mouse IgG, TRITC-conjugated	Goat FITC-coupled, polyclonal antibody targeting mouse IgG	Secondary antibody for immunofluorescence	1:300 in PBS
Anti-mouse IgG, alkaline phosphatase-conjugated	Goat alkaline phosphatase-coupled, polyclonal antibody targeting mouse IgG	Secondary antibody for Western blotting	1:7000 in milk buffer

Tab. 12: Overview of antibodies

2 Methods

2.1 *In silico* analysis

2.1.1 Phylogenetic analysis of KCHs

Putative candidate proteins belonging to the KCH subgroup of Kin-14 were identified on protein level in Swiss-Prot/TrEMBL (<http://www.expasy.org/sprot>) via BLAST search using AtKatD (O86135; Tamura et al., 1999) as bait.

For general phylogenetic analysis, KCH sequences were aligned together with members of the Kin-1 family and additional kinesins belonging to other subgroups of Kin-14 using the ClustalW2 tool at EBI (<http://www.ebi.ac.uk/Tools/clustalw2/index.html>). A detailed phylogenetic analysis of the KCH family was performed using candidate proteins from *Arabidopsis thaliana*, *Gossypium hirsutum*, *Oryza sativa*, *Physcomitrella patens*, *Populus trichocarpa*, *Ricinus communis* and *Vitis vinifera*, aligned in ClustalW2. The alignments were transferred to PhyML Online, a maximum-likelihood based algorithm for phylogenetic analysis (<http://atgc.lirmm.fr/phym1>; Guindon et al., 2005), and phylogenetic trees were generated by heuristic search methods with random stepwise addition of sequences. Bootstrap support values were obtained from 100 replicates. The resulting tree files were visualized in iTOL (<http://itol.embl.de>; Letunic and Bork, 2007) and rooted arbitrarily using either the orphan kinesin ScSMY-1 (Lillie and Brown, 1992) or AtKatA (Marcus et al., 2002) as outgroup.

The Swiss-Prot/TrEMBL accession numbers of all proteins used for phylogenetic analysis were the following: OsKCH1 (Q0IMS9), Q10MN5, Q2QP07, A2WT45, A3CDK9, GhKCH1 (Q5M-NW6), GhKCH2 (A4GU96), Q5JKW1, B9FFM0, B9FL70, A5BH78, A7Q9E6, A5APK4, Q9F-HD2, Q9SS42, A9SJ46, A9SDI6, A9SPL2, B9I798, B9GH20, B9GSE0, B9I2M3, B9GWJ1, B9T1P9, B9T5B8, B9RCC3, B9RFF9, B9SAW6, A5C0F0, A5BG13, AtKatD (O81635), A9S-J46, AtKP1 (Q8W1Y3), Q9FHD2, Q9SS42, A5APK4, B9H9K3, B9T5B8, A9SDI6, A9SJ46, B9N5N8, B9T1P9, B9RFF9, B9I798, B9N4N1, O80491, A2XFQ6, A3AH36, Q84W97, O22260, B9SAW6, B9GSE0, B9I9N7, A7Q0H7, A5C0F0, DmNCD (P20480), A1E130, ScK-ar3 (P17119), EnKlpA (P28739), XlCtk2A (Q5XGK6), RnKIFC1 (Q5XI63), AtKatA (Q07970), AtKatC (S48020), Q7Y1U0, AtZWICHEL (O23102), Q84VE4, HsKinH (P33176), XlKinH (A5XAW2), DmKinH (Q9V7L9), ScSMY-1 (P32364).

2.1.2 Sequence analysis of OsKCH1

SMART-assisted domain analysis

For secondary structure analysis of OsKCH1 a motif and domain prediction was carried out in SMART (<http://smart.embl-heidelberg.de>).

Sequence alignments and comparisons

Sequence alignments of DNA or protein sequences were generally performed using the application AlignX in Vector NTI (Invitrogen, Karlsruhe, Germany). Protein sequences were further analyzed by diagonal dot-matrix plots at a window size of 5 and a stringency of 50 %, as well using AlignX.

COILS-assisted analysis of putative oligomerization sites

A prediction of putative coiled-coils in the OsKCH1 protein sequence was performed in COILS (http://www.ch.embnet.org/software/COILS_form.html) according to the Lupas algorithm (Lupas et al., 1991) using MTIDK as matrix background. To minimize false positives, the analysis was performed at window width of 14, 21, and 28 aa, respectively, and with both a weighted and an unweighted matrix. The results were compared and only sequence stretches that did not differ by more than 20 percent in all analysis were taken into account.

2.1.3 Database search for cDNA clones and knock-out mutants

The genomic sequence of OsKCH1 (accession number Os12g36100) was screened for available cDNA clones and knock-out mutants in RiceGE (<http://signal.salk.edu/cgi-bin/RiceGE>).

A RIKEN cDNA clone (clone name: J013034O12, accession number: AK065586), covering the first 811 aa of the protein, was identified and ordered from the Rice Genome Resource Centre (<http://www.rgrc.dna.affrc.go.jp>). Additionally, two rice *Tos17*-insertion lines *kch1-1* (NF9840) and *kch1-2* (NG1558), generated by the National Institute of Agrobiological Sciences (Tsukuba, Japan), were found in the database and ordered.

2.2 Cultivation techniques

2.2.1 Cultivation of bacteria

Cultures of *E. coli* and *A. tumefaciens* were grown according to standard methods (Sambrook and Russell, 2001) from stock cultures on LB plates containing the appropriate antibiotics at 37 °C over night (*E. coli*) and at 28 °C for 2 to 3 days (*A. tumefaciens*). Liquid cultures were inoculated from single colonies and incubated similarly under constant shaking at 180 rpm. For storage purposes, freshly grown bacterial suspensions were supplemented with 15 % [v/v]

sterile glycerol, frozen in liquid nitrogen and stored at $-70\text{ }^{\circ}\text{C}$. For protein expression in *E. coli*, cultivation temperatures were reduced to $14\text{ }^{\circ}\text{C}$ when the cultures reached an OD_{600} of 0.6.

2.2.2 Cultivation of rice plants

Rice seeds were generally incubated at $43\text{ }^{\circ}\text{C}$ for 4 weeks to break dormancy. Seed husks were removed prior to cultivation.

Rice seedlings for particle bombardment were raised according to Gutjahr et al. (2005). Seeds were fixed with medical adhesive B401 (Factor II, Lakeside, USA) 5 mm below the edge of a microscopy slide and were placed in conventional staining trays in plexiglas boxes (95 x 95 x 60 mm) with the embryo pointing upwards. Plexiglas boxes were filled with deionized water such that the seeds were only partially covered to ensure optimal germination in aerobic conditions. Seedlings were raised at $28\text{ }^{\circ}\text{C}$ in photobiological darkness using black boxes, black cloth and isolated dark chambers for 4-5 days.

Seedlings for coleoptile and root length measurements were grown in agripots (Kirin Brewery Ltd., Tokyo, Japan) on 0.6 % [w/v] water agar under sterile conditions. For sterilizations, 50 - 100 seeds were gently shaken in 5 ml of 70 % [v/v] ethanol in a 50 ml Falcon tube (Eppendorf, Hamburg, Germany) and washed in deionized water. Subsequently they were incubated in NaClO for 20 min on a table top shaker at 95 rpm and again washed 4-5 times with deionized water. 25 seeds per agripot were placed equidistantly in the agar and were raised for 7 days at $28\text{ }^{\circ}\text{C}$ in photobiological darkness as described above. Usually seed germination was higher than 95 % and seedling length among the population varied by less than 5 %.

For seed propagation and phenotyping rice plants were grown from 7 day old seedlings raised in agripots as described above. Seedlings were planted in flower pots into soil supplemented with 4 g/l Osmocote fertilizer pearls (Scotts Celaflor, Salzburg, Austria) and were further cultivated in growth chambers under controlled long day conditions. The photoperiod was set to 16 h day period at $28\text{ }^{\circ}\text{C}$ and 8 h night period at $20\text{ }^{\circ}\text{C}$. The relative humidity was constantly kept at 70 %.

2.2.3 Maintenance of tobacco BY-2 cell cultures

The tobacco cell lines WT BY-2, KCH1 BY-2 and GFP BY-2 were cultivated in liquid MS medium as described by Nagata et al. (1992). The cells were subcultured weekly by inoculation of 1-2 ml of stationary cells into 30 ml of fresh medium supplemented with adequate antibiotics in 100 ml Erlenmeyer flasks. The cell suspensions were incubated at $25\text{ }^{\circ}\text{C}$ in the dark on an orbital shaker (KS250 basic, IKA Labortechnik, Staufen, Germany) at 150 rpm. Stock BY-2 calli were maintained on solid MS medium and were subcultured monthly. Cells for phenotyping experiments were temporarily maintained in the absence of selective pressure for establishment of comparable growth conditions.

2.3 Molecular biological methods

2.3.1 General methods

Agarose gel electrophoresis

Separation and identification of nucleic acids according to their size was performed on 0.8 - 2 % [w/v] agarose in TAE buffer (50x stock: 2 M Tris-HCl, 0.57 % [v/v] acetic acid, 50 mM EDTA; pH 7.5). For detection, 0.5x SYBR Safe (Invitrogen, Karlsruhe, Germany) was added to the liquid agarose. Samples and size markers were mixed with an appropriate volume of 5x loading dye (50 % [v/v] glycerin, 0.05 % [w/v] bromphenol blue, 0.05 % [w/v] xylencyanol) before loading. Gels were run with 75-100 V and bands were visualized on a Safe Imager blue light transilluminator (Invitrogen, Karlsruhe, Germany) and documented using a Rainbow Camera system (Hama, Monheim, Germany).

Determination of nucleic acid concentration

Concentrations of nucleic acids in solution were determined photometrically on a NanoDrop 2000 (ThermoScientific, Wilmington, USA) against the respective H₂O or buffer blank values at a wavelength of 260 nm according to the manufacturers instructions.

Standard polymerase chain reactions

Polymerase chain reactions (PCR) were basically performed according to one of the following two protocols. Tab. 13 gives the typical reaction set-up for analytical PCR purposes, while Tab. 14 shows the standard composition of PCRs for preparative applications.

Component	Amount
Template (cDNA, gDNA, plasmids; 2-500 ng/μl)	1 μl
10x ThermoPol buffer (NEB, Frankfurt, Germany)	2.5 μl
5 mM each dNTP Mix (NEB, Frankfurt, Germany)	1 μl
20 μM primer forward	0.5 μl
20 μM primer reverse	0.5 μl
*100 % [v/v] DMSO	1 μl
*5 M betaine	2.5 μl
5 U/μl Taq Polymerase (NEB, Frankfurt, Germany)	0.1 μl
dd H ₂ O	15.9 μl

Tab. 13: Standard set-up for analytical PCRs (25μl)

* Added optionally depending on the respective PCR requirements.

Component	Amount
Template (cDNA, gDNA, plasmids; 2-500 ng/ μ l)	1 μ l
5x HF Phusion buffer (NEB, Frankfurt, Germany)	10 μ l
5 mM each dNTP Mix (NEB, Frankfurt, Germany)	2 μ l
20 μ M primer forward	1 μ l
20 μ M primer reverse	1 μ l
2 U/ μ l Phusion Polymerase (NEB, Frankfurt, Germany)	0.1 μ l
dd H ₂ O	34.9 μ l

Tab. 14: Standard set-up for preparative PCRs (50 μ l)

PCRs were run in a Primus 96 Advanced or Cyclone 25 thermocycler (PeQlab, Erlangen, Germany). The denaturation, annealing and elongation times and temperatures varied depending on each application and were chosen according to guidelines for each polymerase given by the manufacturers. Optimal annealing temperatures (T_A) for the different primer sets are listed in Tab. 5-8. In case of primers for Gateway-cloning the first 5 PCR cycles were run with a $T_1 = T_A - 6$ °C, the second 5 cycles with a $T_1 = T_A - 3$ °C. For the remaining cycles the listed T_A was used. This inverse touch-down approach was chosen in order to increase PCR efficiency, taking into account the long *att* sequences in the primers. These *att* sequences are required for subsequent Gateway recombination of the PCR products but do not have reverse complementary target sequences within the first cycles of PCR, resulting in a decreased effective primer annealing temperature during this period. PCR programs were generally carried out with 25 to 40 cycles of repetition.

DNA digestion with restriction endonucleases

All restriction enzymes were obtained from NEB (Frankfurt, Germany) and used with the adequate buffers according to the conditions recommended by the manufacturer. Typically, 1 - 5 U enzyme were applied for digestion of 200 ng to 1 μ g of DNA. Samples were incubated for 1 h to over night, analyzed on agarose gels, and, if required, further purified and used for cloning procedures.

DNA ligation

T4 DNA Ligase for standard ligation reactions was purchased from NEB (Frankfurt, Germany) and applied according to the manufacturers instructions. Ligation reactions were typically performed over night at 16 °C in a reaction volume of 15 μ l, using 100 ng vector and a 10-fold molar excess of insert.

Transformation of *E. coli*

Chemically competent *E. coli* cells (XL1blue, DH5 α , BL21) were generated according to a published protocol (Sambrook and Russell, 2001). 250 ml SOC medium were inoculated with 3 ml of an *E. coli* overnight culture and grown to an OD₆₀₀ of 0.6 at 37 °C under constant shaking. Subsequently, the culture was incubated on ice for 10 min, the cells were harvested by centrifugation (5000 rpm, 10 min, 4 °C) in a Hermle Universal centrifuge (Hermle, Wehningen, Germany) and resuspended in ice-cold TB solution (10 mM PIPES-KOH, 55 mM MnCl₂, 15 mM CaCl₂, 250 mM KCl, pH 6.7). Following another centrifugation step, the cells were resuspended in 20 ml TB and supplemented with 7 % [v/v] DMSO. The cells were frozen in small aliquots in liquid nitrogen and stored at -70 °C until transformation.

Competent *E. coli* cells were generally transformed by heat-shock. 25-50 μ l of cells were slowly thawed and incubated on ice with 0.5 μ l vector or 2-7 μ l ligation reaction for 30 min. For heat-shock, the mixture was placed at 42 °C for 30 s, followed by incubation on ice for 2 min and addition of 1 ml SOC medium. The cells were incubated at 37 °C for 1 h under constant shaking and finally plated on LB agar plates containing the required antibiotics for selection.

2.3.2 Purification of nucleic acids

Isolation of genomic DNA from plant material

For purification of genomic DNA, leaf material of 4 to 8 week old rice plants was harvested, frozen in liquid nitrogen, grounded up in a TissueLyser (Qiagen, Hilden, Germany) and stored at -70 °C until preparation. Genomic DNA was isolated out of samples of 100-200 mg pulverized plant material following a chloroform-isopropanol extraction protocol as described by Sambrook and Russell (2001).

700 μ l of DNA isolation buffer (200 mM Tris-HCl pH 7.5, 250 mM NaCl, 25 mM EDTA pH 8.0, 0.5 % [w/v] SDS), freshly supplemented with 50 μ g/ml Proteinase K, was added to the frozen material and the samples were vortexed vigorously prior incubation at 65 °C in a water bath for 2 h. Subsequently, 700 μ l of chloroform were added and the suspensions were shaken for 20 min at maximum speed on a Thermomixer (Eppendorf, Hamburg, Germany). Aqueous and organic phase were separated by centrifugation at 16500 g for 10 min. The upper, aqueous layer was transferred to a fresh tube and mixed with 500 μ l isopropanol to precipitate DNA. Samples were centrifuged at 10000 g for 5 min and the DNA pellets were washed with 500 μ l of 70 % [v/v] ethanol.

After drying in a Speedvac (Eppendorf 5301 Concentrator; Eppendorf, Hamburg, Germany), the pellets were dissolved by shaking at 1200 rpm for 30 min in 50 μ l TE (1 mM Tris-HCl, 1 mM EDTA, pH 8.0) supplemented with 5 μ g Rnase H (Qiagen, Hilden, Germany). Genomic DNA was generally stored at 4 °C.

Isolation of total RNA from plant material

For isolation of total RNA, rice tissue or BY-2 cell culture material was frozen in liquid nitrogen, grounded up in a TissueLyser (Qiagen, Hilden, Germany) and stored at -70 °C until further preparation. Total RNA was purified from samples of 100 mg of pulverized plant material using an RNeasy Plant Mini Kit (Qiagen, Hilden, Germany) including on-column digest of genomic DNA with RNase-free DNase I (Qiagen, Hilden, Germany) according to the manufacturers instructions. All RNA preparations were checked for purity and integrity on 1 % [w/v] agarose gels and stored at -20 °C until Reverse Transcription.

Preparation of plasmids from *E. coli*

Plasmid DNA mini-preparations from 3 ml of *E. coli* overnight cultures were performed with a NucleoSpin Plasmid Kit (Macherey-Nagel, Düren, Germany) following the recommended protocol.

For midi-preparations of plasmid DNA from 200-400 ml of *E. coli* overnight cultures, a Nucleo-Bond Plasmid Midi Kit (Macherey-Nagel, Düren, Germany) was used according to the manufacturers instructions.

All preparations were assessed for sample purity and nucleic acid concentrations by photometric measurement.

Purification of plasmids and PCR products from agarose gels

The desired DNA fragments or PCR products were cut out off agarose gels under blue light illumination and purified using a NucleoSpin Extract II Kit (Macherey-Nagel, Düren, Germany) according to the enclosed protocol.

2.3.3 Molecular analytics

DNA sequencing

Sequencing of plasmid DNA and PCR products was performed by GATC (Konstanz, Germany) according to published methods (Sanger et al., 1977) using an ABI 3730XL automated sequencer (Applied Biosystems, Darmstadt, Germany). The obtained data was analyzed and aligned with the target sequences using the AlignX tool of VectorNTI (Invitrogen, Karlsruhe, Germany).

Genotyping of rice mutants

Rice *Tos17* insertion mutants were generally screened for their genotypes using a PCR-based method with two independent PCR reactions. One reaction was targeting the insert at the specific site of integration and a second reaction was aiming at the gene sequence surrounding the putative site of integration as described by Winkler and Feldmann (1998).

Chromosomal DNA of plants and seedlings was isolated as described above and used as template for the two PCR set-ups, one containing a *Tos17* border-specific primer in combination with a sequence-specific primer and a second containing two sequence-specific primers, targeting a sequence stretch that spans over the site of *Tos17* insertion. The different primer pairs for genotyping of plants of the mutant lines *kch1-1* (NF9840) and *kch1-2* (NG1558) are listed in Tab. 5, together with the sequence of a primer targeting the left border of the retrotransposon *Tos17*. The reactions were run according to the described standard protocol for analytical PCRs and the products were separated on 1 % [w/v] agarose gels.

Quantification of gene expression levels

Gene expression levels in rice tissues and tobacco BY-2 cell cultures were quantified via real-time PCR or semiquantitative RT-PCR in two-step protocols. All primers used for real-time PCR analysis and semiquantitative RT-PCR are listed in Tab. 6.

In a first step cDNA was synthesized from 1 µg of total RNA extracts by reverse transcription with MuLV Reverse Transcriptase (NEB, Frankfurt, Germany) or using a Dynamo cDNA Synthesis Kit (Finnzymes, Espoo, Finland) as described by the manufacturer. In order to check for completeness of genomic DNA digestion, control reactions without addition of Reverse Transcriptase were run for each RNA sample and were analyzed in parallel in the subsequent quantitative PCRs.

Quantitative real-time PCR analysis of cDNA samples was performed using an iQ SYBR Green Supermix (Bio-Rad, München, Germany) according to the manufacturers instructions. The PCR was run in a DNA Engine Opticon 2 cycler (Bio-Rad, München, Germany) with the following cycler conditions: 3 min, 95 °C, 40× (10 s, 95 °C; 1 min, 60 °C). OsKCH1 cDNA from rice was amplified with the primer set NF 41 and NF 42. Ubiquitin was used as endogenous control gene for normalization and was detected with the primers Rubg237F and Rubg304R (Riemann et al., 2008). Samples were run as triplicates and relative gene expression values were calculated by the $\Delta\Delta C_t$ -method using the softwares MJ Opticon Monitor 3.1 (Bio-Rad, München, Germany) and Microsoft Office Excel 2003 (Microsoft, Redmont, USA) for quantification.

For semiquantitative RT-PCR, following reverse transcription, a PCR was set up with standard Taq polymerase (NEB, Frankfurt, Germany) as described in Tab. 13. The cDNA was detected using the following PCR conditions: 2 min, 94 °C, 32× (30 s, 94 °C; 1 min, 60 °C; 30 s 72 °C), 5 min, 72 °C. The cycle numbers for PCR were chosen such that the amplifications of templates for all primers were still in an exponential range and the products were clearly visible on agarose gels, making a subsequent quantification possible and reproducible. OsKCH1 cDNA from rice was amplified with the primers NF 41 and NF 42. For detection of KCH cDNA levels in tobacco BY-2 a set of degenerated primers (NF 73, NF 74) was designed. For this purpose an alignment of KCH sequences from rice, *Arabidopsis*, cotton, *Vitis* and *Populus* was used as template and the primers were set to highly conserved sequence parts outside the CH and the motor domain. The degenerated primers were tested on rice, tobacco and tobacco BY-2 cDNA for their functionality, and products were verified by sequencing prior application of the primers in semi-

quantitative RT-PCR (see Fig. 34 in appendix for sequence information). Ubiquitin was used as endogenous control gene and was detected with the primers Rubg237F and Rubg304R (Riemann et al., 2008) in both rice and tobacco BY-2. The PCR products were separated by 2 % [w/v] Agarose gels, stained with SYBR Safe (Invitrogen, Karlsruhe, Germany) and images were taken. Bands were quantified by gray value analysis in ImageJ (NIH, Bethesda, USA) and the ratios between sample RNA and Ubiquitin calculated to normalize for initial variations in sample concentration, and as a control for reaction efficiency. Mean values and SE were calculated from at least three independent experiments.

2.3.4 Cloning and manipulation of plasmids

All cloning procedures involving any OsKCH1 sequence parts were based on a RIKEN cDNA clone of OsKCH1. The cDNA clone (name: J013034O12) was obtained from the Rice Genome Resource Centre (<http://www.rgrc.dna.affrc.go.jp>) and can be found under the following accession number: AK065586. The clone covers the first 2331 bp of the sequence which correspond to the amino acids 1-811 of the protein. Fig. 7 illustrates exemplarily the vector maps of two constructs for fluorescent protein fusion and recombinant protein expression.

Generation of fluorescent protein fusion constructs

Plasmids for stable and transient plant transformation were constructed via Gateway-based cloning. The sequences corresponding to three different length variants of OsKCH1 (fl: residue 1-800, mot: residue 300-500, ch: residue 1-473) were amplified by PCR using the respective primers listed in Tab. 7, all containing specific Gateway *att* recombination sites.

The PCR products were purified and recombined into the Gateway entry plasmid pDONR/Zeo (Invitrogen, Karlsruhe, Germany) via standard BP reactions as follows: 50 fmol of both PCR product and entry plasmid were mixed and incubated with 4 μ l BP Clonase Enzyme Mix (Invitrogen, Karlsruhe, Germany) in a total reaction volume of 12 μ l for 2-3 h at 25 °C. To arrest recombination, 1 μ l Proteinase K was added and the mixture incubated for 10 min at 37 °C prior transformation in chemically competent DH5 α cells. Plasmid DNA of transformants was analyzed by analytical restriction digests and sequencing.

Successfully recombined entry plasmids were applied as donor molecules into subsequent LR reactions together with the respective destination vectors for transient or stable plant transformation and BIFC-assays (Tab. 9). The LR reactions were set-up according to the manufacturers instructions with molar equivalents of donor and destination vector in a total reaction volume of 10 μ l, containing 2 μ l of LR Clonase Enzyme Mix (Invitrogen, Karlsruhe, Germany). The mixture was incubated overnight at 25 °C. Then the recombination was arrested through addition of 1 μ l Proteinase K and incubation at 37 °C for 10 min. The reaction mixture was transformed into chemically competent DH5 α cells and the plasmid DNA of transformants was analyzed by analytical restriction digests and sequencing for successful recombination. Tab. 11 gives an overview of all fluorescent protein fusion constructs generated in the course of this work.

Generation of constructs for recombinant protein expression

Plasmids for recombinant protein expression were generated using a conventional cloning approach. The sequences corresponding to four different length variants of OsKCH1 (cc3: residue 1-769, mot: residue 300-500, cc2: residue 1-398, cc1: residue 1-319, sh: residues 1-250) were amplified by PCR from the cDNA clone using the respective primers listed in Tab. 7. All primers were designed such that they contain specific recognition sites for restriction enzymes upstream of the target sequences; *Bam*HI sites in case of all forward primers and *Not*I sites for reverse primers. The PCR products were purified and were subsequently cloned into the pET21b expression vector (Novagene, San Diego, USA) via the *Bam*HI and *Not*I sites. For this purpose, the PCR products as well as the target vector were restriction digested with both enzymes, purified and sticky-end ligated as described in section 2.3.1. The ligation mixture was transformed into chemically competent BL21 cells and the plasmid DNA of transformants was analyzed by analytical restriction digests and subsequent sequencing. An overview of all constructs for recombinant protein expression generated in the course of this work is given in Tab. 10.

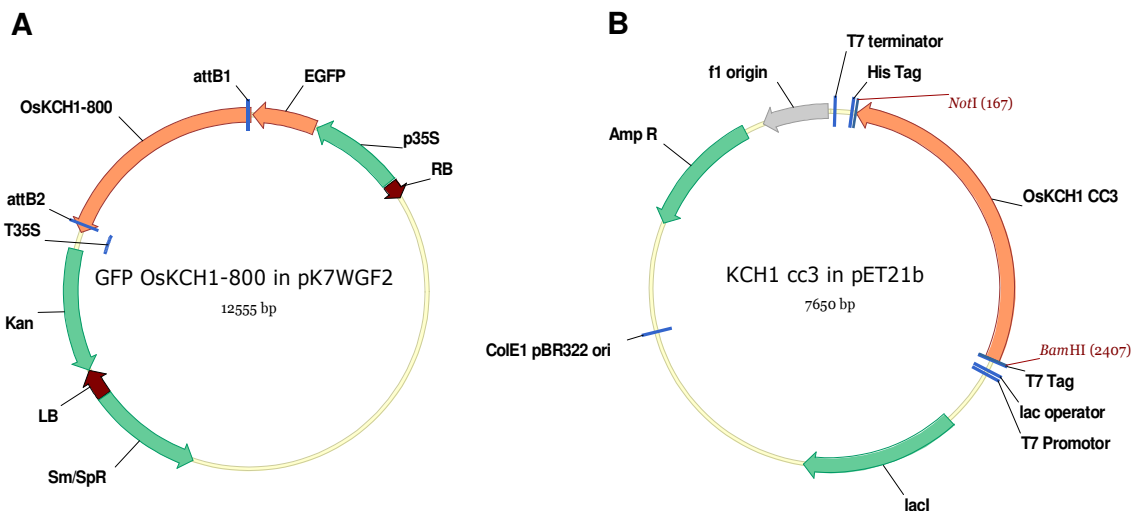


Fig. 7: Constructs for fluorescent protein fusions and recombinant protein expression

[A] Representative diagram of a fluorescent protein fusion construct. The vector map shows the fusion of GFP with residues 1-800 of OsKCH1 (orange arrows) in the binary Gateway plasmid pK7WGF2 under control of the 35S-CaMV promoter (p35S/T). Other abbreviations: *attB1/2* – recombinations sites for Gateway cloning; LB/RB – left and right boarder for *Agrobacterium*-mediated transformation. Kanamycin (*Kan*) and Spectinomycin (*Sm/SpR*) represent markers for antibiotic selection. [B] Representative diagram showing a construct for recombinant protein expression. Residues 1-769 of OsKCH1 were cloned via the *Bam*HI and *Not*I restriction sites as C-terminal 6x His-Tag into the pET21b expression plasmid. Expression is controlled via the T7 promoter system and under control of the lac operon. Ampicillin (*Amp*) is used as selection marker.

2.4 Cell biological methods

2.4.1 Plant transformations

Biolistic, transient transformation of tobacco BY-2 cells and rice seedlings

For biolistic transformation, 60 mg of gold particles (1.5-3.0 μm) were suspended in 50 % [v/v] sterile glycerol by mixing on a platform vortexer (Bender & Hobein, Zurich, Switzerland). For each transformation, 12.5 μl (0.75 mg) of the gold suspension were transferred to a 1.5 ml microcentrifuge tube and were coated with 1 μg of the respective target DNA vector construct under continuous vortexing and successive addition of DNA, 12.5 μl of 2.5 M sterile CaCl_2 , and 5 μl of 0.1 M sterile spermidine. Following additional mixing for 3 minutes, the DNA-coated gold particles were spun down briefly. The supernatant was discarded and the gold particles were washed with 125 μl of absolute ethanol and resuspended in 40 μl of absolute ethanol. The DNA-coated gold particles were loaded in 10 μl steps onto a macrocarrier (BIO-RAD, Hercules, USA). Particle bombardment on BY-2 cells or rice coleoptiles was performed immediately after total evaporation of the ethanol.

For biolistic transformation of BY-2 cells, a suspension of 3 day old cells was transferred to solid MS medium in PetriSlides (Millipore, Schwalbach, Germany). Slides were placed in a particle gun (Finer et al., 1992) and the cells were bombarded by three shots at a pressure of 1.5 bar in the vacuum chamber at -0.8 bar.

For transformation of rice coleoptiles, 4 day old, etiolated rice seedlings were arranged on a glass slide under green safety light according to a published method (Holweg et al., 2004). Caryopses of the seedlings were glued next to each other, in a stacked way resembling a zipper, along the edge of the glass slide such that the coleoptiles of all seedlings pointed towards the center of the slide. The slides were then placed in the particle gun and the coleoptiles were bombarded by three shots at a pressure of 1.5 bar in the vacuum chamber at -0.9 bar.

Following bombardment, both BY-2 cells and rice coleoptiles were incubated in the dark at 25 °C for 3 to 24 h and examined by fluorescence microscopy.

***Agrobacterium*-mediated stable transformation of tobacco BY-2 cells**

Tobacco BY-2 cells were stably transformed via *Agrobacterium*-mediated transformation. The binary vector construct OsKCH1-fl GFP was first introduced into *Agrobacterium tumefaciens* by heat shock. 100 μl of an overnight culture of the transformed *A. tumefaciens* were then co-incubated for 3 days at 27 °C with 4 ml of a 3 day old BY-2 cells as described by An (1985).

Subsequently, the cells were washed three times in liquid medium containing 100 mg/l cefotaxim and were plated onto solid MS medium containing 100 mg/l kanamycin and 100 mg/l cefotaxim.

After four weeks of incubation in the dark at 25 °C kanamycin-resistant calli appeared, were transferred to new plates and cultured separately until they reached approximately 1 cm in diameter. Cell suspension cultures were established from these calli and were maintained as described above.

2.4.2 Visualization of actin filaments and microtubules in fixed cells

Staining of actin microfilaments by Rhodamin-phalloidin

Actin filaments for colocalization studies were visualized following basic protocols by Kakimoto and Shibaoka (1987) and Olyslaegers and Verbelen (1998). BY-2 cells were fixed for 10 min in 1.8 % [w/v] paraformaldehyde (PFA) in standard buffer (0.1 M 1,4-piperazin-diethane sulfonic acid (PIPES) pH 7.0, supplemented with 5 mM MgCl₂ and 10 mM EGTA). After a subsequent 10 min fixation in standard buffer containing 1 % [v/v] glycerol, cells were rinsed twice for 10 min with standard buffer. 0.5 ml of the resuspended cells were then incubated for 35 min with 0.5 ml of 0.66 μM tetramethyl rhodamine isothiocyanate (TRITC)-phalloidin prepared freshly from a 6.6 μM stock solution in 96 % [w/v] ethanol by dilution (1:10 [v/v]) with phosphate buffered saline (PBS; 0.15 M NaCl, 2.7 mM KCl, 1.2 mM KH₂PO₄, and 6.5 mM Na₂HPO₄, pH 7.2). Cells were washed three times for 10 min in PBS and observed immediately.

Staining of microtubules by indirect immunofluorescence

Microtubules were visualized by indirect immunofluorescence basically as described by Nick et al. (2000). After fixation for 30 min with 3.7 % [w/v] paraformaldehyde in microtubule stabilizing buffer (MSB; 50 mM PIPES, 2 mM EGTA, 2 mM MgSO₄, 0.1 % [v/v] Triton X-100, pH 6.9), cells were washed in PBS three times for at least 5 min to remove excess paraformaldehyde. Subsequently, the cell wall was digested using 1 % [w/v] Macerozym (Duchefa, Haarlem, The Netherlands) and 0.2 % [w/v] Pectolyase (Fluka, Taufkirchen, Germany) in MSB for 5 min. After washing for 5 min with PBS, unspecific binding sites were blocked for 20 min with 0.5 % [w/v] BSA, diluted in PBS. Cells were subsequently directly transferred into a 1:300 PBS-dilution of the primary antibody DM1A (see Tab. 12 for details). The primary antibody was allowed to bind overnight at 4 °C. After removing unbound primary antibody by washing the cells three times for at least 5 min in PBS, the samples were incubated for 1 h at 37 °C with a secondary TRITC-conjugated antibody which is targeted against mouse IgG (Tab. 12). Again, unbound secondary antibody was removed by washing with PBS. If required, the DNA was additionally stained by Hoechst as described below.

DNA staining by Hoechst

For a detailed analysis of mitosis in tobacco BY-2 cells, staining of the DNA was required. BY-2 cell suspensions were either fixed in Carnoy fixative (3:1 [v/v] of 96 % [v/v] ethanol and glacial acetic acid, 0.25 % [v/v] Triton X-100) or immunolabeled as described above. The DNA was subsequently stained with 2'-(4-Hydroxyphenyl)-5-(4-methyl-1-piperazinyl)-2,5'-bi-(benzim-

idazole)-trihydrochloride (Hoechst 33258; Sigma, Taufkirchen, Germany). For this purpose, a final concentration of 1 $\mu\text{g/ml}$ Hoechst, prepared as a 0.5 mg/ml filter-sterilized stock solution in distilled water, was added to either Carnoy-fixed or immunolabeled BY-2 cells and the samples were immediately investigated under the microscope. For staining of living cells, the samples were incubated with 1 $\mu\text{g/ml}$ Hoechst 33258 under constant shaking for 12 h and subsequently investigated under the microscope.

2.4.3 Treatments of tobacco BY-2 cells with microtubule and actin drugs

BY-2 cells stably expressing OsKCH1-fl GFP were treated with 10 μM Oryzalin or 2 mM Colchicine to eliminate microtubules and were directly investigated by fluorescence microscopy for a duration of 2.5 h to observe changes in protein localization pattern. To disrupt actin microfilaments, cells were treated with either 100 μM Cytochalasin D or 10 μM Latrunculin B and as well examined for a time course of 2.5 h. In order to avoid bleaching, z-stack images were recorded only once every 30 min. In all cases controls were performed by treating the cells with the corresponding volume of solvent (DMSO) and investigating them in the same way.

2.4.4 Microscopy and image analysis

BY-2 cells were examined under an AxioImager Z.1 microscope (Zeiss, Jena, Germany) equipped with an ApoTome microscope slider for optical sectioning and a cooled digital CCD camera (AxioCam Mrm, Zeiss, Jena, Germany) for imaging.

TRITC and RFP fluorescence were observed through the filter set 43 HE (excitation at 550 nm, beamsplitter at 570 nm, and emission at 605 nm). YFP and GFP fluorescence were recorded through the filter sets 46 HE (excitation at 500 nm, beamsplitter at 515 nm, and emission at 535 nm) and 38 HE (excitation at 470 nm, beamsplitter at 495 nm, and emission at 525 nm), respectively. The filter set 49 HE (excitation at 365 nm, beamsplitter at 395 nm, and emission at 445 nm) was used for investigation of DAPI fluorescence and 47 HE (excitation at 436 nm, beamsplitter at 455 nm, and emission at 480 nm) for CFP fluorescence.

BY-2 cells were generally observed with either a 63x plan apochromat oil-immersion objective or a 40x objective. Stacks of optical sections were acquired at different step sizes between 0.5 and 0.8 μm . For phenotyping, cells were examined with a 20x objective and differential interference contrast (DIC) illumination.

Images were processed with respect to contrast and brightness and analyzed using the AxioVision software (AxioVision, Rel. 4.5; Zeiss, Jena, Germany) according to the manufacturers instructions. ImageJ (NIH, Bethesda, USA) was used for quantitative image analysis, such as gray value determinations and analysis of time series. Time space plots (kymographs) were generated using an EMBL-plugin for ImageJ (www.embl.de/eamnet/html/kymograph.html) according to the corresponding detailed instructions from the website.

2.5 Phenotyping methods

2.5.1 Phenotyping of tobacco BY-2 cell lines

Determination of cell length and width

Length and width of BY-2 cells were determined using the length measurement function of the AxioVision software (Zeiss, Jena, Germany). DIC images were recorded at day 3 after subcultivation from 3 independent experimental series comprising 300 cells each. Mean values and standard errors (SE) were calculated and the results were tested for significance by Student's t-test for unpaired data at a 95 % confidence level.

Determination of mitotic indices

Mitotic indices (MI) were determined microscopically in tobacco BY-2 cell suspensions after fixation and Hoechst staining as described above. MI were calculated as the number of cells in mitosis divided by the total number of counted cells. For each time-point 450 cells obtained from three independent experimental series were scored, and the results were tested for significance by Student's t-test.

Determination of the position of the nucleus

Nuclear positions (NP) in tobacco BY-2 were assessed at different time-points after subcultivation (0-6 d) from DIC images of central sections of the cells using the length measurement function of the AxioVision software (Zeiss, Jena, Germany). NP were determined as relative values by division of the shortest distance between the middle of the nucleus and the cell wall, and the total cell diameter (see Fig. 25 in results section for illustration). Typical values for mean NP ranged between 0.15 and 0.5 and were clustered into three main intervals indexed by the attributes lateral (NP \in [0.15, 0.29]), intermediate (NP \in [0.3, 0.39]) and central (NP \in [0.4, 0.5]). For each time-point and cell line 3 times 500 cells were measured and mean values, SE and occurrence distributions calculated. The results were tested for significance by Student's t-test.

2.5.2 Phenotyping of rice *kch1* mutants

Determination of coleoptile and root length of seedlings

Coleoptile length was determined in etiolated rice seedlings 7 days after germination. Macroscopic images of the seedlings were recorded and coleoptiles and roots measured using the periphery tool of ImageJ (NIH, Bethesda, USA). At least 50 seedlings, collected cumulatively over a minimum of 3 independent experimental series, were investigated and mean values and SE were calculated. Differences between mutants and wildtypes were tested for significance using Student's t-test for unpaired data sets at a confidence level of 95 %.

Determination of cell length and cell number in rice coleoptile

For determination of the mean cell length and the overall cell number in coleoptiles of wildtype and mutant rice plants, cross walls per cell file were counted in the field of vision at the microscope (see Fig. 19 in the results section for illustration). The mean length of the cells (l) was calculated by dividing the diameter of the field of vision ($1115 \mu\text{m}$) by the counted number of cross

walls (n) per cell file (n) in the following way: $l = \frac{1115 \mu\text{m}}{n}$. The number of cells per cole-

optile (N) was determined by dividing the total length of the coleoptile (L) by the cell length (l)

as follows: $N = \frac{L}{l}$. Mean values and SE for both the cell length and the overall cell number

were determined from a total of 150 analyzed cell files, collected cumulatively from 15 coleoptiles. All observed differences were tested for significance by Student's t-tests.

2.6 Biochemical methods

2.6.1 Standard methods

SDS-Polyacrylamide gel electrophoresis (SDS-Page)

Proteins were separated on discontinuous SDS-polyacrylamide gels (Laemmli, 1970).

Component	Separation Gel	Stacking Gel
Acrylamide (29.2 % [v/v] acrylamid 0.8 % [v/v] bisacrylamid)	6.7 ml	1.7 ml
Buffer S (1.5 M Tris-HCl, pH 8.8)	5 ml	--
Buffer C (0.5 M Tris-HCl, pH 6.8)	--	2.5 ml
H ₂ O	8 ml	3.3 ml
10 % [w/v] SDS	200 μl	100 μl
10 % [w/v] APS	80 μl	80 μl
TEMED	10 μl	10 μl

Tab. 15: Composition of 10 % SDS-polyacrylamide gels

The gels were run in a miniPAGE chamber (Atto, Tokyo, Japan) at 25 mA per gel for 90 min in running buffer (25 mM Tris, 192 mM glycine, 0.15 % [w/v] SDS).

Samples and high molecular weight standard (Sigma-Aldrich, Steinheim, Germany) were mixed with 3 x sample buffer (30 % [v/v] glycerin, 300 mM DTT, 6 % [w/v] SDS, 48 % [v/v] stacking gel buffer, 0.05 % [w/v] bromophenol blue), incubated at 95 °C for 5 min and immediately loaded onto the gel.

Gels were stained for 60 min to overnight in Coomassie staining solution (0.04 % [v/v] Coomassie Brilliant Blue R250, 40 % [v/v] ethanol, 10 % [v/v] acidic acid), rinsed with H₂O

and destained in 30 % [v/v] ethanol supplemented with 10 % [v/v] acetic acid. For documentation, gels were scanned using a HP ScanJet 3400C (Hewlett-Packard, Palo Alto, USA) and dried for long term storage.

Western blotting

Western blotting of protein gels was performed by semi-dry blotting according to Towbin et al. (1979) with minor modifications.

For preparation, the polyvinylidene fluoride (PVDF) membrane (Pall Gelman Laboratory, Dreieich, Germany) was activated by incubation in methanol for 30 sec and the blotting paper (Whatman, Dassel, Germany) soaked for 1 min in transfer buffer (14.4 g/l glycine, 12.07 g/l Tris-HCl, 20 % [v/v] MeOH). The blot was set-up in Trans-Blot SD Semi-Dry Transfer Cell (Bio-Rad, München, Germany) from the anode onwards as follows: 3 layers of blotting paper, PVDF membrane, the SDS-PAGE, 3 layers of blotting paper.

Proteins were transferred to the membrane at a constant current of 100 mA for 60 minutes per gel. After blotting, the membrane was blocked with milk buffer (2.5 % [w/v] in TBS) for 60 min and rinsed twice in TBS (20 mM Tris-HCl, 150 mM NaCl, 1 % [v/v] Triton-X 100) for 1 min. The blot was incubated overnight at 4 °C with the according primary antibody described in Tab. 12. The membrane was washed 3 times for 15 min in TBS prior incubation with the secondary antibody listed in Tab. 12 for 60 min. The secondary antibody was washed away by rinsing the blot once in milk buffer and twice for 5 min in TBS.

The membrane was developed using an alkaline phosphatase-based development method. For this purpose, the blot was incubated for 15 min in staining buffer (100 mM Tris-HCl, 100 mM NaCl) freshly supplemented with 1/10 magnesium stock (500 mM). The membrane was developed in 5 ml freshly prepared developer solution consisting of 66 µl nitrobluetetrazolium (NBT; 75 mg/ml in 75 % [v/v] dimethylformamide) and 33 µl 5-bromo-4-chloro-3-indoxylphosphate-p-tuloidin (BCIP; 50 mg/ml in 75 % [v/v] dimethylformamide) in 5 ml staining buffer with 1/10 magnesium stock solution for 15-30 min. Blots were typically scanned for documentation.

Determination of protein concentration

Protein concentrations were generally determined with Bradford assays (Bradford, 1976). For this purpose, 1 ml of Bradford reagent (100 mg/l Coomassie Brilliant Blue G250, 5 % [v/v] EtOH, 10 % [v/v] phosphoric acid) was mixed with 10 µl of protein solution, incubated for 15 min and measured photometrically at 595 nm using an BioPhotometer (Eppendorf, Hamburg, Germany). A standard curve with bovine serum albumin (BSA) was measured in parallel and the protein concentration was calculated in reference to the standard.

In cases of a high degree of impurity in the protein purifications, it is not possible to determine the concentration through Bradford assays. Instead, a comparative approach was chosen and the concentration of the protein of interest was assessed by comparison of the band intensities of the

target protein with a standard BSA dilution series on SDS-gels. After staining of the gels, the intensity of each BSA band and of the protein of interest is quantified by densitometric measurement using ImageJ (NIH, Bethesda, USA). A standard curve is generated, and the protein concentration is calculated in reference to the standard.

2.6.2 Protein expression and purification

Recombinant expression of kinesin constructs

All expression plasmids were transferred into the *E. coli* expression strain BL21 Codon Plus (DE3). Recombinant protein expression was performed in 200-2000 ml culture flasks containing LB medium supplemented with ampicillin.

Flasks were inoculated with 1/100 culture volume of overnight precultures and cells were grown until an OD₆₀₀ of 0.6-0.8 was reached. After cooling down for 15 min at 4 °C, protein expression was induced with 50 μM isopropyl-β-D-thiogalactopyranoside (IPTG). The cultures were subsequently incubated for 2-3 days at 14 °C. Cells were harvested by centrifugation at 9000 g and 4 °C for 10 min (Hermle Universal centrifuge, Wehingen, Germany) and washed in ground buffer (GB; 50 mM Tris-HCl pH 7.8, 300 mM NaCl, 1 mM ATP). Cells were spun down by another centrifugation step and resuspended in 1/10 of the original culture volume in GB before freezing in liquid nitrogen and storing at -70 °C.

Affinity purification of kinesin constructs

The proteins KCH1-sh, -cc1, -cc2, -mot and -cc3 were expressed in an at least partially soluble form, and purified under native conditions via nickel affinity chromatography at 4 °C in a cold room.

The frozen cell slurry was thawed slowly on ice and cells were extracted using a French pressure cell in two intervals at 1000 psi (Thermo Fisher Scientific, Schwerte, Germany). Debris and membranes were sedimented by centrifugation (25000 g, 30 min, 4 °C) in a Hermle Universal centrifuge (Hermle, Wehingen, Germany). The supernatant was applied to an affinity column of 25 ml Ni²⁺-NTA agarose matrix (Qiagen, Hilden, Germany), preequilibrated with binding buffer (BB; 50 mM Tris-HCl pH 7.8, 300 mM NaCl, 1.4 mM β-mercaptoethanol, 1 mM ATP). The proteins were bound to the resin for 30 min under constant gentle shaking, before unbound material was washed off the column with washing buffer (WB; BB supplemented with 10-40 mM imidazole). The proteins were eluted in fractions of 1.5 ml with 250 mM imidazole in BB. All fractions were checked for their protein content by measurements of E₂₈₀. Eluates containing sufficient amounts of protein were pooled and concentrated via ammonium sulfate (AmS) precipitation with 50 % [v/v] AmS and centrifuged at 25000 g and 4 °C for 20 min (Hermle Universal centrifuge, Hermle, Wehingen, Germany). Protein sediments were taken up in the according buffers (see respective sections) either for microtubule- or actin-binding assays or for SEC.

The protein KCH1-ch was expressed in insoluble form and purified under denaturing conditions and subsequent refolding. Sedimented cell debris after French pressure cell extraction was sus-

pended in solubilization buffer (SB; 50 mM TrisHCl pH 7.8, 300 mM NaCl, 8M urea, 1.4 mM β -mercaptoethanol) and incubated for 30 min under constant gentle shaking. The mixture was centrifuged (25000 g, 4 °C, 20 min; Hermle Universal centrifuge, Hermle, Wehingen, Germany) and the supernatant, containing the resolubilized protein, was applied to an SB-equilibrated nickel affinity column. The protein was bound to the resin for 30 min under constant gentle shaking before unbound material was washed off the column with SB. The protein was rena-tured on the column using a stepwise 8-0 M urea gradient in BB and finally eluted with 250 mM imidazole in BB. For buffer exchange, eluates were concentrated using Amicon Ultra centrifugal filter devices (Millipore, Schwalbach, Germany) and diluted in the required buffers for subsequent assays.

Protein concentrations for both solubly purified and insolubly purified proteins were generally determined as described in section 2.6.1. For storage purposes, protein aliquots were supplemented with 10 % [v/v] glycerol, frozen in liquid nitrogen and stored at -70 °C.

Activity purification of kinesin constructs

To verify the activity of motor proteins, recombinantly expressed and affinity purified kinesin constructs were tested for their ability for microtubule-binding and subsequent release.

200 - 500 μ l of affinity purified proteins or 2-3 ml of protein raw extract were preclarified from protein agglomerates at 40000 rpm and 4 °C for 20 min in a Beckman tabletop ultracentrifuge (TLA-100 rotor, Beckman, Krefeld, Germany) and incubated for 15-30 min at room temperature with 200 μ l of taxol-stabilized microtubules under presence of 200 μ M AMP-PNP, apyrase (1 U/ml) and 20 μ M taxol. The kinesin-microtubule-complexes were sedimented (42000 rpm, TLA-100 rotor, 30 min, 22 °C), and the supernatant discarded. The sediment was washed once with AP100 (100 mM PIPES-KOH, 2 mM MgCl₂, 1 mM EGTA, pH 6.8), resuspended in 100-200 ml KCl-buffer (AP100 supplemented with 50 mM KCl, 10 μ M taxol, 200 μ M AMP-PNP), and spun through a sucrose cushion (40 % [w/v] sucrose in AP100) to remove unpolymerized tubulin at 22 °C and 80000 rpm in a TLA-100 rotor for 10 min. The sediment was resuspended in 50-100 μ l release buffer (AP100 with 10 mM ATP, 10 mM MgCl₂, 200 mM KCl, 10 μ M taxol) and incubated 30 min at room temperature to ensure complete release of active motors. Microtubules were sedimented (80000 rpm, TLA-100 rotor, 10 min, 22 °C) and the supernatant containing the active motor proteins were removed and stored on ice. The release procedure was repeated once.

Proteins in the sediment and release fractions were identified via SDS-PAGE and – in case of similar concentrations in both fractions – they were pooled. Aliquots were supplemented with 10 % [w/v] glycerol, frozen in liquid nitrogen and stored at -70°C.

2.6.3 Preparation of pig brain tubulin

Purification of tubulin

Pig brain tubulin was purified in three successive steps of polymerization and depolymerization, followed by ion exchange chromatography (Mandelkow et al., 1985). All centrifugation steps during the purification process were performed in Beckman ultracentrifuges using the appropriate rotors purchased from Beckman (Krefeld, Germany), unless otherwise stated.

Fresh pig brains were obtained at the local slaughterhouse, immediately put on ice and separated from blood vessels and connective tissue. A mixture of 700 g of brain with 700 ml buffer A (0.1 M PIPES- NaOH, 2 mM EGTA, 1 mM MgSO₄, 1 mM DTT, 100 μM ATP) was homogenized in a Warring Blender (Braun, Kronberg, Germany) and clarified at 13000 rpm and 4 °C for 70 min in Sorvall RC centrifuge equipped with a GSA rotor (Thermo Fisher Scientific, Waltham, USA). The supernatant was inoculated with 25 % [v/v] glycerol and 2 mM ATP. For polymerization, the mixture was incubated in a 35 °C water bath for 30 min under constant gentle shaking. Microtubules were sedimented by ultracentrifugation at 32 °C and 42000 rpm for 45 min in a Ti 45 rotor. The sediments were resuspended in 100 ml buffer C (0.1 M PIPES- NaOH, 1 mM EGTA, 1 mM MgSO₄, 1 mM DTT, 1 mM ATP) and homogenized on ice using a glass potter (Wheaton Science Products, Millville, USA). For depolymerization, microtubules were incubated for 25 min on ice and the mixture was clarified by ultracentrifugation (36000 rpm, 30 min, 4 °C, Ti 45 rotor). After addition of 2 mM ATP, the supernatant was repolymerized at 35 °C for 30 min and spun down again at 32 °C and 33000 rpm for 60 min in a Ti 45 rotor. The sedimented microtubules were weighed, frozen in liquid nitrogen, and stored at -70 °C.

Last traces of microtubule-binding proteins were removed by ion-exchange chromatography on a phosphocellulose column containing 50 ml of activated P-11 phosphocellulose material (Whatman, Dassel, Germany). While the column was equilibrated with 3 volumes of buffer D (0.1 M PIPES- NaOH, 1 mM EGTA, 1 mM MgSO₄, 1 mM DTT, 50 μM ATP) at a constant flow rate of 1 ml/min in an FPLC (Amersham Pharmacia, München, Germany), microtubule sediments were thawed, homogenized on ice in 50-100 ml buffer B (0.5 M PIPES- NaOH, 1 mM EGTA, 1 mM MgSO₄, 1 mM DTT, 1 mM ATP) and depolymerized through incubation on ice for 25 min. After centrifugation (Ti 45 rotor, 36000 rpm, 30 min, 4 °C), polymerization of the supernatant was induced through addition of 10 % [v/v] DMSO and 2 mM ATP under constant gentle shaking at 35 °C for 30 min. The microtubules were spun down at 32 °C and 33000 rpm for 60 min in a Ti 45 rotor and resuspended and homogenized in 5-7 ml buffer D and depolymerized on ice for 25 min. The mixture was clarified (Ti 70 rotor, 34200 rpm, 30 min, 4 °C) and the supernatant was loaded onto the phosphocellulose column and washed with buffer D at a constant flow of 0.16 ml/min. While microtubule associated proteins bind to the column, tubulin is eluted in a distinct protein peak. For tubulin detection, elution fractions of 1 ml were collected and tested for their protein content via standard Bradford assay. Peak fractions were pooled, supplemented with 0.1 mM GTP, frozen in aliquots of 100 μl in liquid nitrogen, and stored at -70 °C.

Rhodamine-labeling of tubulin

For fluorescent visualization of microtubules, purified pig brain tubulin was labeled with the fluorescent dye Rhodamine. The labeling procedure involved chemical coupling of the reactive 5(6)-Carboxytetramethylrhodamine N-succinimidyl ester (TAMRA-SE; Sigma-Aldrich, Steinheim, Germany) to polymerized microtubules, thereby protecting residues important for microtubule assembly (Peloquin et al., 2005). High pH conditions were required to optimize the reaction efficiency. Therefore the functionality of tubulin was tested after labeling by several cycles of polymerization and depolymerization. All centrifugation steps during the labeling process were performed in Beckman ultracentrifuges using the appropriate rotors purchased from Beckman (Krefeld, Germany).

3-5 ml of purified tubulin were thawed quickly, supplemented with 1 mM GTP and stored on ice for 5 min. To promote polymerization, DMSO was added to a final concentration of 10 % [v/v] and the mixture transferred to 37 °C for 30 min. Polymerized tubulin was layered onto 4 ml of high-pH cushion (0.1 M Na-HEPES, 1 mM MgCl₂, 1 mM EGTA, 60 % [v/v] glycerol, pH 8.6) and sedimented at 25 °C and 80000 rpm for 15 min (Ti 70 rotor). The pH cushion was carefully removed and the sediment resuspended in 1-2 ml labeling buffer (0.1 M Na-HEPES, 1 mM MgCl₂, 1 mM EGTA, 40 % [v/v] glycerol, pH 8.6). A 10-20 fold molar excess of TAMRA-SE, dissolved in anhydrous DMSO, was added and incubated for 30-40 min at 37 °C under constant gentle mixing every 2-3 min. Following the labeling, an equal volume of quench-solution (2x BRB80, 100 mM K-glutamate, 40 % [v/v] glycerol) was added, mixed thoroughly and incubated for another 5 min. The quenched reaction mixture was layered onto 3 ml of low pH cushion (1x BRB80 with 60 % [v/v] glycerol) and sedimented (TLA-100 rotor, 80000 rpm, 10 min, 25 °C). The cushion was carefully removed and the pellet was resuspended in 1 ml of ice-cold 1x IB (10x IB stock: 500 mM K-Glutamate, 5 mM MgCl₂, pH 7.0) using a pre-cooled potter until a homogeneous suspension was obtained. The mixture was incubated for 30 min on ice to allow depolymerization and was subsequently clarified by centrifugation (TLA-100 rotor, 80000 rpm, 10 min, 2°C). The supernatant was removed carefully, supplemented to 1x with BRB80 (5x BRB80 stock: 400 mM PIPES, 5 mM MgCl₂, 5 mM EGTA, pH 6.8) and 1 mM GTP and incubated on ice for 3 min. After equilibrating the reaction mixture for 2 min at 37 °C 33 % [v/v] glycerol was added, and tubulin was polymerized for 30 min at 37 °C. Microtubules were layered onto 1 ml of low pH cushion and sedimented at 25 °C and 80000 rpm in a TLA-100 rotor for 15 min. The cushion was removed carefully, the pellet resuspended in 0.2 - 0.4 ml ice-cold IB and depolymerized for 20 - 30 min on ice prior to a clarification step via ultracentrifugation (TLA-100 rotor, 80000 rpm, 10 min, 2 °C). The supernatant was frozen in liquid nitrogen in small aliquots of 2-4 µl and stored at -70 °C.

2.6.4 *In vitro* polymerization of microtubules and actin filaments

Polymerization of microtubules

Depending on the specific experimental requirements for biochemical analysis or microscopic investigation, either unlabeled or labeled microtubules were polymerized from the tubulin preparations. Typically a total volume of 100 μ l of unlabeled tubulin was used for polymerization and, if necessary, supplemented with 2-4 μ l of Rhodamine-tubulin. Prior to polymerization, inactive, aggregated tubulin had to be removed through ultracentrifugation (80000 rpm, 4 °C, 10 min; TLA-100 rotor, Beckman, Krefeld, Germany) to make a subsequent accurate determination of microtubule concentration possible. The resulting supernatant was supplemented with 1 mM GTP and polymerized at 37 °C for 15 min. 100 μ M taxol (Paclitaxel; Sigma-Aldrich, Steinheim, Germany) was added stepwise for stabilization of microtubules and the mixture was incubated for another 15 min at 37 °C. Unpolymerized tubulin was removed by sedimentation of microtubules through a cushion of 40 % [v/v] sucrose in BRB80 buffer (80 mM PIPES pH 6.8, 1 mM MgCl₂, 1 mM EGTA) at 80000 rpm and 25 °C for 10 min in a TLA-100 rotor. The microtubule sediment was washed once and then resuspended in BRB80 buffer supplemented with 100 μ M taxol. The concentration of tubulin was typically determined by Bradford assays, as described in section 2.6.1.

In some cases, the accurate microtubule concentration was not relevant for the assay. Here, tubulin was thawed and quickly polymerized by adding 1 mM GTP and incubated for 30 min at 37 °C. Microtubules were again stabilized by addition of 100 μ M taxol during polymerization.

Biotinylation of microtubules

For several assays biotinylated microtubules were required. Taxol-stabilized microtubules were thus prepolymerized as described above. Subsequently, 1 mg/ml biotin-XX N-hydroxysuccinimide ester (biotin-XX NHS; Jena Bioscience, Jena, Germany) and 100 μ M NaHCO₃ were added to the microtubules. The mixture was incubated for another 45 min at 37 °C. Then, unpolymerized tubulin and unbound biotin were removed by sedimentation of microtubules through a cushion of 40 % [v/v] sucrose in BRB80 buffer (80 mM PIPES pH 6.8, 1 mM MgCl₂, 1 mM EGTA) at 80000 rpm and 25 °C for 10 min in a TLA-100 rotor. The microtubule sediment was washed once and finally resuspended in BRB80 buffer supplemented with 100 μ M taxol.

Polymerization of actin

Actin filaments were polymerized from monomeric rabbit skeletal muscle actin purchased from Cytoskeleton (Denver, USA) according to the manufacturers instructions. Monomeric actin was diluted to a final concentration of 0.4 mg/ml in buffer A (5 mM Tris-HCl pH 8.0, 0.2 mM CaCl₂, 50 mM KCl, 2 mM MgCl₂) and clarified by centrifugation (20000 rpm, 10 min, 4 °C; TLA-100 rotor, Beckman, Krefeld, Germany). The supernatant containing monomeric actin was supplemented with 1 mM ATP and 0.5 mM DTT and then polymerized at room temperature for 1 h. Actin filaments could be stored for 24 h at 4 °C.

Fluorescein-labeling of actin filaments

For bundling assays, fluorescently labeled actin was required. FITC-labeled filaments were thus generated by addition of a molar ratio of 1:1 Fluorescein isothiocyanate (FITC)-phalloidin from a 6.6 μM stock solution in 96 % [w/v] ethanol to prepolymerized actin filaments. The mixture was incubated for 1 h to overnight at 4 °C (VanBuren et al., 1998).

2.6.5 Protein analysis

Microtubule-binding assays

The binding behavior and the affinity of OsKCH1 to microtubules were investigated via concentration-dependent cosedimentation tests as described by Xu et al. (2007). Recombinantly expressed KCH1 preparations were preclarified at 80000 rpm and 22 °C for 15 min in a TLA-100 rotor (Beckman, Krefeld, Germany) prior to each microtubule-binding experiment. Subsequently, 0.3 μM of kinesin was mixed with varying concentrations of taxol-stabilized microtubules (0-15 μM) in a 70 μl reaction volume in BRB80 buffer (80 mM PIPES pH 6.8, 1 mM MgCl_2 , 1 mM EGTA) supplemented with 1 mM ATP and 20 μM taxol. The samples were incubated for 15 min at room temperature and then centrifuged at 80000 rpm for 10 min at 22 °C in a TLA-100 ultracentrifuge (Beckman, Krefeld, Germany). For control, KCH1 proteins were incubated in the absence of microtubules and treated the same way. The supernatants of all samples were carefully removed and mixed with 3x SDS sample buffer. The sediments were resuspended in BRB80, in a volume equal to the supernatants, and as well mixed with 3x SDS sample buffer. Equal amounts of the sediment and supernatant samples were separated on 10 % [w/v] SDS-PAGE and either stained with Coomassie or detected via Western blotting with anti-penta His antibodies. The gels or blots were scanned and affinity constants describing the binding of KCH1 variants to microtubules were determined as described below.

Actin-binding assays

For characterization of the binding behavior and the affinity of OsKCH1 to microfilaments, concentration-dependent cosedimentation assays were performed according to Srivastava (2008). Preceding each cosedimentation assay, recombinantly expressed KCH1 proteins were preclarified at 50000 rpm and 22 °C for 20 min in a TLA-100 rotor (Beckman, Krefeld, Germany). Subsequently, 0.3 μM of kinesin was incubated for 1 h at 22 °C with varying concentrations of actin microfilaments (0-7 μM) in a 50 μl reaction volume in actin-binding buffer (10 mM Tris-HCl pH 7.0, 1 mM EGTA, 0.1 mM CaCl_2 , 2 mM MgCl_2 , 0.5 mM DTT, 1 mM ATP). For control treatments, the proteins were incubated in the absence of actin under similar conditions. The samples were centrifuged at 50000 rpm for 20 min at 22 °C in a TLA-100 ultracentrifuge (Beckman, Krefeld, Germany) to sediment the filaments and the filament-bound proteins. The supernatants were carefully separated and mixed with 3x SDS sample buffer. The sediments were resuspended in a similar volume of actin-binding buffer and as well mixed with sample buffer. Equal amounts of the sediment and supernatant samples were separated by 10 % [w/v]

SDS-Page and either stained with Coomassie or detected via Western blotting with anti-penta His antibodies. The gels or blots were scanned and affinity constants, describing the binding of KCH1 to actin filaments, were determined as described below.

Determination of affinity constants

The dissociation constant K_d was determined for both microtubule and actin-binding of KCH1 variants as a measure of the binding affinities of the proteins. The following paragraph exemplarily describes the determination of the K_d value for microtubule-binding of KCH1. The K_d value for actin-binding was calculated in the same way.

The amount of bound and unbound protein in sediment and supernatant fractions of the cosedimentation assays with microtubules was quantified by gray value analysis of the corresponding bands from SDS-Page or Western Blot using the program ImageJ (NIH, Bethesda, USA). The gray values were normalized on the total amount of KCH1 protein used in the assays, and the percentage of filament-bound protein was calculated and plotted against the microtubule concentration. The dissociation constant K_d , which corresponds to the microtubule concentration at which half of the protein is filament-bound and partitions to the sediment fraction, was determined by non-linear least-square fit of the data to a curve generated using the hyperbolic equation

$$c[KCH1-MT] = f_{max} \cdot \left(\frac{c[MT_{tot}]}{c[MT_{tot}] + K_d} \right).$$

Here, $c[KCH1-MT]$ represents the fraction of microtubule-bound KCH1 during the reaction equilibrium, f_{max} the saturation coefficient, $c[MT_{tot}]$ the total concentration of microtubules used per sample, and K_d the dissociation constant (Goodrich and Kugel, 2007).

Depolymerization assays with microtubules

The ability of OsKCH1 to depolymerize microtubules was investigated *in vitro* via microtubule depolymerization assays basically following a protocol by Ovechkina et al. (2002). Recombinantly expressed KCH1-mot was preclarified at 80000 rpm (22 °C, 15 min; TLA-100 rotor, Beckman, Krefeld, Germany) and the protein concentration was determined. Subsequently, 1 μ M of kinesin was mixed with 2 μ M of taxol-stabilized microtubules in a 70 μ l reaction volume in BRB80 buffer (80 mM PIPES pH 6.8, 1 mM $MgCl_2$, 1 mM EGTA) supplemented with 1 mM ATP and either 3 or 20 μ M taxol. The mixtures were incubated at room temperature for 30 min, and then centrifuged at 22 °C and 80000 rpm for 10 min in a TLA-100 ultracentrifuge (Beckman, Krefeld, Germany). Both supernatants and sediments were assayed for the presence of tubulin on Coomassie-stained SDS-Page and the gels were calibrated and quantified using ImageJ (NIH, Bethesda, USA). For normalization purposes, the amount of tubulin in the supernatant of no-motor control reactions was subtracted from the amount present in the supernatant of the motor-containing reactions. The ratios of tubulin in both sediment and supernatant fractions were calculated as mean values \pm SE of three independent experiments for all samples. The ratios were then compared between the different reaction conditions.

Bundling assays with microtubules and actin filaments

To assess the ability of OsKCH1 to bundle microtubules and actin microfilaments, *in vitro* bundling assays were performed basically following a published method (Cao et al., 2004). Recombinantly expressed variants of KCH1 were clarified from protein aggregates by ultracentrifugation (80000 rpm, 22 °C, 15 min; TLA 100 rotor, Beckman, Krefeld, Germany) and the protein concentrations were determined. 1 μ M of kinesin was subsequently mixed with either 1 μ M of rhodamin-labeled, taxol-stabilized microtubules, 1 μ M FITC-phalloidin-labeled actin filaments, or both, in a reaction volume of 20 μ l of BRB80 buffer (80 mM Pipes pH 6.8, 1 mM MgCl₂, 1 mM EGTA, 1 mM ATP) or actin-binding buffer (10 mM Tris-HCl pH 7.0, 1 mM EGTA, 0.1 mM CaCl₂, 2 mM MgCl₂, 0.5 mM DTT, 1 mM ATP). The mixtures were incubated at room temperature for 30 min and subsequently investigated under the microscope.

Analytical size exclusion chromatography

The native conformations and putative oligomerization states of OsKCH1 were analyzed via analytical size exclusion chromatography (SEC) as described elsewhere (Irvine, 2001). A Superdex 200 HR 10/30 column (Pharmacia, Uppsala, Sweden) was calibrated with six proteins of known molecular sizes between 12.4 and 443 kDa (Sigma-Aldrich, Steinheim, Germany) and a standard elution curve was generated. The column was run at 500 μ l/min with 10 mM Tris-HCl (pH 7.8), 150 mM NaCl, and 1 mM EDTA. Samples of standard proteins as well as of kinesins were loaded via a 100 μ l loop. The elution profile was constantly monitored by photometric measurement of E₂₈₀. Additionally, fractions of 500 μ l were collected and subsequently analyzed via SDS-Page and Coomassie staining. Molecular weights of kinesin samples were determined by comparison with standard proteins.

RESULTS

A tight coordination of cytoskeletal elements is necessary for a variety of different processes during plant cell growth and development. The recently identified plant kinesins with calponin-homology domain (KCHs) represent promising candidates for mediation of such microtubule-microfilament interaction (Tamura et al., 1999; Preuss et al., 2004).

This study aims to further elucidate the specific functions of this interesting group of proteins. In the following, first a computer-based analysis of the KCH subfamily will be given. The second part will focus on the investigation of bifunctional binding to microtubules and actin filaments as characteristic feature of KCHs. The third section will present an analysis of the putative biological role of a new KCH from rice, OsKCH1. In addition, biochemical data on the molecular properties of OsKCH1 will be given. Finally, all findings will be summarized.

1 *In silico* analysis of KCHs

The recently identified plant kinesins with calponin-homology domain (KCH) (Tamura et al., 1999; Preuss et al., 2004) have been linked with a putative role in microtubule-microfilament interaction in the developing cotton fiber (Preuss et al., 2004). Developing cotton fibers represent a cell system that is functionally specialized towards cellulose synthesis and comprises a highly prominent array of cortical microtubules, which is in tight contact with the actin cytoskeleton (Seagull, 1990). To what extent this presumed link between microtubules and actin filaments is a general function of KCH or rather limited to the specialized cotton fiber system has, however, so far remained elusive. An analysis of further KCH candidate proteins in other organisms and in different cell systems is therefore necessary and a major target of this work.

In order to obtain a first overview on the KCH subgroup of kinesins and their members in different organisms, genome and protein databases were thoroughly searched and candidate proteins were identified. Subsequently, a phylogenetic analysis was performed to investigate the evolutionary relationship among the different KCH members, and to choose one candidate protein for further study.

1.1 KCHs form a highly conserved, plant-specific subgroup within the Kin-14 family

A protein BLAST search in Swiss-Prot/TrEMBL was performed using the cotton KCH member GhKCH1 (Preuss et al., 2004) as a template and was followed by a domain analysis of all putative candidates in SMART. The search revealed KCH family members in all higher plants that had been sequenced and proteom-annotated to that time (February 2009), namely the grass model plant *Oryza sativa*, the Rosids *Arabidopsis thaliana*, *Vitis vinifera*, *Populus trichocarpa*, and *Ricinus communis*. Additionally, members were identified in the moss *Physcomitrella patens*. All species contain at least 3 copies of KCH (as in case of *Physcomitrella*), but often

more members were found. An overview of the identified proteins is given in the appendix (Tab. 16), together with their according Swiss-Prot/TrEMBL accession numbers.

Interestingly, putative candidates were neither identified in the green algae *Chlamydomonas reinhardtii*, nor in animal and fungi. Thus, KCHs are so far the only kinesin subgroup exclusively found in higher plants.

To determine the evolutionary relationship between the various KCH members, other representatives of the kinesin-14 (Kin-14) family and of the family of conventional kinesins (Kin-1), a phylogenetic analysis was performed. The corresponding tree is shown in Fig. 8 A.

All identified KCH candidate proteins, including the cotton members GhKCH1 (Preuss et al., 2004), the *Arabidopsis* AtKatD (Tamura et al., 1999), and the rice variant OsKCH1, clustered together into a defined clade. Interestingly, the plant kinesin-14 members AtKatC and AtKatA,

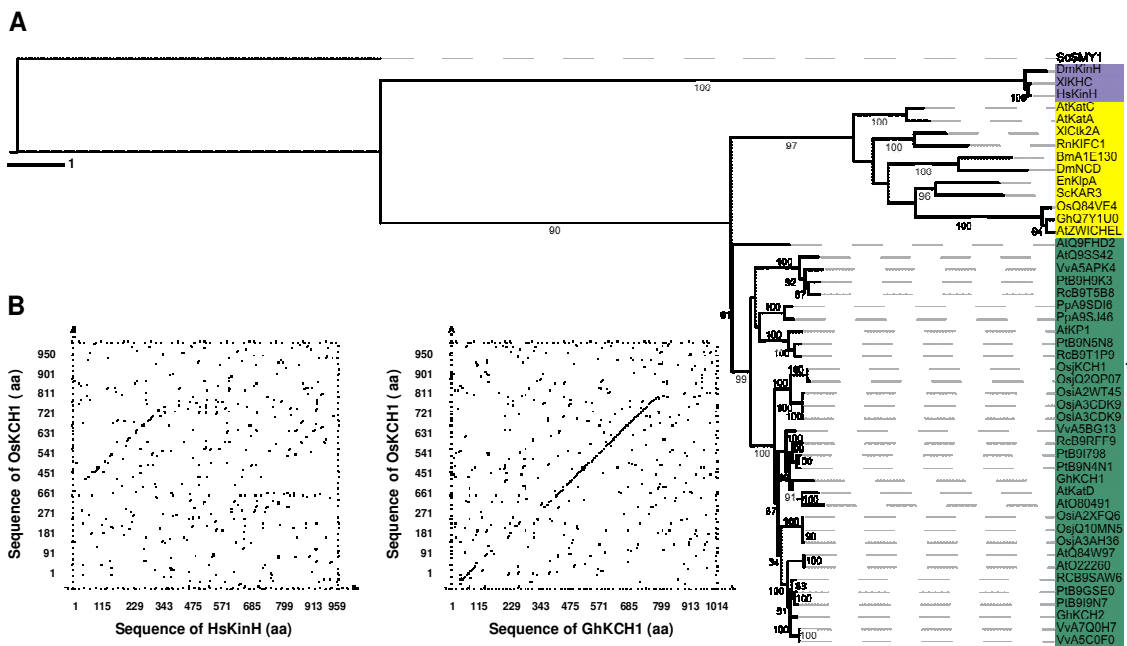


Fig. 8: Sequence analysis of *OsKCH1*

[A] Phylogenetic relationship of *OsKCH1* (marked by an asterisk) with several plant and animal members of the kinesin-14 family (shaded in yellow) and representatives of the kinesin-1 family (shaded in blue), generated by a maximum likelihood approach with a random stepwise addition of protein sequences. The phylogenetic tree was rooted arbitrarily by using the orphan yeast kinesin ScSMY1 (Lillie and Brown, 1992) as outgroup. Bootstrap support values were obtained from 100 replicates, and only values greater than 50 are shown in the tree. The clade containing the KCH kinesins is highlighted by a vertical line and shaded in green. Abbreviations: At – *Arabidopsis thaliana*, Bm – *Bombyx mori*, Dm – *Drosophila melanogaster*, En – *Emericella nidulans*, Gh – *Gossypium hirsutum*, Osi – *Oryza sativa* ssp. *indica*, Osj – *Oryza sativa* ssp. *japonica*, Pp – *Physcomitrella patens*, Pt – *Populus trichocarpa*, Rc – *Ricinus communis*, Rn – *Rattus norvegicus*, Sc – *Saccharomyces cerevisiae*, Hs – *Homo sapiens*, Vv – *Vitis vinifera*, Xl – *Xenopus laevis*. All protein sequence data was obtained from Swiss-Prot/TrEMBL. [B] Comparison of amino acid sequences of *OsKCH1* with *HsKinH* and *GhKCH1*, respectively. Both are presented in a dot matrix plot. Whereas only minor sequence homologies can be found for the pair *OsKCH1* and *HsKinH*, significant homologies are present at the N-terminal and the central regions between *OsKCH1* and *GhKCH1*.

the latter known to be a minus-end directed motor with a C-terminal motor domain (Marcus et al., 2002), formed a branch with members of the KIFC1 family from rat and *Xenopus* instead of clustering with the KCH subgroup. Similarly, representatives of the plant KCBP-family (Reddy et al., 1996; Preuss et al., 2003; Abdel-Ghany et al., 2005) were found to diverge clearly from the KCHs. Thus, plant KCHs form a phylogenetically distinct subgroup within the kinesin-14 subfamily, indicating possibly distinct characteristics and functions.

1.2 OsKCH1 is a KCH member from rice

All previous studies on KCH proteins have so far only focused on dicotyledon family members (Tamura et al., 1999; Preuss et al., 2004; Xu et al., 2007). In order to get an insight in structural and functional conservation within the KCH family, this work was specifically interested in investigating a monocotyledon KCH member. The database search had identified several candidate proteins in the monocotyledon grass model plant *Oryza sativa* ssp. *japonica* (see Fig. 8 and Tab. 16). One of these candidates, OsKCH1 (GenBank accession: Os12g0547500, Swiss-Prot accession: Q0IMS9), was recognized as a close homologue to GhKCH1. It was therefore chosen for further investigations, ensuring the advantage of good comparability of the results from this work with previously published studies.

The predicted OsKCH1 protein consists of 954 amino acids and has a calculated molecular mass of 106 kDa. It shows only low similarity to the conventional human kinesin HsKinH (13 % of sequence identity), but shares about 47 % sequence identity with AtKatD (Tamura et al., 1999), and 45 % with GhKCH1 (Preuss et al., 2004). As visible in dot matrix plots of the respective sequences (Fig. 8 B), in both cases the similarity is mostly pronounced in the N-terminal regions and the central parts. A domain analysis revealed the presence of the typical calponin-homology (CH) domain at the N-terminus of the polypeptide and the highly conserved kinesin motor core in the central part (Fig. 9 A). Sequence analysis using the Lupas algorithm (Lupas et al., 1991) in combination with other sequence routines have additionally defined three putative coiled-coil regions in the OsKCH1 sequence: two in tandem upstream and one downstream of the catalytic core (Fig. 9 B). Furthermore, directly upstream of the catalytic core a 14-aa sequence was identified that matches the consensus neck motif found among kinesins that move towards the minus-end of microtubules (Endow, 1999; Fig. 9 C). Thus, OsKCH1 is probably a microtubule minus-end-directed motor.

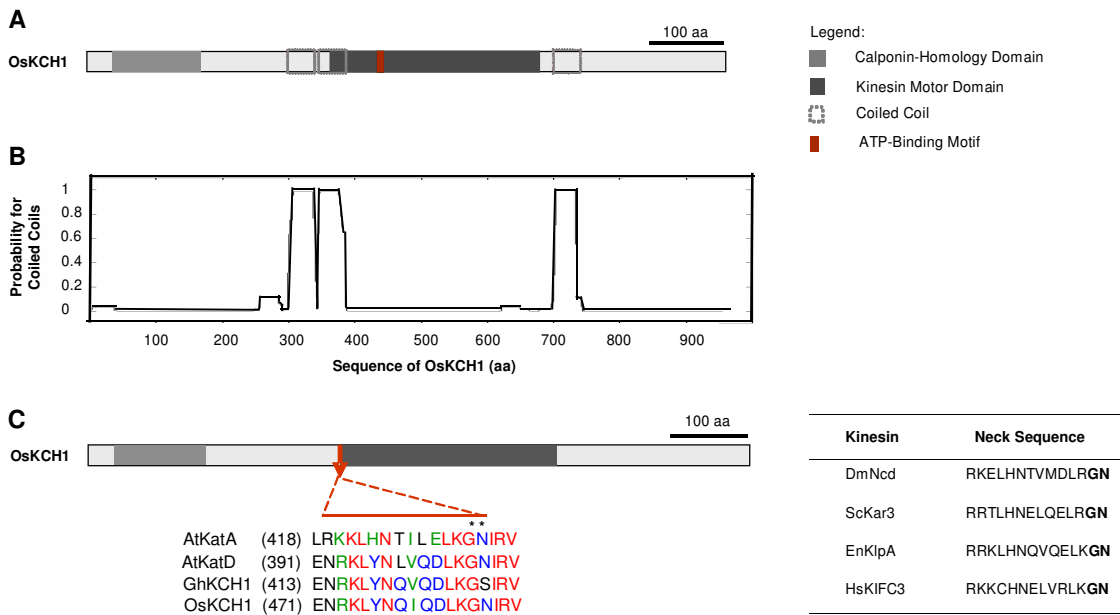


Fig. 9: Domain organization in OsKCH1

[A] Schematic diagram of the domain organization in OsKCH1. The full-length protein OsKCH1 has a size of 954 aa and harbors a putative kinesin-motor domain in the central region, including a conserved ATP-binding motif and a microtubule-binding site. The protein N-terminus includes a calponin-homology (CH) domain. [B] Prediction of coiled-coil motives. A probability > 0.5 indicates that the corresponding region likely forms a coiled-coil. [C] An amino-acid sequence alignment of the putative neck linker region of OsKCH1 and related kinesins shows that the 14-aa stretch associated with minus-end directionality in the kinesin-14 family (Endow, 1999; marked by a red line) is partially conserved. Asterisks indicate the two amino acids known to be mostly connected with kinesin minus-end directed movement. The table includes kinesins with known minus-end directionality from several non-plant species, together with their respective neck sequences.

2 Investigation of OsKCH1 bifunctionality

KCH proteins contain, in addition to the typically microtubule-binding kinesin motor core, a highly conserved CH domain. This domain is widely known as actin-binding motif from a variety of actin-binding proteins, such as in α -actinin, spectrin or fimbrins (Klein et al., 2004). KCHs thus might represent putative bifunctional proteins, and the ability of the cotton KCH member GhKCH1 to interact with both types of cytoskeletal elements was already investigated in developing cotton fibers (Preuss et al., 2004).

To analyze, whether the presumed bifunctionality represents a conserved function among the KCHs, the ability of the rice KCH family member OsKCH1 to bind to both microtubules and microfilaments was investigated. For this purpose, a combination of *in vivo* colocalization studies in different cell types, pharmacological treatments, and *in vitro* binding studies with recombinantly expressed proteins was performed.

2.1 OsKCH1 colocalizes *in vivo* with microtubules and actin

The *in vivo* investigation of the putative bifunctionality of OsKCH1 through localization studies required the generation of a variety of fusion constructs of the target protein OsKCH1 with fluorescent proteins. For cloning purposes, a RIKEN cDNA clone of OsKCH1 was obtained from the Rice Genome Resource Center that covered 2433 bp (811 aa) of the target sequence. Several constructs were generated as N-terminal fusions with either yellow fluorescent protein (YFP) or green fluorescent protein (GFP), each comprising different domains of OsKCH1. A nearly full-length construct (OsKCH1-800: residues 1-800) contained both the CH and the motor domain, while two truncated versions encoded either the N-terminal part with the CH domain (OsKCH1-ch: residues 1-473) or the central region containing the motor core (OsKCH1-mot: residues 300-800; Fig. 10 B).

2.1.1 OsKCH1-800 is expressed in punctate, filamentous structures

The fusion proteins were both transiently and stably expressed *in planta* and the specific localization pattern studied. An expression of the constructs in two functionally different model cell systems, namely etiolated rice coleoptiles as model for cell expansion growth and tobacco BY-2 cells as model for cycling cells, intended to investigate the general and conserved behavior of OsKCH1 in expanding versus dividing cells.

Transient expression of the full-length construct OsKCH1-800 in the homologous system rice coleoptile typically produced a punctate localization pattern of the protein (Fig. 10 A, a). This punctate signals were preferentially found in the cell cortex and were often aligned as beads on the string in a transverse orientation and in helicoidal pattern.

As rice coleoptiles grow exclusively via cell elongation, the heterologous system tobacco BY-2 was used to investigate the localization of OsKCH1-800 in cycling cells. Similar to the results from rice coleoptiles, the expression of OsKCH1-800 in interphasic tobacco BY-2 cells yielded a punctate localization of the protein along transversely oriented filaments in the cell cortex (Fig. 10 A, b and c), and on longitudinally oriented filamentous structures in the cell center (Fig. 10 A, g and h). Fluorescent signals were additionally found around the nucleus (Fig. 10 A, d and f), often in form of a tight perinuclear network (Fig. 10 A, d and e) or as point-like signal accumulations at sites where filaments reached the nuclear envelope. Furthermore, signals localized to filaments that seemed to tether the nucleus to the periphery of the cell (Fig. 10 A, d-h), and especially accumulated on sites where these filaments attached to the cell cortex (Fig. 10 A, f and h).

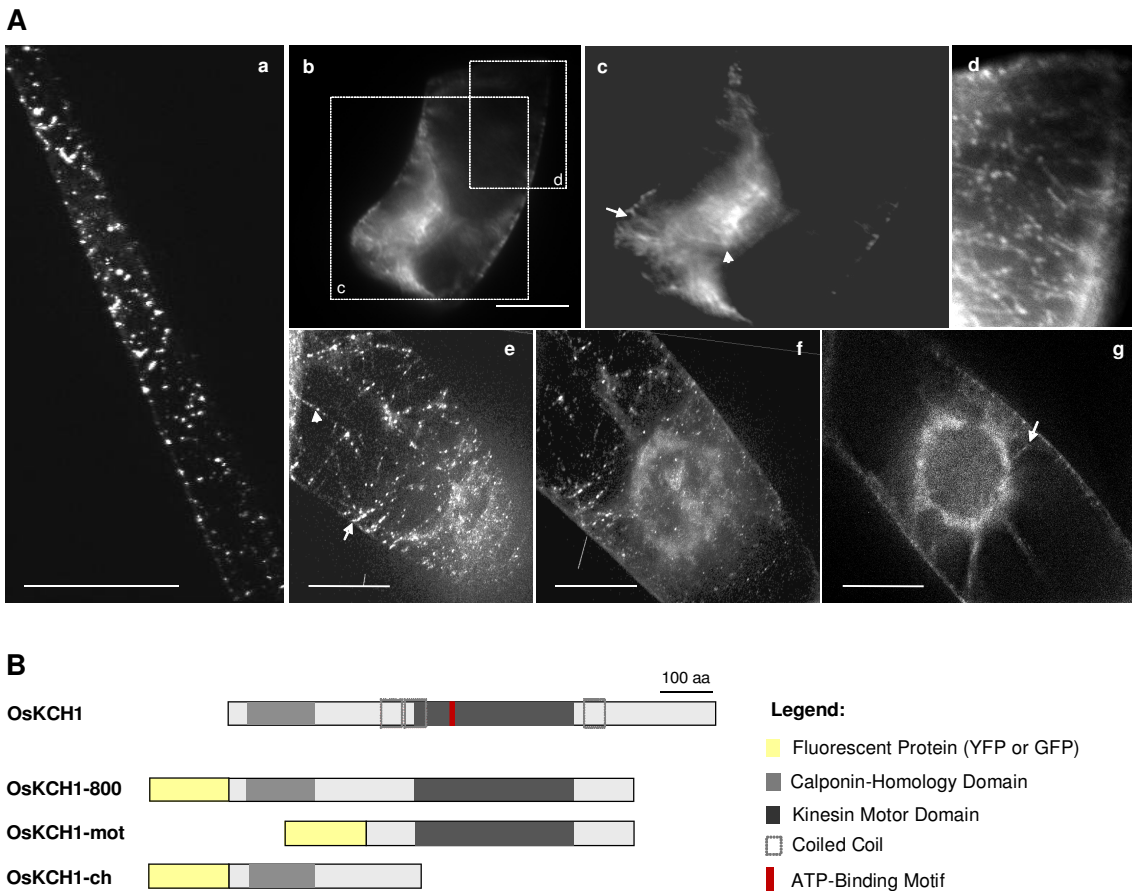


Fig. 10: Localization pattern of *OsKCH1* in rice coleoptiles and tobacco *BY-2* cells

[A] (a) Transient expression of YFP *OsKCH1*-800 in rice coleoptiles. Note the punctate fluorescence that appears to be aligned as beads on a string and produces a helicoidal pattern. (b-d) Transient expression of YFP *OsKCH1*-800 in tobacco *BY-2* cells. Optical section through the cell midplane (b, c). A filamentous fluorescence surrounds the nucleus in a mesh-like structure (c, arrow head) and reaches from the nucleus to the cortex (c, arrow). (d) Detail of the cell cortex. Punctate signals aligned as beads on a string in addition to filamentous structures are visible. (e-g) Stable expression of GFP *OsKCH1*-800 in tobacco *BY-2* cells. A series of individual optical sections from the cell cortex (e) towards the cell-mid plane (f, g) is shown. Note the punctate fluorescence in (e) that is organized in filaments with either transverse (arrow) or longitudinal orientation (arrow head), and the signals around the nucleus and on filamentous structures that tether the nucleus to the periphery (g, arrow). Scale bar = 20 μ m. [B] Schematic diagram of the domain organization in the fluorescent-protein fusions used for localization studies, *OsKCH1*-800 (aa 1-800), *OsKCH1*-mot (aa 300-800), *OsKCH1*-ch (aa 1-480) with respect to the full length protein *OsKCH1*.

2.1.2 OsKCH1-800 and OsKCH1-mot colocalize with cortical microtubules

Transient and stable expressions of OsKCH1-800 have typically revealed the localization of the protein on filamentous pattern in both investigated model cell systems. In order to identify these structures, YFP fusions of OsKCH1 were coexpressed with the microtubule marker MBD-MAP4 (Marc et al., 1998) in fusion with DsRed in etiolated rice coleoptiles. In addition to the

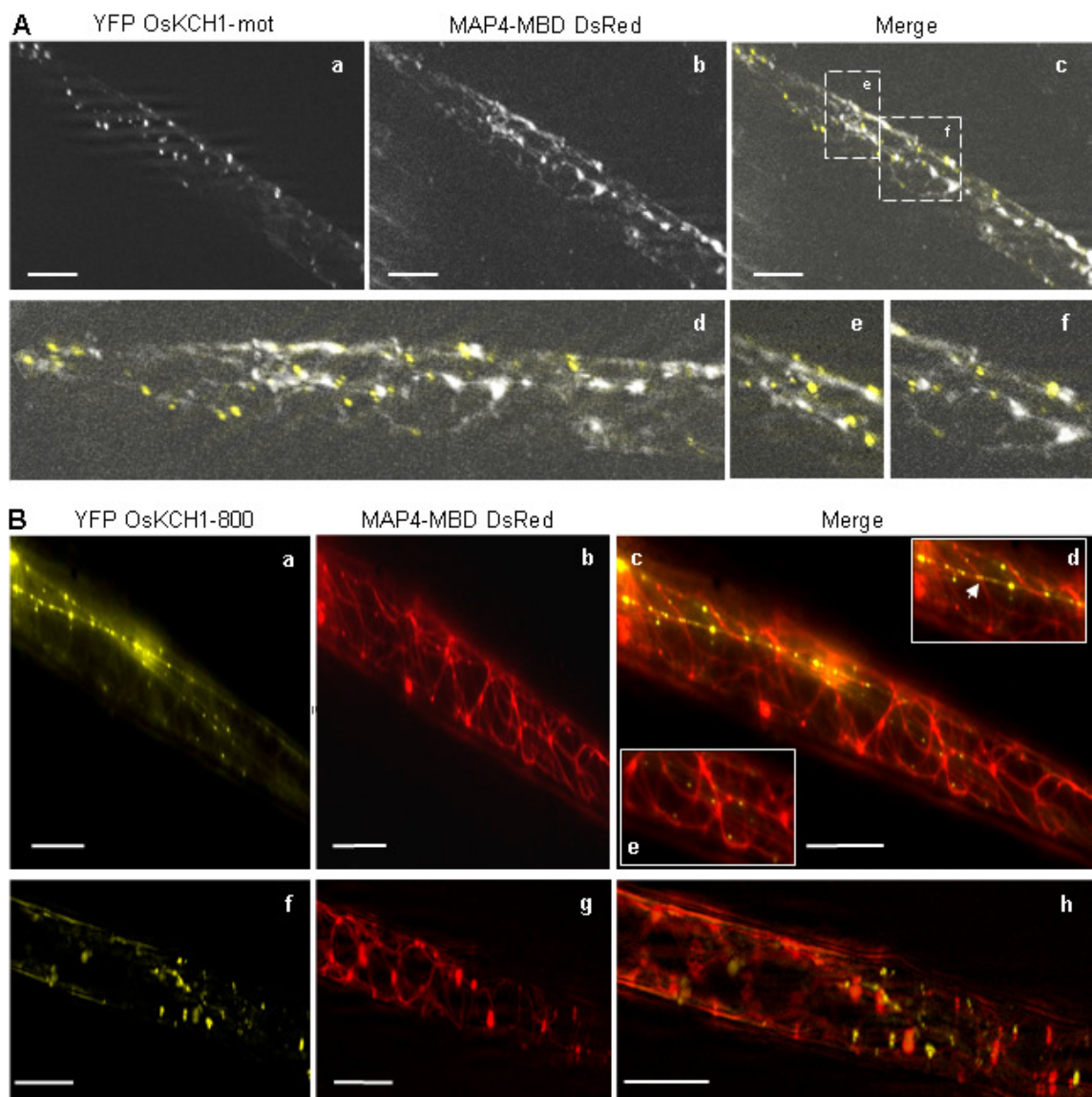


Fig. 11: Colocalization of *OsKCH1* with microtubule markers in rice coleoptile cells

[A] Transient coexpression of *OsKCH1*-mot (encoding the motor domain) in fusion with YFP, and the microtubule marker MAP4-MBD in fusion with DsRed. *OsKCH1*-mot labels microtubules in a punctate manner (c-f). [B] Transient coexpression of *OsKCH1*-800, encoding both the CH and the motor domain in fusion with YFP, and MAP4-MBD in fusion with DsRed in rice coleoptile. The punctate pattern of *OsKCH1*-800 decorates microtubules in the cell periphery (c, e, h), but additionally labels longitudinally oriented filamentous structures that are not stained by the microtubule marker (d). Punctate *OsKCH1*-800 signals accumulate often at crossings between microtubules and these filamentous structures (arrow in d). Scale bar = 20 μ m.

full-length construct, the truncated constructs OsKCH1-mot, encoding only the kinesin motor core, and OsKCH1-ch, harboring the N-terminal part of the protein with the CH domain, were transformed in order to assign localization pattern to individual protein domains. The truncated OsKCH1-mot construct was found to colocalize with microtubules and to label them in a punctate manner (Fig. 11 A, c-f). The signals were especially concentrated in the cortical regions. By contrast, YFP OsKCH1-ch did not show colocalization with microtubules (Fig. 12 B, c-f), but accumulated around the nucleus and labeled filamentous structures that reached from the nucleus to the periphery (Fig. 12 B, a). The full-length construct YFP OsKCH1-800 produced a punctate pattern of fluorescence that colocalized with the microtubule marker. Again, the fluorescence was seen most clearly in the cell cortex (Fig. 11 B, c-e, h). Interestingly, YFP OsKCH1-800 as well labeled longitudinally oriented filamentous structures that were clearly not stained by the microtubule marker (Fig. 11 B, c and d). Furthermore, strong punctate signals were often found at crossings between microtubules and the non-microtubular filaments (Fig. 11 B, c-e).

To test whether the localization of OsKCH1-800 was dependent on the integrity of microtubules pharmacological treatments were performed. We investigated the effects of the microtubule polymerization inhibitors oryzalin (Fig. 14 A) and colchicine (data not shown) on stably transformed tobacco BY-2 cells expressing OsKCH1-800 as fusion with GFP. At 2.5 hours after addition of 10 μ M oryzalin, the majority of GFP OsKCH1-800 signals along fine filamentous structures within the cells was lost and only diffuse signals could be detected (Fig. 14 A, b, g, h). Meanwhile, most signals along thicker, longitudinally oriented filament bundles and on filament networks surrounding the nucleus were still present (Fig. 14 A, b, g and h). Punctate signals in the cell cortex were furthermore clearly diminished after oryzalin treatment, however

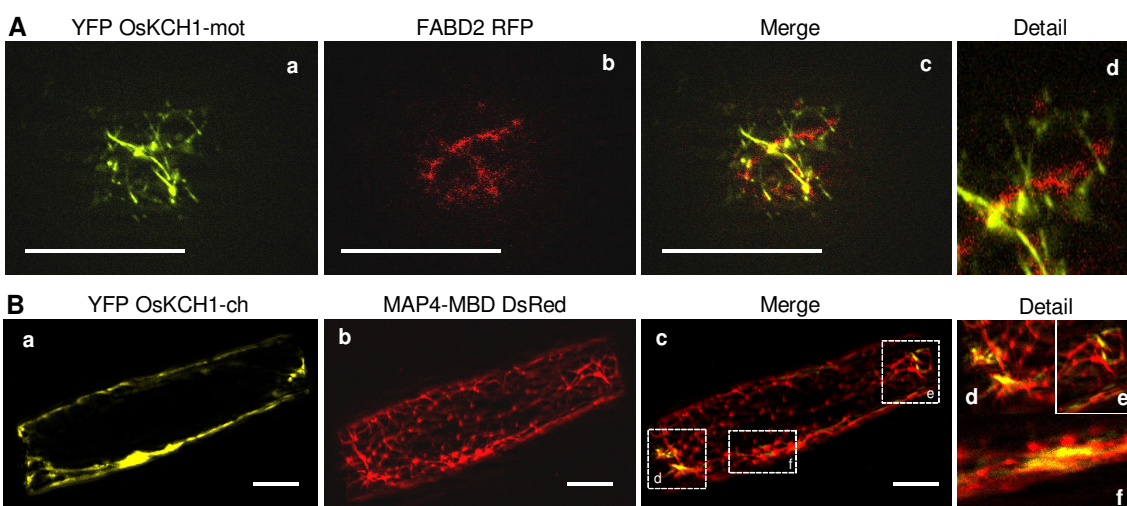


Fig. 12: Transient coexpression of truncated versions of *OsKCH1* with microtubule and actin markers

[A] Coexpression of OsKCH1-mot (encoding the motor domain) in fusion with YFP, and the actin filament marker FABD2 in fusion with RFP in tobacco BY-2 cells. OsKCH1-mot labels filamentous structures in the cortex of a BY-2 cell that do not colocalize with the red signals of the actin marker (c, d). [B] Coexpression of OsKCH1-ch (encoding the CH domain) in fusion with YFP and MAP4-MBD in fusion with DsRed. No colocalization is observed. Scale bar = 20 μ m.

not totally eliminated (Fig. 14 A, g and h). In contrast, OsKCH1-800 signals were clearly preserved in control cells incubated for 2.5 hours under the same conditions but in the absence of the drug (Fig. 14 D, b and c, e).

2.1.3 OsKCH1-800 colocalizes with longitudinally oriented actin filaments

Coexpression experiments with YFP OsKCH1-800 and MBD-MAP4 DsRed showed a colocalization of the protein with microtubules but as well with filamentous pattern that were not associated with the microtubule marker. In order to investigate, whether these filamentous targets of OsKCH1-800 might be actin filaments, OsKCH1-800 in fusion with YFP was transiently coexpressed with an RFP fusion of the actin marker FABD2 in etiolated rice coleoptiles and tobacco BY-2 cells.

Again, the two truncated OsKCH1 constructs were used in parallel to test for the protein domains necessary for localization. The motor domain construct YFP OsKCH1-mot was found to decorate cortical, filamentous structures that were clearly not stained by FABD2 RFP (Fig. 12 A, c and d). The full-length construct YFP OsKCH1-800, by contrast, colocalized in a punctate pattern with actin filaments that either surrounded the nucleus or were bundled and longitudinally oriented (Fig. 13 A, c, f and g). These observations were further supported by TRITC-phalloidin staining of tobacco BY-2 cells that stably expressed GFP OsKCH1-800. Here, OsKCH1-800 preferentially decorated perinuclear actin filaments and thick actin bundles that reached from the nucleus to the periphery (Fig. 13 B, c-e). While OsKCH1-800 matched the actin marker at the nucleus and on prominent actin bundles, a punctate pattern of OsKCH1-800 fluorescence was found in the cell midplane and the cell cortex that did not show a signal overlap with the actin marker (Fig. 13 B, c-e). This finding is analogous to the observation made during the coexpression of OsKCH1-800 and the microtubule marker MBD-MAP4. Here only a certain proportion of filamentous OsKCH1-800 signals could be attributed to microtubules, whereas a significant part labeled filaments that were not associated with microtubules.

To test, whether the localization of OsKCH1-800 was dependent on the integrity of actin filaments, tobacco BY-2 cells stably expressing OsKCH1-800 as fusion with GFP were treated with the actin polymerization inhibitors latrunculin B (10 μ M; Fig. 14 B) and cytochalasin D (100 μ M; data not shown). For both inhibitors, 2 hours after treatment the majority of the punctate OsKCH1-800 signals on perinuclear and longitudinal filaments had disappeared and was replaced by a diffuse distribution of the GFP signal (Fig. 14 B, b and d, g and i). The punctate fluorescence in the cell cortex and on fine filaments in the cell midplane, however, was not affected and thus appeared to be independent of an intact actin cytoskeleton. Again, in control cells incubated for 2 hours under the same conditions, but in the absence of inhibitors, OsKCH1-800 signals were clearly preserved (Fig. 14 D, b and c, e).

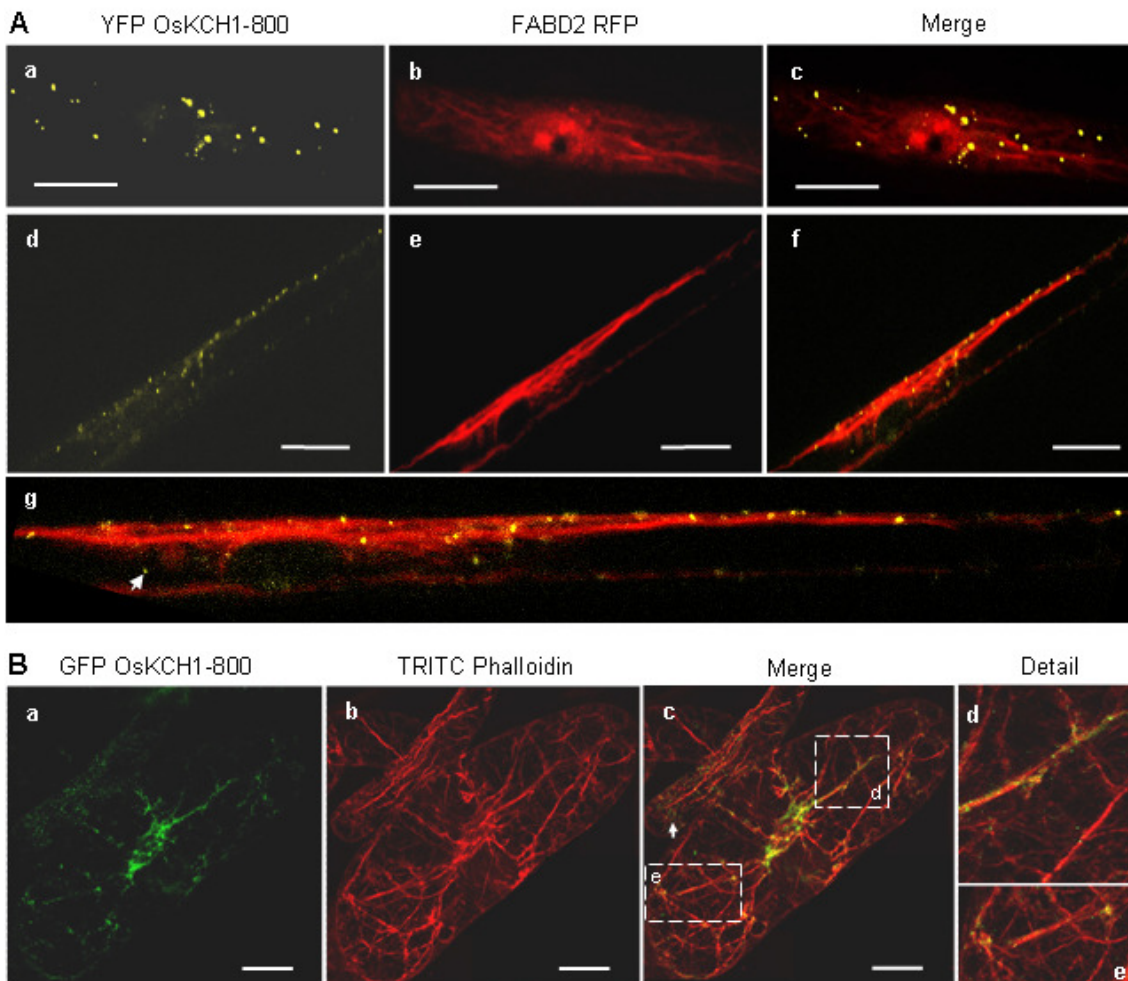


Fig. 13: Colocalization of *OsKCH1* with actin markers in rice coleoptiles and tobacco BY-2 cells

[A] Transient coexpression of *OsKCH1*-800 in fusion with YFP and the actin-filament marker FABD2 in fusion with RFP in rice coleoptile. Colocalization of signals can be seen in a punctate manner along longitudinal actin filaments (c and blow-up in d). Note that at several points the punctate *OsKCH1*-800 signals do not overlap with FABD2 RFP (arrow in d). [B] TRITC-phalloidin staining of actin filaments in BY-2 cells stably expressing GFP *OsKCH1*-800. The punctate signals of *OsKCH1*-800 especially decorate perinuclear actin filaments (c) and actin bundles that tether the nucleus to the periphery (c, d). Note that again at several points, mainly in the cell cortex, the punctate *OsKCH1*-800 signals show no overlap with TRITC-phalloidin. Scale bar = 20 μm .

Treatments of tobacco BY-2 cells stably expressing *OsKCH1*-800 as fusion with GFP with a combination of the microtubule polymerization inhibitor oryzalin (10 μM) and the actin drug latrunculin B (10 μM) resulted in a complete loss of defined fluorescent signals and their replacement by diffuse GFP signals after two hours of incubation (Fig. 14 C, b, e, g), indicating the interdependence of the *OsKCH1* localization pattern with the actin and microtubular networks.

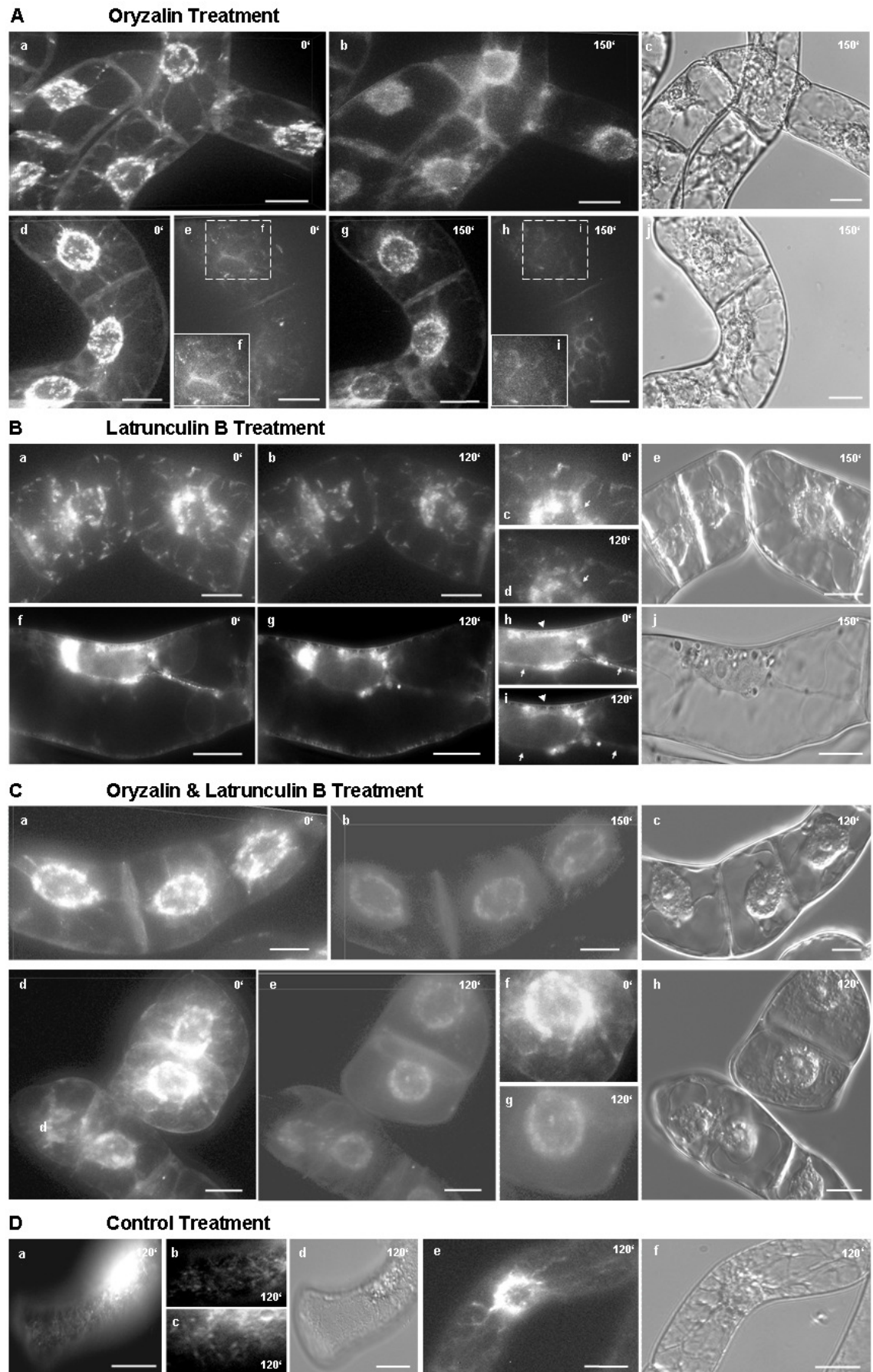


Fig. 14: Response of BY-2 GFP OsKCH1-800 cells to treatments with microtubule and actin drugs (continued on following page)

Fig. 14 continued:

[A] Treatment of tobacco BY-2 cells stably expressing GFP OsKCH1-800 with the microtubule drug oryzalin. Signal localization is shown for two representative samples at 0 min (a, d-f) and 2.5 h (b, c, g-j) after addition of the drug. At 0 min clear OsKCH1-800 signals can be found on filamentous structures in the cells (a and d) and additionally as punctate pattern at the cell periphery (f). After incubation with 10 μ M oryzalin many of the fine filamentous structures within the cells are lost and replaced by diffuse signals. A residual signal is still present, showing independence of microtubules. Additionally, at the periphery only at few points fluorescent stubs are left (f versus i). [B] Treatment of tobacco BY-2 cells stably expressing GFP OsKCH1-800 with 10 mM latrunculin B. Signal localization is shown for two representative samples at 0 min (a, c, f, h) and 2 h (b, d, g, i) after addition of the drug. The treatment clearly alters the punctate perinuclear OsKCH1-800 signals and the signals between nucleus and periphery (arrows; c versus d, h versus i), while OsKCH1-800 signals at the cortical region are still present to some extent (arrow heads; d and e). [C] Combined treatment of tobacco BY-2 cells stably expressing GFP OsKCH1-800 with oryzalin and latrunculin B. Signal localization is shown for two representative samples at 0 min (a, d, f) and 2 h (b, e, g) after addition of the drugs. Note that after 2 h of incubation the majority of OsKCH1 signals at fine filamentous structures within the cell, at the cortex, and surrounding the nucleus have been lost and replaced by diffuse fluorescence. Only residual fractions of the signal remain specifically localized. [D] Control treatments incubated for 2 h in a similar way, but without addition of drugs do not show any signal loss (b, c, e). Scale bar = 20 μ m.

2.2 Recombinant KCH1 cosediments *in vitro* with microtubules and actin

The colocalization experiments had shown that the full-length construct OsKCH1-800 was able to decorate both microtubules and actin microfilaments. The truncated constructs OsKCH1-mot and OsKCH1-ch, in contrast, showed localization pattern that were limited to only one type of cytoskeletal element. This observation points towards a domain-dependency of the interaction and it was therefore important to further verify the binding ability of different domains of OsKCH1 to either actin microfilaments or microtubules. For this purpose *in vitro* cosedimentation assays were performed with recombinantly expressed full-length and truncated OsKCH1 proteins.

2.2.1 OsKCH1 can be recombinantly expressed and purified

A variety of histidine-tagged versions of OsKCH1 was generated for recombinant protein expression. Each of the following constructs comprised different domains of the protein: KCH1-sh (residues 1-250), KCH1-cc1 (residues 1-319), KCH1-cc2 (residues 1-398), KCH1-mot (residues 300-800) and KCH1-cc3 (residues 1-769), as shown in Fig. 15 A. The proteins were solubly expressed in *E. coli*, affinity purified from the cellular extracts via Ni-NTA agarose, and analyzed via SDS-PAGE and Western blotting (Fig. 15 B).

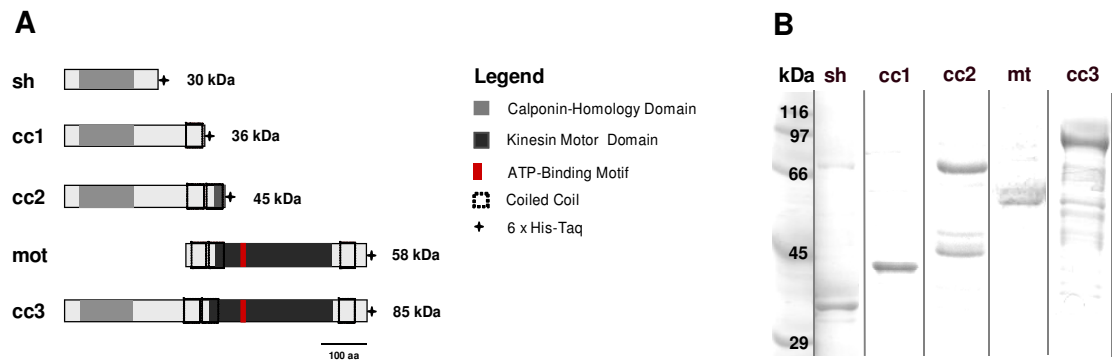


Fig. 15: Expression of recombinant KCH1 proteins

[A] Schematic diagram of domain organization in the recombinantly expressed OsKCH1 variants sh (aa 1-250), cc1 (aa 1-319), cc2 (aa 1-398), mot (aa 300-800), and cc3 (aa 1-769). [B] SDS-PAGE gels stained with Coomassie Brilliant Blue show the recombinantly expressed OsKCH1 variants after purification by Ni-NTA agarose.

2.2.2 OsKCH1 cosedimentation is domain-dependent

The different recombinantly expressed proteins were subsequently tested for their ability to bind to actin and microtubules via *in vitro* cosedimentation assays.

As visible in Fig. 16, the longest construct, KCH1-cc3, which contains the CH domain, the motor core and all putative coiled-coil stretches, showed cosedimentation with both microtubules and actin filaments. In control experiments in absence of microtubules or actin, however, the protein remained predominantly in the supernatant.

The construct KCH1-mot contained the entire protein part upstream of the CH domain, including the motor core and all putative coiled-coil regions. KCH1-mot cosedimented with microtubules, but remained largely in the supernatant in actin-binding assays and control experiments (Fig. 16 A). This underlines the importance of the CH domain for actin-binding. Conversely, the truncated proteins KCH1-cc1 and KCH1-cc2 did not cosedimentation with microtubules. KCH1-cc1 contains only the N-terminal portion of the protein with the CH domain and the first coiled-coil stretch. KCH1-cc2, in addition, includes the second coiled-coil stretch. The motor core, however, is absent in both proteins, underlining the importance of this domain for microtubule-binding.

Both truncated proteins KCH1-cc1 and KCH1-cc2 (data not shown), by contrast, clearly sedimented with actin (Fig. 16 A). Interestingly, the smallest protein truncation, KCH1-sh, including the CH domain but neither the coiled-coil regions nor the motor core, showed only minor sedimentation with actin (data not shown). This indicates that the presence of the first two coiled-coil stretches within the protein is of particular significance for the efficiency of actin-binding. Again, in control experiments without actin the protein was mainly found in the supernatant.

In summary, these results demonstrate the importance of the N-terminal part of OsKCH1, including the CH domain and the first two coiled-coil stretches, for the specific interaction with actin microfilaments. The central protein fragment comprising the motor core, by contrast, seems to be required for microtubule-binding.

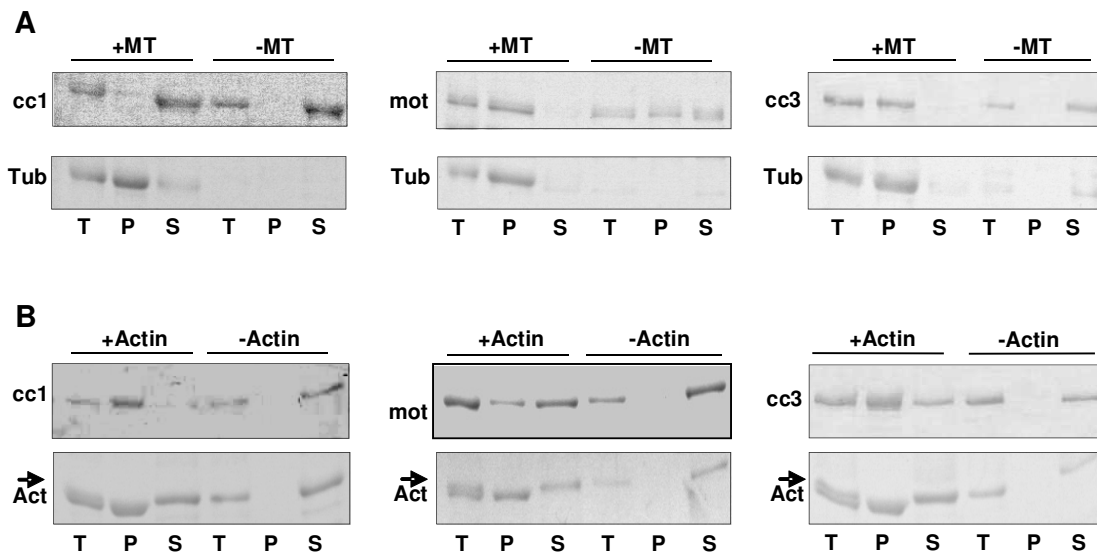


Fig. 16: *Cosedimentation with microtubules and actin microfilaments*

[A] SDS-PAGE gels stained with Coomassie Brilliant Blue of a series of microtubule-binding assays with recombinant OsKCH1 variants encoding either the N-terminal part containing the CH domain (KCH1-cc1), the central part containing the motor domain (KCH1-mot), or both domains (KCH1-cc3). In control experiments without microtubules, all proteins were predominantly found in the supernatant (S). In presence of microtubules, KCH1-mot and KCH1-cc3 were enriched in the precipitates (P). KCH1-cc1, however, did not cosediment with microtubules. For comparison, samples of the mixtures prior centrifugation are as well shown on the gels (T). [B] SDS-PAGE gels stained with Coomassie Brilliant Blue of a series of actin-binding assays with recombinant KCH1 variants of different domains and sizes. After incubation with 1.5 μ M actin microfilaments, KCH1-cc1 and KCH1-cc3 clearly sedimented. In case of KCH1-mot, however, the majority of protein was found in the supernatant. As the protein purifications show minor impurities, an additional protein band of slightly higher molecular weight than actin can be found on the gels in the total and supernatant fractions of the actin-cosedimentation, as well as in the control experiment (marked by an arrow). The protein contamination, however, did not cosediment with actin into the pellet fractions and thus could be neglected.

3 Characterization of the biological role of OsKCH1

As shown in the previous sections, KCHs are highly conserved in structure and function within higher plants and the moss *Physcomitrella patens*. Their ability to bind microtubules and microfilaments makes them interesting candidates for bifunctional mediation between both cytoskeletal elements – a necessary process during plant growth and development. The biological role of KCH proteins has, however, remained elusive so far, although a possible involvement in cotton fiber elongation has been postulated for GhKCH2 (Xu et al., 2009). The putative biological functions of the rice KCH member OsKCH1 were therefore addressed in the course of this work by investigation of both rice *Tos17 kch1* knock-out mutants and a *KCH* overexpression line generated in tobacco BY-2 cells. Additionally, tissue- and development-specificities were analyzed for *OsKCH1* gene expression and all findings further verified by microscopic studies.

3.1 *OsKCH1* gene expression is regulated during development

In order to get insight into potential physiological roles of OsKCH1, the gene expression pattern of *OsKCH1* was quantified in rice in different tissues and developmental stages by real-time PCR. Clear differences in gene expression pattern were detected as shown in Fig. 17. The highest abundance of transcripts was found in tissues with meristematic activity such as primary leaf, primary root, and the developing flower. Additionally, transcripts were abundant in the coleoptile, a rapidly expanding organ exclusively growing via cell elongation.

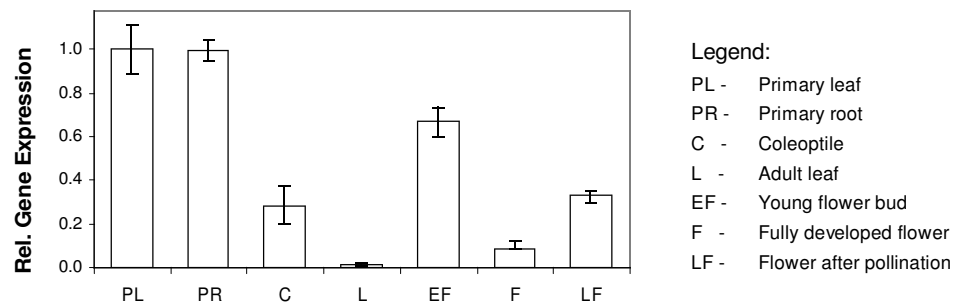


Fig. 17: Gene expression pattern of *OsKCH1* in rice

Expression of *OsKCH1* in rice seedlings and adult plants of the wildtype *Oryza sativa* ssp. *japonica* cv. Nipponbare measured by real-time PCR.

3.2 *kch1* insertion mutants show impaired cell expansion

For further biological characterization of *OsKCH1* a loss-of-function approach was chosen and the rice *Tos17* database (<http://tos.nias.affrc.go.jp>; Miyao et al., 2003) was searched for putative mutants. Two independent mutant lines, NF9840 (*kch1-1*) and NG1558 (*kch1-2*), were identified and showed retrotransposon insertion sites in the 13th and 14th exon of the *OsKCH1* locus, respectively (Fig. 18 A). Heterozygous seeds were obtained from the National Institute of Agro-biological Science (NIAS, Tsukuba, Japan) and segregating mutants and wildtypes were identified by genotyping (Fig. 18 B).

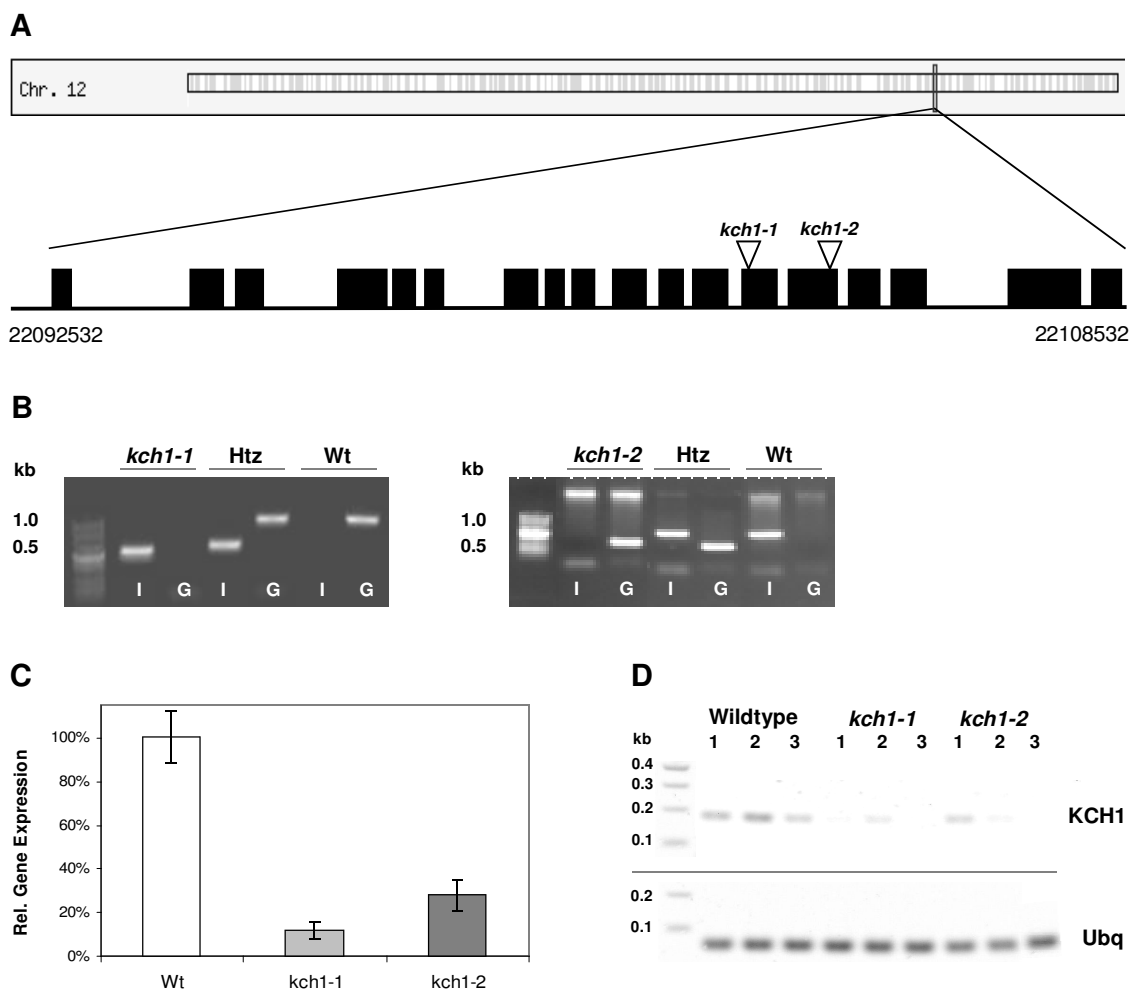


Fig. 18: Genetic analysis of rice *Tos17* lines *kch1-1* and *kch1-2*

[A] Schematic representation of the *OsKCH1* gene structure. Introns are shown as lines, exons as boxes. Positions of *Tos17* insertion sites in *kch1-1* and *kch1-2* are indicated by arrow heads. [B] Representative PCR-based genotyping of segregating populations of the *Tos17* lines *kch1-1* and *kch1-2*. The presence or absence of PCR products for the amplification with gene-specific (G) and insert-specific (I) primers was analyzed using agarose gels. [C] Expression of *OsKCH1* in *Tos17* insertion mutants quantified by real-time PCR in RNA extracts from complete seedlings of the mutant lines *kch1-1* and *kch1-2* as compared to the wildtype control. Additionally, a representative RT-PCR [D] shows the abundance of *OsKCH1* transcripts in seedlings of the wildtype as compared to the mutants *kch1-1* (1) and *kch1-2* (2). Ubiquitin (Ubq) was used as internal standard in all samples.

To estimate the remaining gene expression activity in the *Tos17* mutants, *OsKCH1* gene expression levels were quantified in seedlings of the mutants *kch1-1* and *kch1-2*, and in wildtype seedlings for comparison. As shown in Fig. 18 C and D, transcript abundance in entire rice seedlings was clearly reduced to about 10-25 % of wildtype expression in both *Tos17* lines.

To identify potential morphological phenotypes, etiolated coleoptiles of *kch1-1* and *kch1-2* were investigated. The rice coleoptile represents a system highly suitable for phenotyping studies as they grow rapidly and homogeneously, and are physiologically characterized in great detail (Holweg et al., 2004). The cells that constitute the coleoptile are all formed during late embryogenesis, and following germination no further division occurs. Thus, rice coleoptile growth relies exclusively on cell elongation and therefore records sensitively even small differences in cell growth rates. As shown in Fig. 19 A, coleoptiles were about 10 % shorter in *kch1-1* and *kch1-2* mutants as compared to the segregating wildtypes, to heterozygous plants, or to non-transformed *Oryza sativa* ssp. *japonica* cv. Nipponbare wildtype seedlings. This observed phenotype might either result from a diminished or delayed elongation growth, producing shorter cells in the mutants, or from a reduced number of cells. In order to discriminate between the two alternatives, the average cell length was measured in tangential sections from either the apical or the basal third of the coleoptile (Fig. 19 B). As visible in Fig. 19 C, the average cell length was clearly reduced in both mutant lines with respect to wildtype coleoptiles. This difference was most prominent in the basal region, where mutant cells reached only about 60 % of the length observed in the wildtypes. The observed strong reduction in cell length in the *kch1* insertion mutants was, however, almost compensated by a concomitant increase in the average cell number per coleoptile (Fig. 19 D).

During subsequent development, however, no additional prominent phenotypes were identified. Both mutant and wildtype plants showed normal growth, flowering and seed production under constant long-day conditions.

To test whether the lack of a phenotype in adult plants might be due to functional redundancy between different KCHs, the molecular phylogeny of known KCH members was analyzed. Fig. 20 shows a phylogenetic tree displaying the relationship between KCHs from the grass model plant *Oryza sativa*, the Rosids *Arabidopsis thaliana*, *Populus trichocarpa*, *Vitis vinifera*, *Ricinus communis*, and the moss *Physcomitrella patens*. KCH from higher plants cluster into 4 different clades that each contain at least one KCH member from all species. *OsKCH1* sorts into the most expanded branch, together with two additional KCH family members from rice, indicating a close relation and possibly conserved functions among these proteins. Interestingly, the KCH members from *Physcomitrella* were not resolving into the four prominent clades, but form a solitary branch, indicating evolutionary divergence of these proteins.

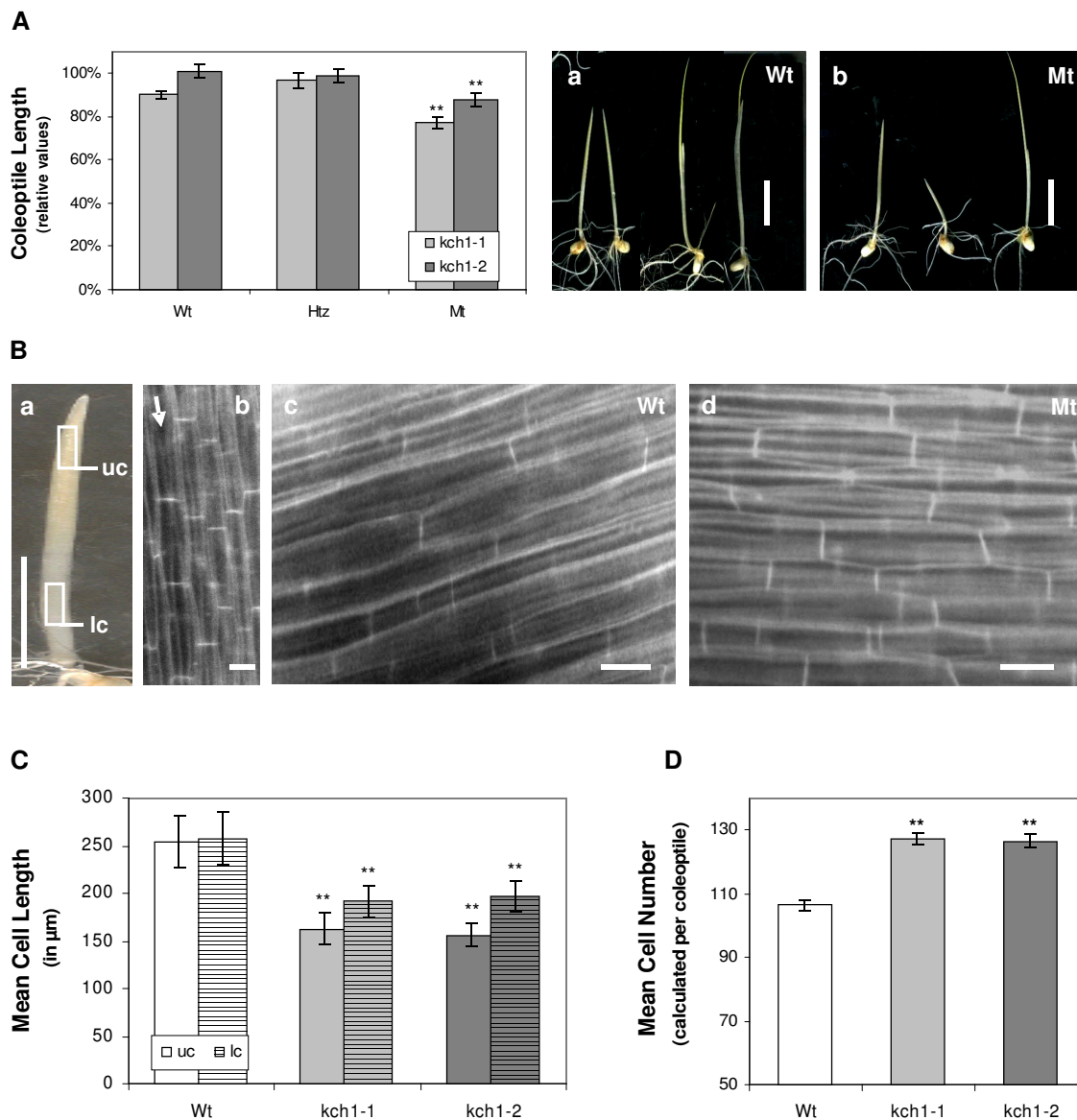


Fig. 19: Phenotypes of *Tos17* insertion mutants

[A] Coleoptile length in etiolated seedlings 7 d after germination. For both mutant lines *kch1-1* (light gray) and *kch1-2* (dark gray) in addition to homozygous mutant plants (Mt), heterozygotes (Htz) and segregating wildtypes (Wt) were analyzed. Coleoptile lengths were plotted relative to the length measured for the cultivar *Oryza sativa* ssp. *japonica* cv. Nipponbare that represents the background for the mutants. Mean values \pm SE of a total of at least 50 measurements are given, collected cumulatively over several independent experimental series. Asterisks (**) indicate significant differences ($P < 0.01$) in both mutant lines between Mt and Wt/Htz as assessed by a t-test for unpaired data. Representative images of both Wt (a) and Mt (b) seedlings. Scale bar = 10 mm. [B+C] Cell length measurements in coleoptiles of etiolated seedlings 7 d after germination for *kch1-1* (light gray), *kch1-2* (dark gray) and wildtype (Wt, white) plants, determined in the upper part (uc, open bars) and in the lower part (lc, hatched bars) of the coleoptile as indicated in (a). Data represent mean values \pm SE of a total of at least 150 analyzed cell files, collected from 15 coleoptiles. Asterisks (**) indicate significant differences ($P < 0.01$) between Mt and Wt as assessed by a t-test for unpaired data. Representative fluorescence images of coleoptile cells are shown in (c) for the wildtype and in (d) for the mutant. Scale bars = 10 mm in (a); 20 μ m in (b)-(c). [D] Mean cell numbers in coleoptiles of etiolated seedlings 7 d after germination for *kch1-1* (light gray), *kch1-2* (dark gray) and wildtype (Wt, white) plants. Mean values \pm SE were estimated from the cell lengths determined in a total of at least 150 analyzed cell files as described in [C]. Asterisks (**) indicate significant differences ($P < 0.01$) between Mt and Wt in t-tests for unpaired data.

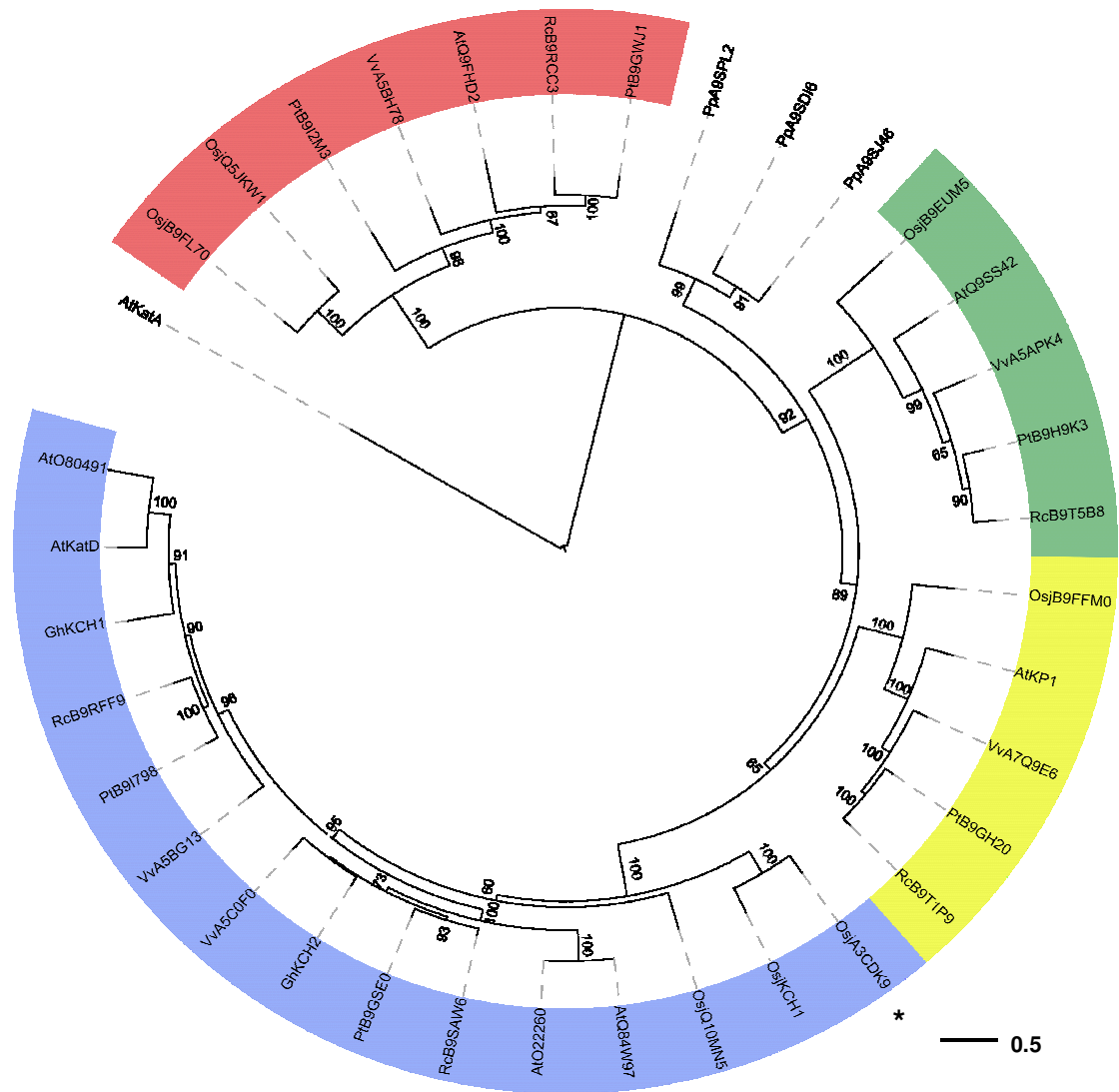


Fig. 20: Phylogenetic analysis of KCH family members

Phylogenetic tree for the KCH family members from several higher plants and from the moss *Physcomitrella patens* obtained by a maximum likelihood approach with random stepwise addition of protein sequences and arbitrary rooting using the Kin-14A family member *AtKatA* as outgroup (Marcus et al., 2002). Bootstrap support values were obtained from 100 replicates and only values greater than 50 are shown in the tree. KCH members from higher plants cluster into four clades, all shaded in different colors. *OsKCH1* (marked by an asterisk) resolves into the most expanded branch, together with two additional KCH family members from rice. Abbreviations: Osj – *Oryza sativa* ssp. *japonica*, At – *Arabidopsis thaliana*, Gh – *Gossypium hirsutum*, Vv – *Vitis vinifera*, Pp – *Physcomitrella patens*, Pt – *Populus trichocarpa*, Rc – *Ricinus communis*. All protein sequence data were obtained from Swiss-Prot/TrEMBL.

3.3 *KCH1* overexpressors show impaired cell division

The expression pattern of *OsKCH1* in rice, along with the observed coleoptile phenotype of rice *kch1* mutants, would allow two different interpretations of the function of OsKCH1. The protein could either be involved in cell division during late embryogenesis when the coleoptile is laid down, or during postgerminative growth when the coleoptile cells expand. In order to further discriminate between these two possibilities, the effect of an overexpression of OsKCH1 on cell division or cell elongation should be investigated. Since rice coleoptiles grow exclusively via cell elongation, they do not represent an adequate model system for this question. We therefore turned towards the well-characterized and reliable tobacco BY-2 system, as widely studied model for cycling cells (Nagata et al., 1992).

As already described in detail in section 2.1.1, a tobacco BY-2 cell line (BY-2 KCH1) was generated that stably expressed a fusion of a GFP reporter with OsKCH1, driven by the constitutive CaMV-35S promoter. The functionality of the exogenously expressed OsKCH1 protein in BY-2 was verified by investigation of intracellular localization pattern of this GFP fusion. As visible

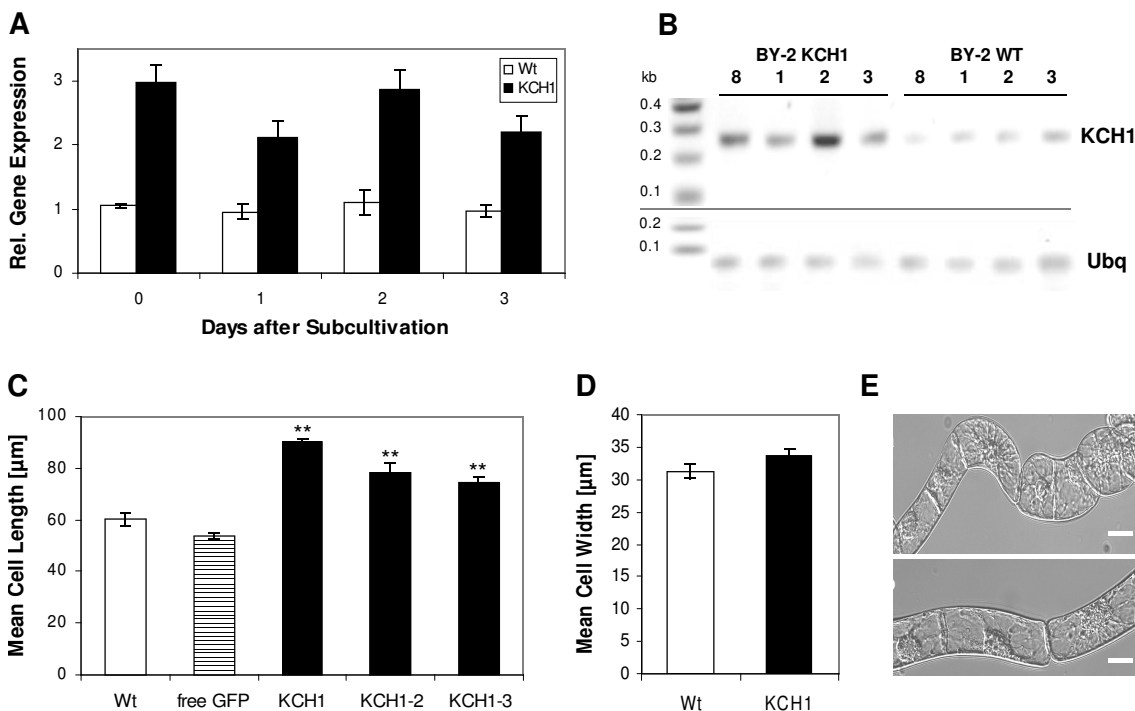


Fig. 21: BY-2 cells overexpressing *OsKCH1* are more elongated than wildtype cells

[A] Relative gene expression of KCH in non-transformed BY-2 wildtype cells (Wt, white) and BY-2 cells stably overexpressing *OsKCH1* (KCH1, black). [B] Representative RT-PCR detection of KCH expression levels in BY-2 Wt and BY-2 KCH1. Ubiquitin (Ubq) was used as internal standard in all samples. [C] Cell length in BY-2 Wt (white), BY-2 free GFP (hatched) and three independent lines overexpressing *OsKCH1*, BY-2 KCH1, BY-2 KCH1-2 and BY-2 KCH1-3 (all black). Mean values \pm SE of a total of 300 analyzed cells per sample, collected cumulatively in 3 independent experimental series are given. Asterisks (**) indicate $P < 0.01$ as evaluated by a t-test for unpaired data. [D] Cell width in BY-2 Wt and BY-2 KCH1. For details refer to [C]. [E] Representative DIC images of (a) BY-2 Wt and (b) BY-2 KCH1 cells to show the differences in cell length. Scale bars = 20 μm .

in Fig. 10 and Fig. 14, the protein clearly localized in a punctate pattern to both microtubules and actin filaments, emphasizing the functionality of the protein in the heterologous system.

Since sequence information for tobacco homologues of *OsKCH1* are not available yet, the expression levels of *KCH* genes in BY-2 had to be assessed with degenerated primers that were designed using an alignment of *KCH* sequences from rice, *Arabidopsis*, cotton, *Vitis* and *Populus* as template. The primers were tested for their general performance on rice cDNA and specifically amplified the region of interest, as verified by sequencing. The primer functionality was further verified on tobacco BY-2 wildtype cDNA, and the obtained PCR products were additionally analyzed by sequencing. The primer amplified sequence stretches from tobacco BY-2 that were highly similar to the target *KCH* sequences from the other plants and thus most likely correspond to the expected region tobacco (for details see Fig. 34 in appendix). The abundance of *KCH* transcripts was then measured by semiquantitative RT-PCR in both BY-2 Wt and BY-2 KCH1 cells at different stages of the cell cycle. In BY-2 KCH1 the *KCH* expression level was consistently elevated about 2.5- to 3-fold as compared to the non-transformed Wt cells (Fig. 21 A+B), confirming overexpression of the transgene.

The BY-2 KCH1 cell line grew homogeneously at a normal growth rate and generated the pluricellular files typical for BY-2. However, a detailed phenotypic investigation showed that BY-2 KCH1 cells were about 1.5 fold longer than the non-transformed BY-2 Wt cells (Fig. 21 C+E). In contrast, the cell width was not significantly altered (Fig. 21 D+E). The observed morphology in BY-2 KCH1 was underlined by investigation of two additional BY-2 cell lines KCH1-1 and KCH1-2, which had been independently transformed with the same reporter construct and yielded similar elongation phenotypes (Fig. 21 C).

To test whether this altered morphology was caused by overexpression of a transgene *per se*, all phenotypical traits were assessed and quantified in a cell line stably expressing free-GFP under control of a CaMV-35S promoter. This line, however, did not show any significant differences to the non-transformed BY-2 Wt (Fig. 21 C), suggesting that the observed elevated cell elongation in BY-2 KCH1 cells is a specific effect.

3.4 KCH1 overexpressors show delayed but morphologically normal mitosis

In order to investigate whether the observed increase in cell length might be caused by alterations in mitosis, the mitotic index (MI) was followed through the culture cycle in both BY-2 KCH1 and BY-2 Wt. As shown in Fig. 22 A, the MI in BY-2 KCH1 was decreased at day 1 and 2 as compared to the non-transformed wildtype. From day 3 on, however, the MI reached the wildtype level and remained similar to the wildtype levels for the rest of the analyzed period. This indicated that the onset of the growth phase was delayed in BY-2 KCH1, but subsequently proceeded normally.

The functionality of mitosis was further confirmed by microscopic investigation and comparison of mitotic spindle structures in BY-2 KCH1 and BY-2 Wt. For this purpose, microtubules were stained by immunofluorescence in both cell lines, and chromosomes were visualized by Hoechst. As shown in Fig. 22 B, spindle microtubules in BY-2 KCH1 appeared completely normal and the spindle apparatus showed no structural alterations from the non-transformed wildtype. Thus, mitosis in general did not seem to be disturbed by overexpression of OsKCH1, its onset, however, was delayed.

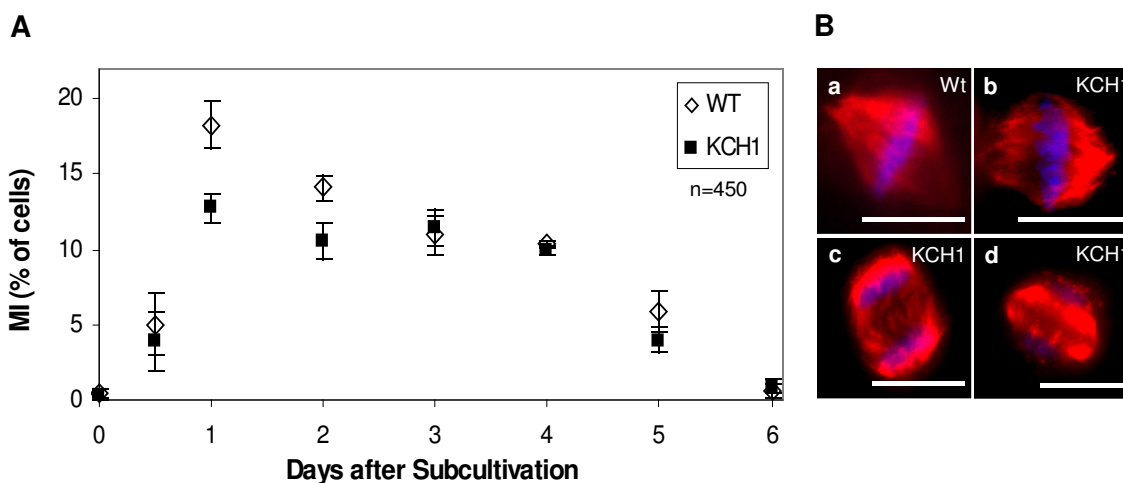


Fig. 22: Analysis of mitosis in BY-2 Wt and BY-2 KCH1

[A] Time course of mitotic indices (MI) in BY-2 Wt and BY-2 KCH1. Mean \pm SE are given in percent of cells of a total of 450 analyzed cells per time-point and sample, collected cumulatively from 3 independent experimental series with 150 cells per series. [B] Microscopic analysis of mitotic spindles in BY-2 Wt (a) and BY-2 KCH1 (b-d). Microtubules were stained by immunofluorescence, DNA was visualized by Hoechst staining. Scale bars = 20 μ m.

3.5 OsKCH1 is dynamically repartitioned during the cell cycle

In order to further assess a potential role of KCH1 in the cell cycle, the localization of GFP-OsKCH1 was followed through the cell cycle in tobacco BY-2 cells (Fig. 23, Fig. 24). As visible

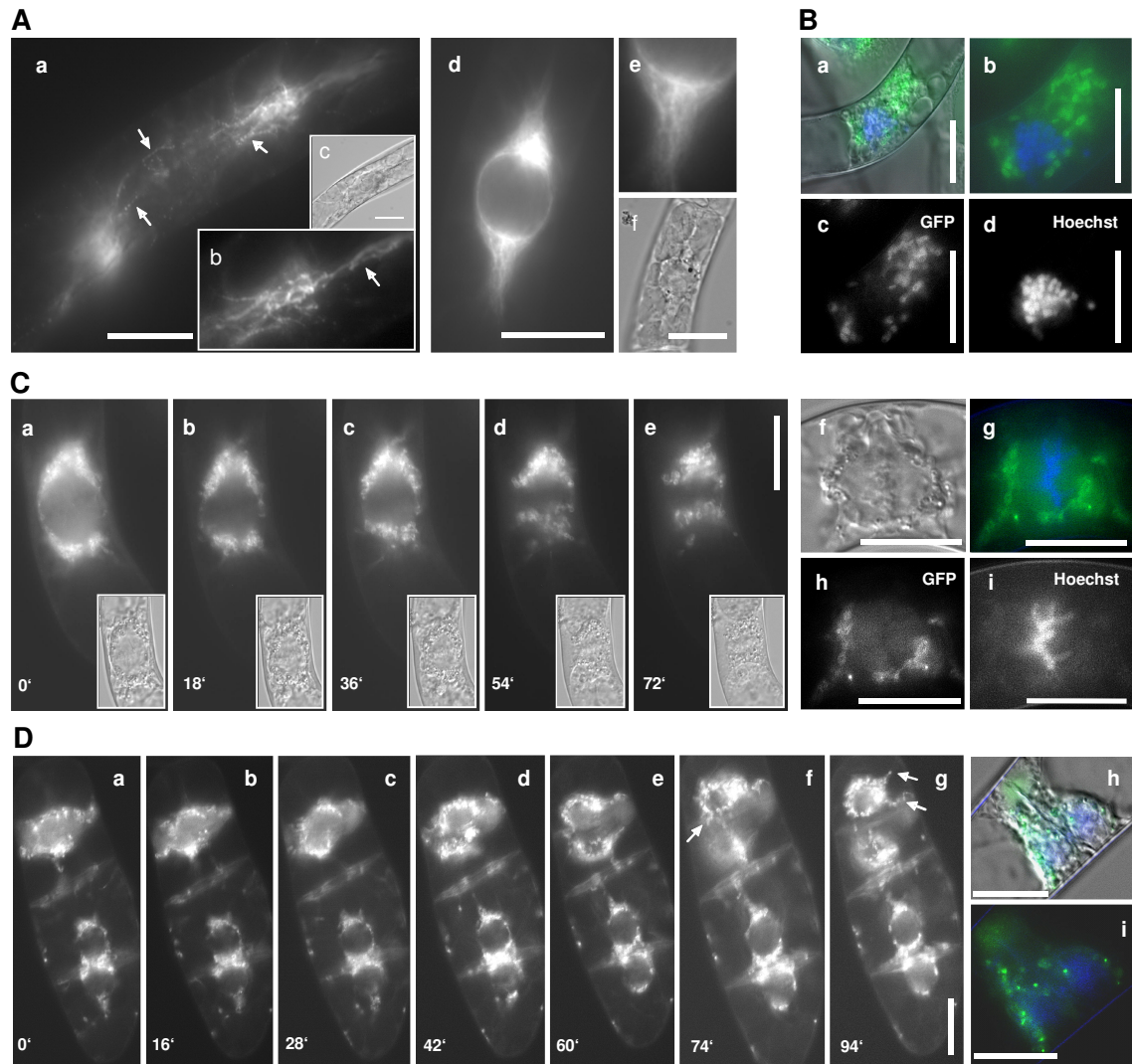


Fig. 23: Localization of *OsKCH1* during mitosis

[A] Transient expression of a YFP-fusion with OsKCH1-800 in tobacco BY-2 cells. Optical sections through the cell midplanes of premitotic BY-2 cells at different focus levels (a+b, d+e). The corresponding DIC images are given in (c, f). Arrows highlight punctate pattern on perinuclear filaments. [B-D] Pre-prophasic and prophasic tobacco BY-2 cells stably expressing a GFP-fusion with OsKCH1-800. The DNA was stained with Hoechst to determine the stage of mitosis. [B] Section through the cell midplane. Merge images of GFP (c) and Hoechst (d) are given in (a) and, at higher magnification, in (b). [C] A time-lapse series shows GFP OsKCH1 signals in tobacco BY-2 cells during early stages of mitosis, from prophase to early anaphase, together with the corresponding DIC images (a-e). Additionally, a double-staining of GFP OsKCH1 (h) with Hoechst (i) during metaphase is shown (see merge in g). The corresponding DIC image is given in (f). [D] Time-lapse series of GFP OsKCH1 localization in tobacco BY-2 cells during late telophase and beginning cytokinesis. A double-staining of GFP OsKCH1 with Hoechst is additionally shown in (i) together with a merge including the DIC image (h). Arrows highlight filaments that tether the nuclei to the periphery (g) and bridge the nucleus and the new cell wall (f). See supplemented data CD for corresponding movies. Scale bars = 20 μ m.

in Fig. 23 A, in premitotic cells OsKCH1 was clearly aligned as punctate pattern along filamentous, mesh-like structures on both sides of the nucleus and on perinuclear filaments spanning over and surrounding the nucleus. At the onset of mitosis (Fig. 23 B-D) OsKCH1 retracted and was subsequently mainly found at both sides of the nucleus. The protein was neither found in preprophase bands (Fig. 23 B+C), nor in the spindle apparatus (Fig. 23 C) or at the division plate (Fig. 23 D). During late telophase and beginning cytokinesis, OsKCH1 signals were repar-

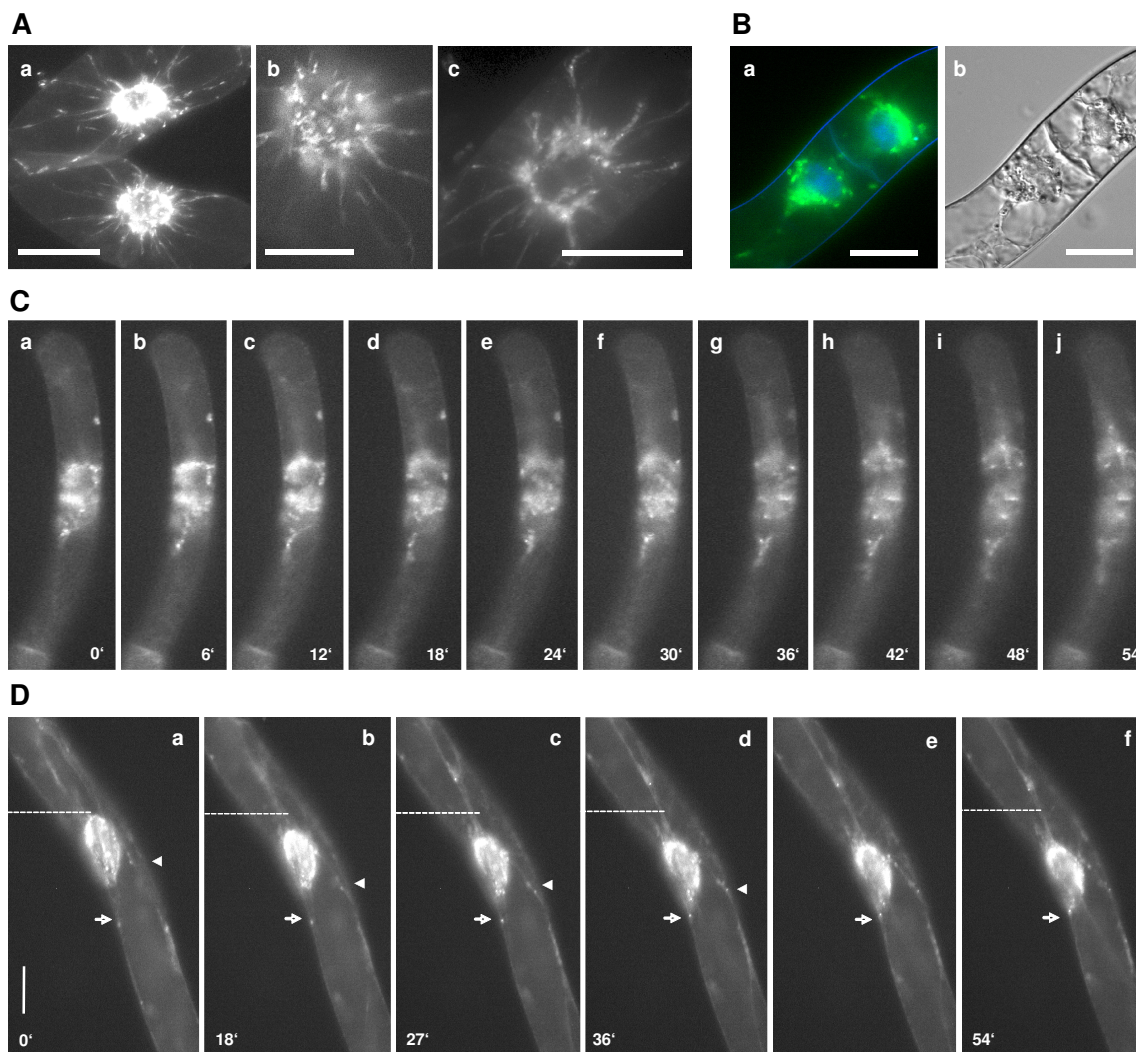


Fig. 24: Localization of *OsKCH1* during nuclear positioning

[A-C] Tobacco BY-2 cells stably expressing a GFP fusion of OsKCH1-800. [A] Optical sections from the cell midplane of interphasic cells. [B] Merge image showing GFP OsKCH1-800 fluorescence and DNA signals stained by Hoechst in a cell after mitosis (a). The corresponding DIC image is given in (b). [C] Time-lapse series of cells after mitosis (a-j). A merge image is additionally given in (k) and shows GFP OsKCH1-800 fluorescence and DNA signals stained by Hoechst. The corresponding DIC image is given in (l). [D] Time-lapse series of nuclear movement in an interphasic cell. The original position of the nucleus in each image is indicated by a dotted line. Arrows highlight filaments that span to the periphery while arrow heads point to OsKCH1 accumulations on cortical anchor points. See supplemented data CD for corresponding movies. Scale bars = 20 μm .

tioned and subsequently mainly found surrounding the newly forming nuclei and on filaments that tethered these nuclei to the periphery and the new cell wall (Fig. 23 D, Fig. 24 B+C).

Similar signals were also found during later steps of cytokinesis, on filaments that spanned longitudinally from the nuclei towards the cell poles as shown in Fig. 24 B+C. Interestingly, the fluorescent signals were accumulating in the interspace between these filaments and the leading edge of the migrating nuclei, as if the nucleus was guided (Fig. 24 C). In interphasic cells OsKCH1 typically localized to fine filaments, tethering the nucleus to the periphery (Fig. 24 A+D). Punctate signals accumulated at the nucleus, often located at the sites, where the filaments reached the nuclear envelope or attached to the cell cortex (Fig. 24 A+D).

3.6 KCH1 overexpressors show delayed nuclear positioning

Phenotypic and microscopic analysis had shown that mitosis in general was not severely altered in BY-2 KCH1. The structure of mitotic spindles was normal and mitosis occurred at most of the investigated time-points with normal rate, indicating that the division process itself can proceed normally in the cells. The onset of mitosis, however, was clearly delayed in BY-2 KCH1, resulting in a reduced MI at early time-points after subcultivation. In plant cells that prepare for division, typically a migration of the nucleus occurs towards the site where the future cell plate will form (for review see Nick, 2008). Especially for the first division the nucleus has to cover a considerable distance from the cell periphery. During the subsequent divisions, however, it

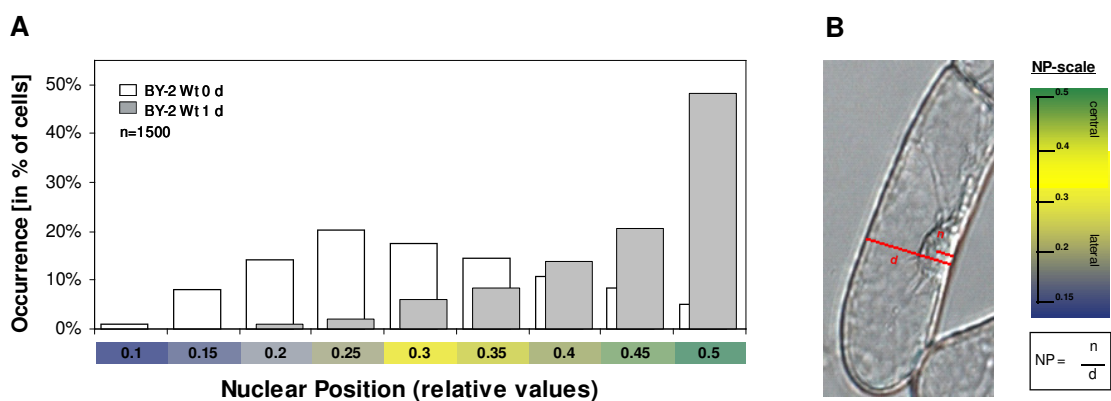


Fig. 25: Development of a method to analyze nuclear positioning

The nuclear position (NP) is determined as relative value by division of the shortest distance between cell wall and the middle of the nucleus n , and the total cell diameter d . Refer to the DIC image in [B] for illustration. The adjacent scale shows the typical values for mean NP, ranging between 0.15 and 0.5, together with a color code. Three main intervals can be defined for the position of the nucleus in a cell of interest: a central location (NP \in [0.4, 0.5], shaded in green), a lateral position (NP \in [0.15, 0.3], shaded in blue), or an intermediate state (NP \in [0.3, 0.4], shaded in bright yellow). The histogram in [A] displays the distribution of measured NP values in ranges of 0.05, together with their respective occurrence in percent of analyzed cells as determined for BY-2 Wt cells before subcultivation (0 d, white bars) and 1 day after subcultivation (1 d, gray bars). Note that the NP within the cell populations shifts with high homogeneity from a lateral position peak at day 0 to a central position peak at day 1.

remains near the cell center and premitotic migration is then as consequence less prominent. Interestingly, the detailed microscopic investigations of the localization of GFP OsKCH1 in tobacco BY-2 cells have revealed that OsKCH1 signals during nuclear migration in cytokinetic and premitotic cells were predominantly found at the leading edge of the migrating nucleus, pointing towards a possible connection to this process.

In order to investigate whether premitotic migration might be impaired in BY-2 KCH1, a method was developed to follow the mean nuclear position (NP) in BY-2 KCH1 and BY-2 Wt during the culture cycle (Fig. 25 B). For validation of the method, the distributions of NP values were determined on one hand in stationary BY-2 Wt cells before subcultivation, and on the other hand in cells that had already reentered the cell cycle at day 1 after subcultivation. As clearly visible in Fig. 25 A, the nuclear positions in BY-2 Wt cells shift within this one day from lateral towards central positions.

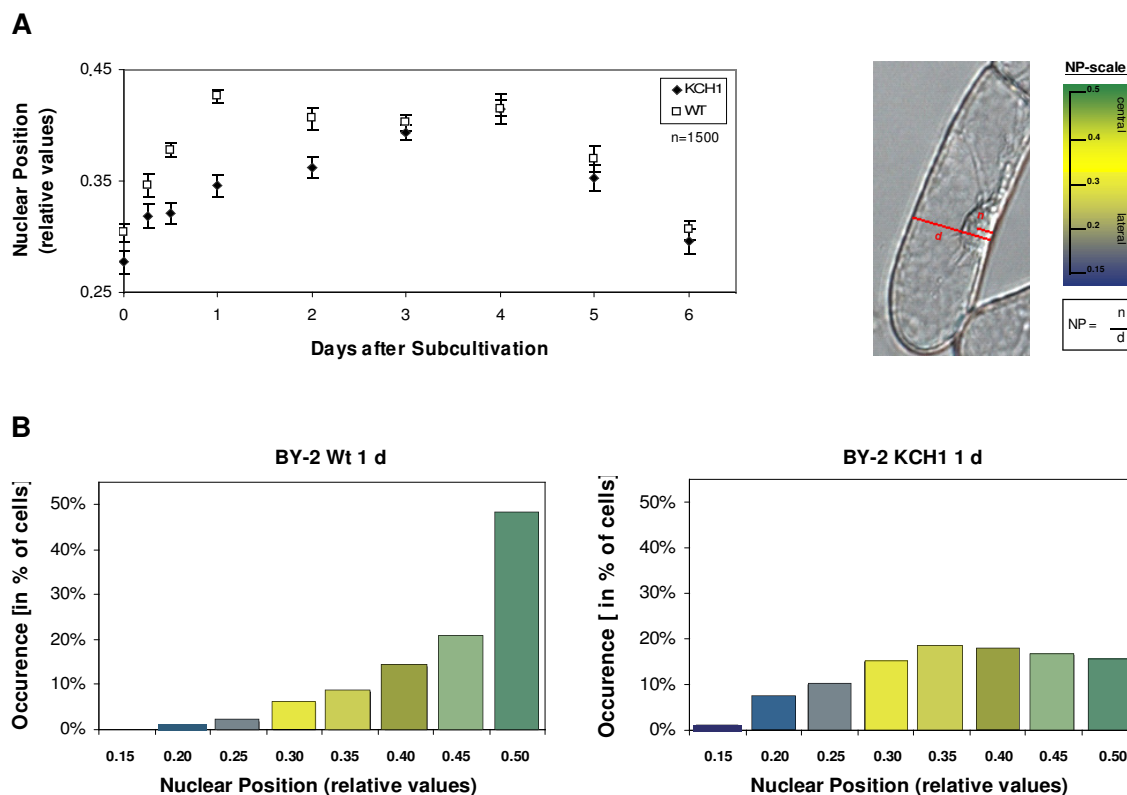


Fig. 26: Influence of *OsKCH1* on nuclear positioning

[A] Time course of nuclear migration in BY-2 KCH1 and BY-2 Wt through the culture cycle at different time-points after subcultivation. The adjacent scale again shows the values for mean nuclear positions (NP), ranging between 0.15 and 0.5 together with their color code (for details refer to Fig. 25). For each time-point and cell line 3 times 500 cells were measured, and mean values were plotted as a function of time together with the respective SE. Differences between mean NP values were positively tested for significance at days 0.5, 1 and 2 (unpaired t-tests, $P < 0.01$). [B] Comparison between the NP value distributions in BY-2 Wt and BY-2 KCH1 at day 1. The histograms display the NP values in ranges of 0.05, color-coded as described in Fig. 25 A, together with the respective occurrence in % of cells. Note that in BY-2 Wt at 1 d in about 70 % of cells the nuclei are centrally located (NP greater than 0.4) while at the same time-point in BY-2 KCH1 this is only the case in about 28 % of cells.

Subsequently, the mean nuclear positions were followed in both BY-2 KCH1 and BY-2 Wt cells during the culture cycle (Fig. 26 A). Interestingly, at days 0.5, 1, and 2 after subcultivation, the mean NP in BY-2 Wt and BY-2 KCH1 were significantly different. While in the non-transformed Wt the nuclei had already started to shift from their original lateral into a more central position at day 0.5, most BY-2 KCH1 nuclei were still located at the periphery, indicating a delay in premitotic nuclear movement in the OsKCH1 overexpressor. At day 1 and 2 in BY-2 Wt cells nuclei had already reached the cell center while in BY-2 KCH1, this position was only reached at day 3 after subcultivation. The histograms in Fig. 26 B exhibit the relative frequencies of the NP values in 1800 cells of both the BY-2 Wt and the BY-2 KCH1 cell line at day 1, respectively, and illustrate the differences in nuclear positions even more clearly. Thus, in Wt cells at 1 d in about 70 % of the cells the nuclei were centrally located while at the same time-point in KCH1 cells this was the case only for about 28 % of the population.

4 Analysis of the cytoskeletal binding of OsKCH1

The previous chapter described the investigation of the putative biological role of OsKCH1 and demonstrated antagonistic cell division and expansion phenotypes as results of knock-down and overexpression of the protein. The reported dynamic repartitioning of OsKCH1 during the cell cycle and the delay in nuclear positioning and mitosis in BY-2 as results of *KCH* overexpression, in combination with the observation that OsKCH1 has the general ability to bind to microtubules and actin microfilaments, points towards a putative role of the protein as linker between both cytoskeletal elements during nuclear positioning.

In order to discriminate between two principal models that describe putative contributions of OsKCH1 to nuclear movement (Fig. 33), further biochemical analysis were necessary. The following sections thus focus on a further elucidation of the structural and functional binding characteristics of OsKCH1 to actin and microtubules. The binding strength of the protein to both types of cytoskeletal elements was assessed via quantitative analysis of the specific binding kinetics. The putative oligomerization of OsKCH1 into multifunctional complexes was analyzed and specifically investigated in relation to a possible filament-bundling ability of the protein. Finally, the microtubule-depolymerization activity and the dynamic properties of OsKCH1 were assessed in order to obtain a better understanding of the characteristic properties of the protein as molecular motor.

4.1 OsKCH1 shows high affinity to actin and lower affinity to microtubules

The interaction of OsKCH1 with microtubules and actin microfilaments has been assessed both *in vivo* and *in vitro* by detailed qualitative analysis (see section 2). For a better understanding of the putative binding preferences of the protein, however, a more quantitative investigation is required. The strength of protein interactions is typically described by their equilibrium dissociation constant K_d .

For determination of the specific K_d values for the interaction of OsKCH1 with either actin microfilaments or microtubules, concentration-dependent cosedimentation assays were performed with varying concentrations of actin and microtubules, respectively, and fixed concentrations of the recombinantly expressed variants of OsKCH1 (for details on the proteins refer to Fig. 15). The proportion of OsKCH1 that partitioned together with the filaments into the sediment fractions was measured by SDS-Page and Western blotting, and the percentage of filament-bound protein was plotted against the microtubule concentration to determine the K_d values by hyperbolic fits of the data.

Fig. 27 shows the typical hyperbolic functions obtained for the interactions of KCH1-mot, expressing the central part of OsKCH1 including the microtubule-binding domain, with microtubules and KCH1-cc1, encoding the N-terminal part of OsKCH1 including the CH domain, with actin filaments. The gels of representative sedimentation assays clearly show that increasing concentrations of microtubules and actin filaments, respectively, cause a progressive redistribution of KCH1-mot and KCH1-cc1 into the sediments.

While the K_d value determined for the interaction of KCH1-mot with microtubules was $6.7 \pm 0.25 \mu\text{M}$ and thus rather high (Fig. 27 A), the dissociation constant of the complex between KCH1-cc1 and actin filament was only $1.76 \pm 0.38 \mu\text{M}$, indicating a high affinity of the protein to actin (Fig. 27 B). For comparison, an overview of the K_d values determined for a variety of actin- and microtubule-binding proteins is given in Fig. 27 C.

The K_d values for the full-length protein KCH1-cc3 and the truncated version KCH1-mot were in a similar range (7.74 and $6.77 \mu\text{M}$), indicating that the ability of the motor domain of KCH1 to bind to microtubules is not altered by the presence of other domains within the protein, such as the CH domain. Interestingly, for the interactions of the KCH1-cc3 and KCH1-cc1 with actin filaments, clearly different K_d values were obtained (4.80 and $1.76 \mu\text{M}$). Thus, the binding affinity of the full-length KCH1 to actin is clearly lower than the affinity determined for the truncated protein, indicating mutual interactions of different domains.

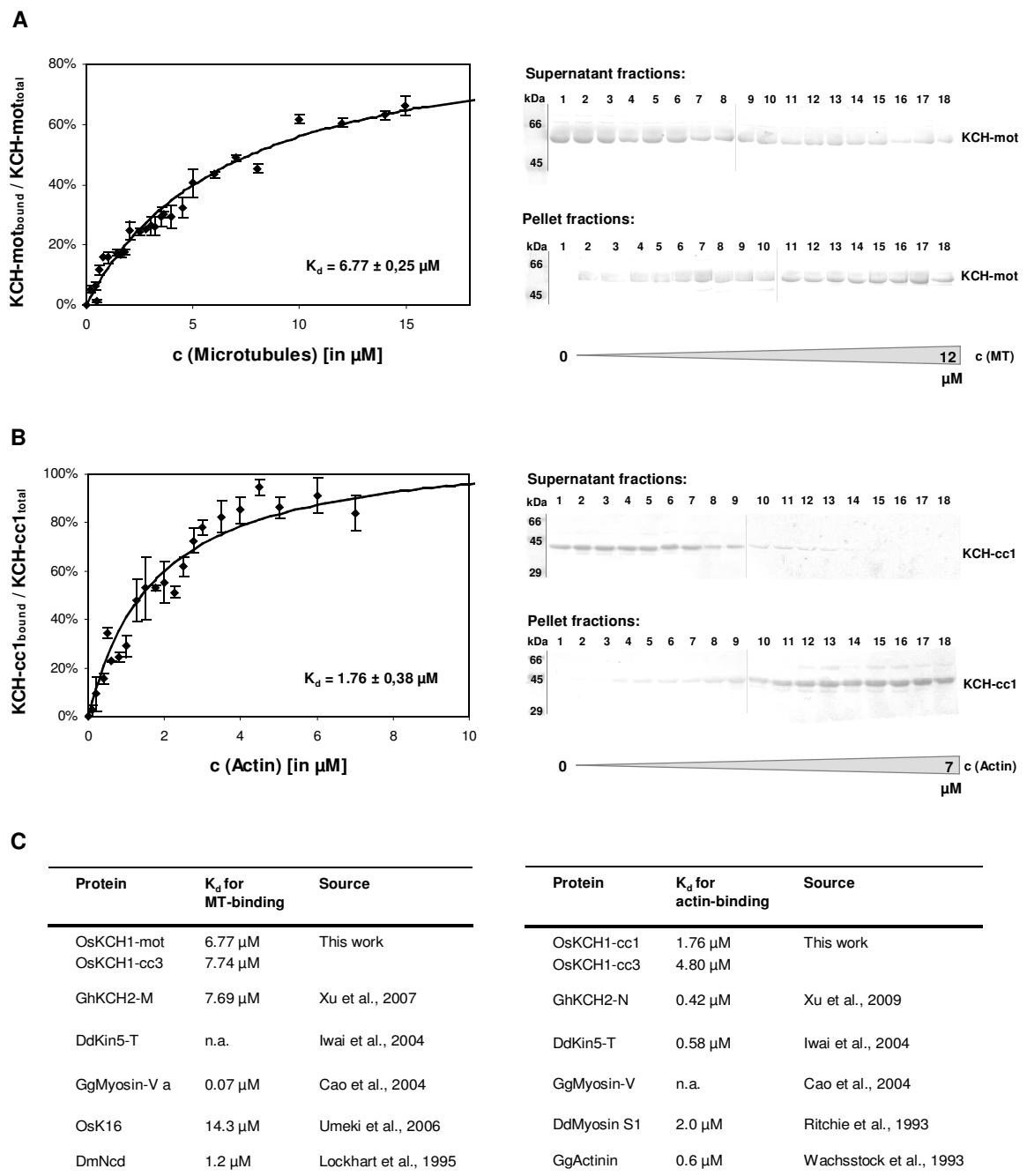


Fig. 27: Quantification of OsKCH1 binding to microtubules and actin microfilaments

[A] Recombinantly expressed KCH-mot protein was mixed with varying concentrations of microtubules and the fractions of bound and unbound protein were separated by ultracentrifugation. The ratio of microtubule-bound kinesin to total kinesin was determined for each sample and plotted over the respective microtubule concentrations. The dissociation constant K_d was calculated from a least-square fit of the data to a curve following the hyperbolic equation given in methods section 2.6.5. SDS-gels show the amount of KCH protein in both the supernatant and pellet fractions of representative sedimentation assays with the following concentrations of microtubules (in μ M) for samples 1 to 18: 0, 0.2, 0.4, 0.8, 1, 1.2, 1.4, 1.8, 2, 2.8, 3.2, 3.6, 4, 5, 6, 8, 10, 12. [B] The binding of recombinantly expressed KCH-cc1 protein to actin was assessed as described in [A]. For titration, the following concentrations of actin (in μ M) were used for samples 1 to 18: 0, 0.1, 0.2, 0.4, 0.8, 1, 1.25, 1.5, 1.75, 2, 2.5, 2.75, 3, 3.5, 4, 5, 6, 7. [C] Overview of the K_d values determined for the different variants of OsKCH1, together with typical K_d values of two other bifunctional microtubule and actin-binding proteins (DdKin4-T and GgMyo-V) and several monofunctional proteins binding only to microtubules (OsK16, DmNcd) or actin (DdMyosin, GgActinin).

4.2 OsKCH1 oligomerization is required for microtubule and actin bundling

The ability of OsKCH1 to bind directly to microtubules and actin filaments was shown by qualitative as well as quantitative biochemical investigations (see results, sections 2.2 and 4.1). Especially the tight association of the protein with actin filaments is most intriguing, as KCHs contain only a single CH domain but actin-binding typically requires two CH domains in tandem (Gimona and Mital, 1998; Gimona et al., 2002). One possibility to explain the observed tight association of the protein with actin would involve the formation of dimeric or multimeric complexes of OsKCH1 that, in turn, would contain more than one functional domain. In fact, protein oligomerization is known as structural feature for numerous kinesin proteins from diverse organisms and is tightly associated with typical kinesin characteristics, such as processivity and microtubule-dependent gliding. Hence, the ability of OsKCH1 to assemble into oligomeric complexes was investigated, and the results will be described in the following section. The oligomerization of OsKCH1 would create a multifunctional protein that could be free to confer simultaneous interactions with either one type of cytoskeletal elements, or both. A second part of the chapter will thus investigate the ability of OsKCH1 to induce filament-bundling.

4.2.1 OsKCH1 forms oligomers *in vitro* and *in vivo*

The results in section 1.2 has already described a general analysis of the domain organization of OsKCH1 and has revealed the presence of three putative coiled-coil regions in the protein sequence, two in tandem upstream and one downstream of the catalytic core (Fig. 9 B). Coiled-coils are often associated with protein oligomerization and contain characteristic periodic repeats of seven amino acid residues, where positions a and d are mostly hydrophobic and e and g are often charged or hydrophilic (Lupas, 1996; Lupas et al., 1991). In order to test ,whether this prediction holds true for OsKCH1, possible oligomerization was analyzed *in vivo* using Bimolecular Fluorescence Complementation (BiFC) assays and *in vitro* via size-exclusion chromatography (SEC) with recombinantly expressed protein.

The BiFC method (Hu et al., 2005; Stolpe et al., 2005) relies on expression of two proteins of interest as translational fusions either to the N-terminal (YN) or C-terminal (YC) halves of yellow fluorescent protein (YFP). Neither of the two halves is capable of fluorescence. Only upon close interaction of the fused proteins they can form a functional YFP fluorophore, which can be detected by standard epifluorescence microscopy (Hu and Kerppola, 2003; Hu et al., 2005).

A series of constructs (Fig. 28 C) was generated to express OsKCH1 variants, fused with either YN or YC in transient transformations of plant cells using particle bombardment. Combinations of all different plasmids were introduced together with transformation control marker plasmids into both etiolated rice coleoptiles as well as tobacco BY-2 cells. Clear YFP-signals were obtained in rice as well as in BY-2 when OsKCH1-800 YN was co-transformed with OsKCH1-800 YC, indicating that the two proteins form a complex *in cellula* presumably due to dimeriza-

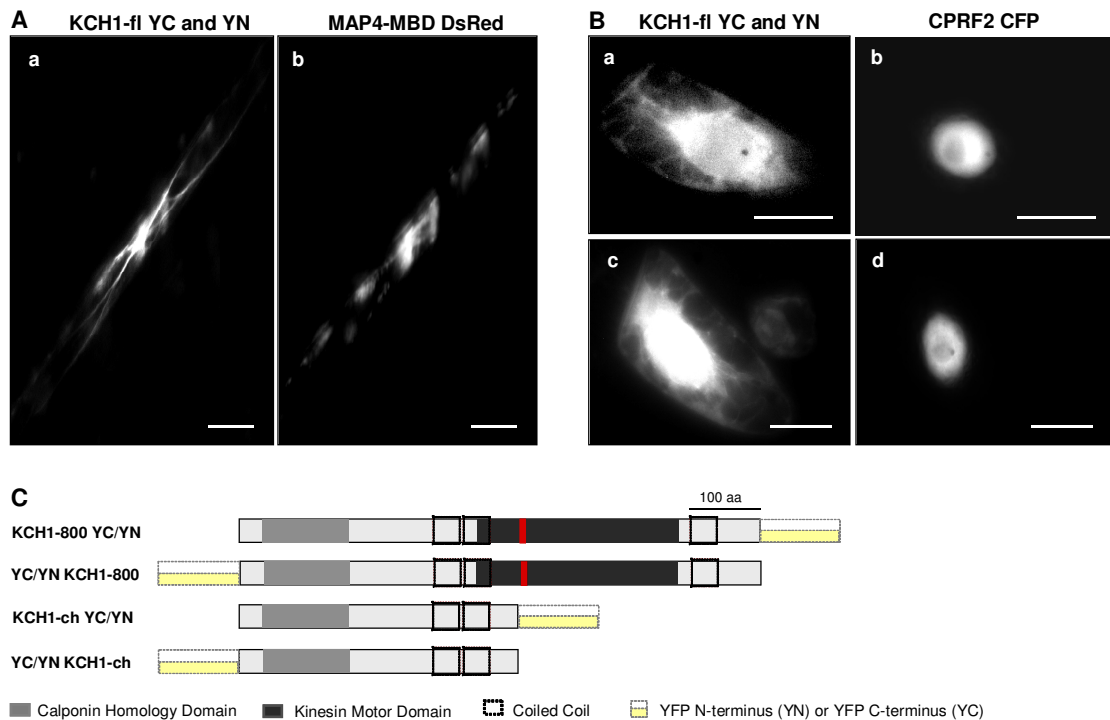


Fig. 28: *Bimolecular Fluorescence Complementation (BiFC) analysis of OsKCH1 oligomerization*

Reconstitution of Split-YFP signals in rice coleoptiles [A] and tobacco BY-2 cells [B] after transient transformation with KCH1-800 YN and KCH1-800 YC. The microtubule marker MAP4-MBD DsRed and the nuclear marker CPRF2 CFP were used as transformation controls. Scale bar = 20 μm [C] Schematic diagram of different Split-YFP fusion constructs of OsKCH1 that were generated and tested for signal reconstitution *in vivo*. In addition to the two constructs KCH1-800 YC and KCH1-800 YN no other of the tested construct combinations led to a signal reconstitution.

tion via the coiled-coil regions (Fig. 28 A and B). In both expression systems the signals became visible as filamentous structures that had the appearance of actin filaments, indicating the functionality of the constructs. The reconstituted YFP-signal was highly specific, because all other construct combinations did not produce any YFP-signals although the transformation control plasmids were successfully expressed in the samples. This stringent limitation of complementation to only very few or even one combination is consistent with previous reports on BiFC (Hu and Kerppola, 2003; Hu et al., 2005).

In accordance with the BiFC results, SEC gelfiltration of recombinantly expressed OsKCH1-mot, containing the coiled-coil domains and the motor core, clearly showed the oligomerization of the protein *in vitro*. A major protein peak corresponding to the predicted molecular weight of the tetramer was observed and accompanied by smaller peaks corresponding to the predicted weight of the dimer and, occasionally, the putative monomer (Fig. 29).

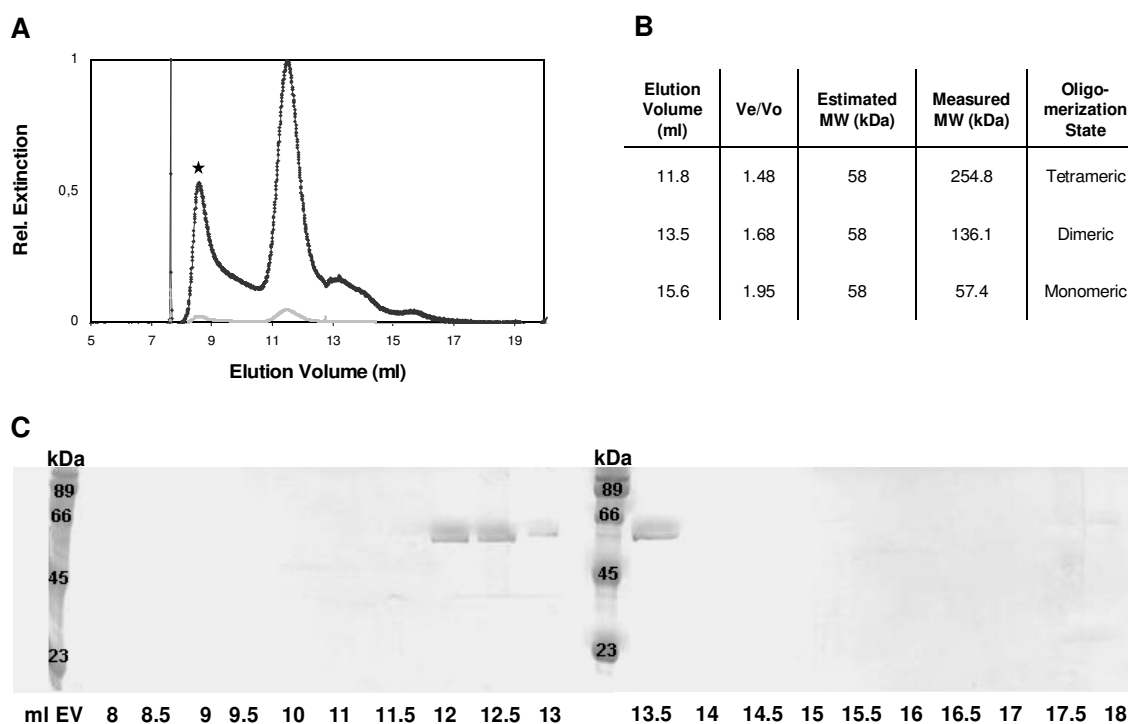


Fig. 29: SEC analysis of *OsKCH1* oligomerization state

[A] Typical elution profile of recombinantly expressed *OsKCH1*-mot protein in SEC gel filtration. As shown on the accompanying SDS-Page [C], the protein elutes in one major and one minor peak at about 12 ml and 13.5 ml. One additional peak was found at about 8.5 ml (marked by an asterisk) but did not yield any protein signal on the gel. [B] Comparison of estimated molecular weights (MW) of *OsKCH1*-mot and the MW determined by gel filtration. For estimation of the MW, several reference proteins were plotted over their ratio of elution-volume (V_e) / void-volume (V_o). A standard curve was generated and used for the measurement of the apparent MW of *OsKCH1*-mot.

4.2.2 *OsKCH1* bundles and cross-links microtubules and actin filaments *in vitro*

As described in detail in sections 2 and 4.1, *OsKCH1* is able to interact both *in vivo* and *in vitro* with microtubules and actin microfilaments. In addition, *OsKCH1* was found to assemble into dimers and tetramers – a structural feature known from numerous kinesins from various organisms. *OsKCH1* could thus be envisaged as an oligomeric protein that is, by consequence, multifunctional and contains several domains which are free to interact with microtubules and actin. Hence the question arises whether *OsKCH1* is capable to generate functional linkages between either filaments of one kind, or between both microtubules and actin microfilaments?

Fluorescence microscopy was therefore used to examine various mixtures of microtubules, actin filaments, and recombinantly expressed variants of *OsKCH1*. FITC-phalloidin labeled actin filaments and TAMRA-labeled microtubules occurred as randomly distributed filaments in control reactions (Fig. 30 A, a, g). The addition of 0.1 μ M of recombinantly expressed *KCH1*-cc3 to

suspensions of either actin filaments (Fig. 30 A, f) or microtubules (Fig. 30 A, l), however, induced their bundling and cross-linking.

The filament-bundling ability of KCH1 was clearly domain-dependent, and appeared also to be tightly associated with the presence of coiled-coil domains within the molecule. While the nearly full-length KCH1-cc3 induced strong actin-bundling throughout the suspension (Fig. 30 A, f), the shorter construct KCH1-cc2 – containing only two of the in total three coiled-coil regions in addition to the CH domain – induced bundling to a clearly lesser extend (Fig. 30 A, d). The even shorter truncations KCH1-cc1 and KCH1-sh, by contrast, did not lead to any aggregation of actin filaments (Fig. 30 A, b and c). Both proteins contain the actin-binding CH domain, but only one or none of the coiled-coil stretches, respectively. This finding thus clearly underlines the importance of the coiled-coil regions and presumably of protein oligomerization for filament bundling.

While KCH1-mot – encoding the kinesin motor core together with all coiled-coil stretches – did not induce bundling of actin filaments (Fig. 30 A, e), it led to aggregation of microtubules (Fig. 30 A, k). All other protein truncations contain only the proteins N-terminus including the CH domain but lack the motor core, and did not lead to microtubule bundling (Fig. 30 A, h-j).

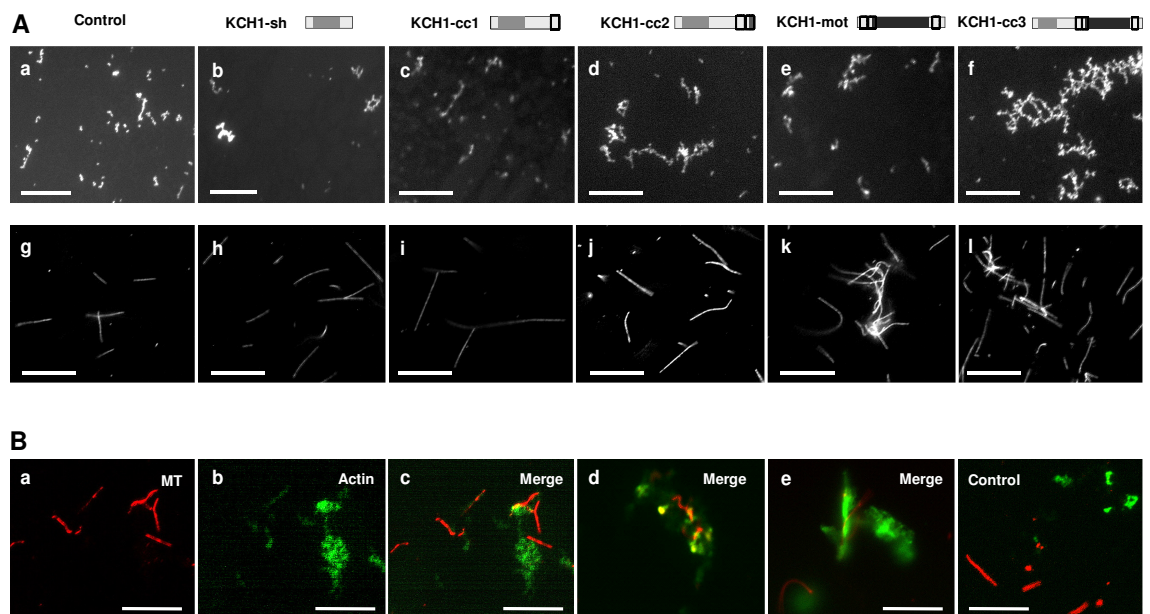


Fig. 30: *In-vitro bundling of actin filaments and microtubules*

[A] Fluorescence images of 0.1 μM of actin filaments stained by FITC-phalloidin (a-f), or 0.1 μM of microtubules labeled with TAMRA (g-l). The filaments were visualized in absence (a, g) or presence of 0.1 μM recombinantly expressed full-length KCH1-cc3 (f, l), and the different truncations KCH1-sh, -cc1, -cc2, and -mot (b-e, and h-k). Schematic diagrams indicate the domain organization in the different KCH1 variants that are added to the respective reactions. The CH domain is shown in light gray, the kinesin motor core in dark gray. Regions of coiled-coil are marked by dashed boxes. For details on the different constructs refer to Fig. 15. [B] Fluorescence images of mixtures of actin filaments (green) and microtubules (red) in presence of KCH1-cc3 in three independent reaction set-ups (c-e). A control shows a mixture of both types of filaments in presence of the truncated protein KCH1-mot (f). Scale bars = 20 μM .

To assess whether OsKCH1 is not only able to bundle either microtubules or actin filaments, but as well to cross-link and co-align both types of cytoskeletal elements, further experiments were necessary. 0.1 μM of microtubules and 0.1 μM actin filaments were thus mixed in presence of 0.1 μM of either the full-length KCH1-cc3, or – as controls – the truncated protein KCH1-mot which contains the microtubule-binding core but lacks the CH domain, or reaction buffer without added protein. Both actin and microtubules remained as distinct, single filaments that were scattered randomly throughout the suspension in the control set-ups (Fig. 30 B, control). The addition of 0.1 μM OsKCH1-cc3 – containing both the CH domain and the kinesin motor core – however, led to their bundling, co-alignment, and aggregation (Fig. 30 B, c-e).

Taken together, these results underline the ability of OsKCH1 to bind to microtubules and actin, and to act as bifunctional mediator between both types of cytoskeletal elements. The observed *in-vitro* cross-linking and co-alignment of actin and microtubules by OsKCH1 could further point towards a putative role of the protein as linker in the structural coordination of the actin and microtubule networks within the cell.

4.3 OsKCH1 harbors certain dynamic properties

Their bifunctional molecular properties make KCHs interesting candidates for the spatiotemporal coordination of microtubules and actin filaments (see results, section 2 and 4.2.2; Preuss et al., 2004; Xu et al., 2009). Interestingly, the cellular phenotypes that can be derived from over-expression or knock-down of OsKCH1 (see results, section 3) point towards an involvement of the protein in premitotic nuclear positioning – a process that in plants requires a tight coordination of microtubule as well actin networks (Katsuta and Shibaoka, 1988; Katsuta et al., 1990; Chytilova et al., 2000; Ketelaar et al., 2002).

Our knowledge of the molecular properties of OsKCH1 has, however, remained incomplete. A detailed analysis of the domain organization has revealed that KCH proteins belong to the kinesin superfamily and contain a characteristic motor core together with the neck-linker sequence known to confer the minus-end directed motility of many kinesin-14 family members (see results, section 1.2). Could KCH proteins possibly as well be associated with directed microtubule-based motility? Or might KCHs rather be involved in the regulation of cytoskeletal dynamics, as known from several other kinesins with internally-located motor cores? The characteristic properties of OsKCH1 as a molecular motor protein were thus further analyzed, and the results will be displayed in the following sections.

4.3.1 OsKCH1 does not induce microtubule depolymerization

Within the cell, microtubules are rigid in comparison to other cytoskeletal elements. Nevertheless, they are able to undergo dynamic instability by rapidly depolymerizing and repolymerizing at their ends to facilitate cytoplasmic remodeling and rapid responses to cell signaling events (reviewed by Mandelkow and Mandelkow, 1989; Nick et al., 2008). These dynamic properties

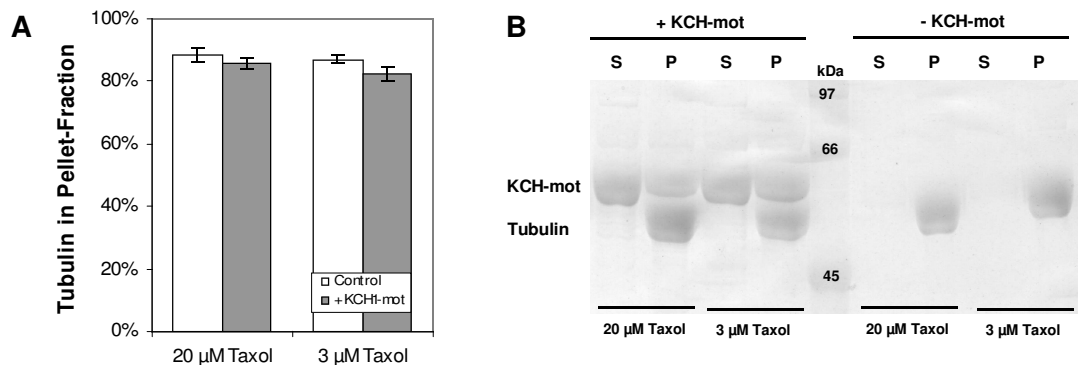


Fig. 31: *In vitro* microtubule depolymerization assay

[A] Depolymerization of microtubules is assessed under two different concentrations of taxol (3 μ M, 20 μ M) in both control samples without motor protein (white bars), and samples containing recombinantly expressed KCH1-mot (gray bars). The fraction of polymerized and unpolymerized tubulin were separated by ultracentrifugation and the amount of tubulin in the pellet fractions quantified by densitometric analysis of the corresponding SDS gels. The proportion of tubulin in the sediment is given as mean values \pm SE calculated of three independent experiments. [B] SDS-Page showing the amount of tubulin detected in supernatant fractions (S) and precipitates (P) of a representative depolymerization assay.

of microtubules are critical for many cellular functions and are spatially and temporally controlled by microtubule accessory proteins.

Several members of the kinesin-8 and kinesin-13 superfamily with centrally located motor domains are known to be involved in microtubule destabilization (reviewed by Wordeman, 2005; Howard and Hyman, 2007). We therefore tested whether recombinantly expressed OsKCH1-mot, encoding the central part of the protein including the kinesin motor core (see Fig. 15 for details), was able to trigger microtubule destabilization *in vitro*. For this purpose, purified OsKCH1-mot was added to taxol-stabilized microtubules and incubated at room temperature in the presence of 1 mM ATP to induce kinesin activity.

The amounts of sedimentable, polymerized tubulin versus soluble tubulin dimers was monitored by SDS-Page and compared to controls, where the motor protein had been omitted. Fig. 31 shows the SDS-Page of a representative *in vitro* depolymerization assay together with the assay quantification. As clearly visible, the majority of tubulin fractionated into the sediments in both the control reactions and in presence of the motor protein, indicating that OsKCH1-mot does not destabilize microtubules under the *in vitro* assay conditions.

4.3.2 OsKCH1 shows slow motility *in vivo*

An intrinsic characteristic of many kinesins is their ability to walk unidirectionally along microtubules. OsKCH1 contains as structural characteristic the typical kinesin motor core, together with the conserved neck-linker sequence that is found among many microtubule minus-end directed kinesins. Previous binding assays with microtubules already showed that the protein is able to associate directly with microtubules. But, is OsKCH1 only able to bind to microtubules,

or does the protein as well possess dynamic properties? In order to analyze the question of motility, two different approaches are widely used in the literature. The so-called gliding-assay investigates *in vitro* if the motor protein – attached to a glass surface via its long coiled-coil stalk – is able to transport microtubules along this surface (Howard et al., 1989). *In vivo* tracking, instead, follows the movement of fluorescent protein fusions of the motor directly inside the cell (Lee et al., 2003; Cai et al., 2007).

Gliding assays were performed with recombinantly expressed nearly full-length OsKCH1-cc3, and OsKCH1-mot, encoding only the central part of the protein including the kinesin motor core (see Fig. 15 for details on the constructs). Although both proteins were able to attach microtubules to the surfaces, no gliding of microtubules could be observed in time-lapse microscopy (data not shown). However, a successful accomplishment of a gliding assay depends on a variety of factors (Uppalapati et al., 2009). These include an appropriate concentration of active motor protein on the surface, as well as the requirement that the motor possesses a long enough

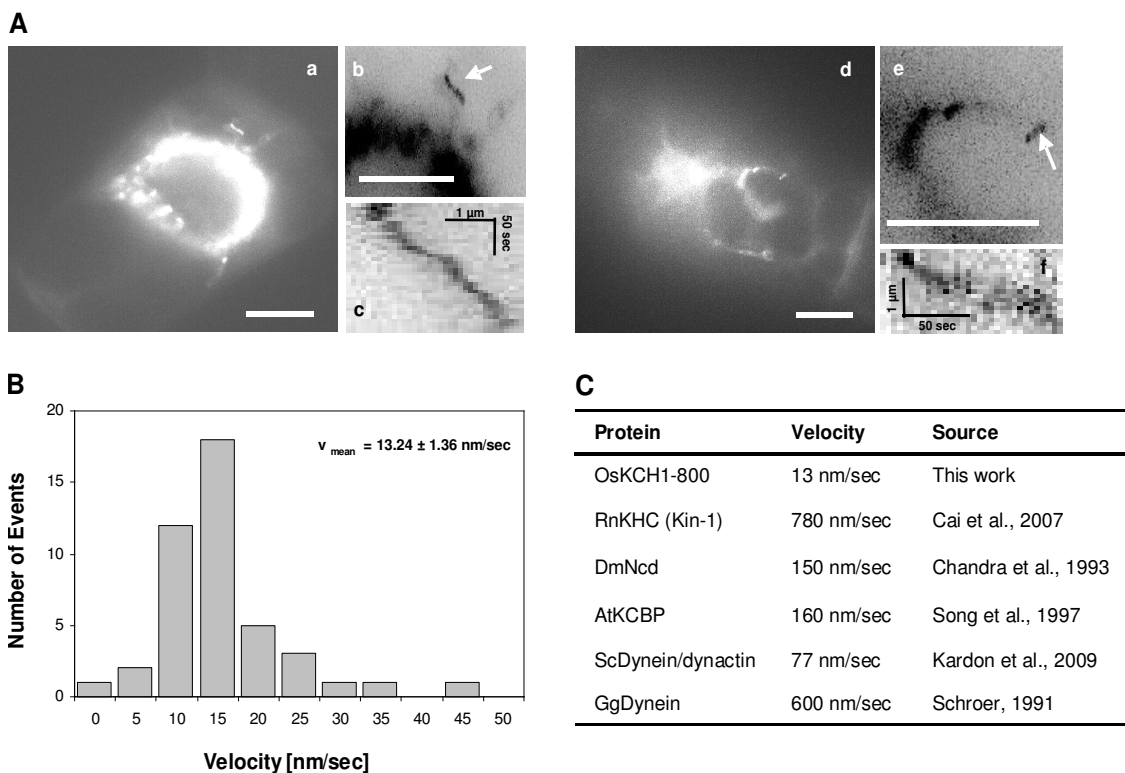


Fig. 32: *In vivo* tracking of cortical movement of *OsKCH1*

[A] Time-tracking of fluorescence pattern of GFP *OsKCH1*-800 stably expressed in tobacco BY-2 cells. (a, d) Z-projection of an image time series. Pictures were taken every 5 sec over a total of 185 sec. Overlays were generated in ImageJ (NIH, Bethesda, USA). (b, e) Blow-ups of the pictures shown in (a) and (d). For better visualization of the fluorescent tracks, the picture color was inverted. Arrows indicate the tracks that were further analyzed in time space plots. The corresponding kymographs, generated in ImageJ, are shown in (c) and (f). Scale bar = 10 μ m. Scale bars in (c) and (f) as indicated in the pictures. [B] Velocity distribution of *OsKCH1*-800 movement in tobacco BY-2 cells. The velocities of *OsKCH1* were measured from kymographs using the PlugIn cited above. The number of particles moving within the indicated velocity ranges was counted. A few outlying points are truncated from the histogram for display purposes. [C] Comparison of the velocities determined *in vivo* for *OsKCH1*-800, for other typical kinesins and for dyneins that are involved in different cellular processes.

stalk region to avoid the attachment of the motor core to the glass surface, as the motor domain in this case would be deactivated. OsKCH1 has a quite unusual domain structure with the motor core located in the center of the protein and only very short coiled-coil regions. It thus cannot be excluded that sterical factors influence the protein activity in the *in vitro* assay set-up.

Therefore, additional *in vivo* investigations were performed in BY-2 cells that stable express OsKCH1-800 in fusion with GFP (refer to Fig. 10 B for details). Fluorescent spots of OsKCH1-800 were tracked by time-lapse microscopy. Subsequently, their dynamics were analyzed using time space plots (kymographs). As visible in Fig. 32, OsKCH1-800 shows slow dynamics *in vivo*, with a mean movement velocity of 13.24 ± 1.36 nm/sec. Dynamic behavior of OsKCH1 was primary found near the cell cortex. Fluorescent spots of OsKCH1 that localized surrounding the nucleus, by contrast, did not alter position during the investigation, indicated that the activity of OsKCH1 might undergo distinct intracellular regulations.

In conclusion, the observed dynamic behavior could point towards a putative role of OsKCH1 as not only structural but as well dynamic coordinator of actin and microtubule networks within the cell. In order to obtain a better understanding of specific dynamic properties of OsKCH1, a more detailed biochemical investigation of the motor characteristics will, however, be required.

5 Summary of results

The recently identified plant kinesins with calponin-homology domain (KCH) have been linked with a putative role in microtubule-microfilament interaction in plant cells (Tamura et al., 1999; Preuss et al., 2004). A scope of this study was to analyze if the presumed link between microtubules and actin filaments represents a general function of KCHs. Secondly, this work aimed at investigating in which cellular processes a rice member of this group, OsKCH1, might be implicated in.

Database searches revealed candidate proteins from the KCH subgroup in all land plants including the mosses, but neither in green algae, nor in animals and fungi. A subsequent phylogenetic analysis showed that the KCHs form a highly conserved clade within the kinesin-14 family. In order to get a deeper insight into structural and functional conservation within the KCH subfamily, a KCH member from rice, OsKCH1, was chosen for further investigation.

Fluorescent protein fusions of OsKCH1 were cloned and transiently and stably expressed in elongating rice cells, as well as in cycling tobacco BY-2 cells. In both cell types, the expression yielded punctate pattern with mainly transverse orientation in the cell cortex. In addition, the fluorescence accumulated along longitudinal and perinuclear filamentous structures in the cell midplane. Colocalization studies with cytoskeletal markers assigned these pattern to microtubules and actin filaments. Pharmacological treatments furthermore demonstrated the sensitivity of the fluorescent structures to microtubule and actin inhibitors.

In vitro binding studies with recombinantly expressed OsKCH1 showed that the association of the protein with both microtubules and actin filaments is due to direct binding. The application

of truncated proteins in these binding studies further pointed out that the association is clearly domain-dependent. The N-terminal part of OsKCH1, including the CH domain and the first coiled-coil stretch, conferred the interaction with actin microfilaments, while the central protein fragment, comprising the motor core, established the binding to microtubules.

Due to their ability to bind both microtubules and microfilaments, KCHs are interesting candidates for bifunctional mediation between both cytoskeletal elements – a function that is required for many processes during plant cell growth and development. To obtain a first insight into their putative biological role, the gene expression pattern of the rice KCH member OsKCH1 was studied via real-time PCR in different tissues and developmental stages. The expression of *OsKCH1* showed clear tissue and developmental regulation, with highest transcript abundances in meristematic tissues such as the primary leaf and root.

The subsequent investigation of rice *kch1 Tos17* insertion mutants and a *KCH* overexpression line generated in tobacco BY-2 cells showed consistent, antagonistic cellular phenotypes. The knock-down of *kch1* resulted in diminished cell elongation and increased cell numbers, while the overexpression of *KCH* led to increased cell elongation and diminished cell numbers due to a delay in division. Although the onset of mitosis was delayed in the *KCH* overexpressor, the division subsequently proceeded normally and the mitotic structures did not show morphological alterations. A detailed microscopic investigation of the localization of GFP OsKCH1 in tobacco BY-2 cells showed the dynamic repartitioning of the protein during the cell cycle. In premitotic cells OsKCH1 was clearly aligned as punctate pattern along filamentous, mesh-like structures surrounding the nucleus. Furthermore, punctate signals accumulated at sites, where the filaments reached the nuclear envelope or connected to the cell cortex. During nuclear migration in cytokinetic and premitotic cells, OsKCH1 signals were predominantly found at the leading flank of migrating nuclei.

In order to investigate whether the process of premitotic nuclear migration might be impaired in BY-2 cells overexpressing *KCH1*, a method was developed to follow the mean nuclear position during the culture cycle. A comparison of the nuclear positions in BY-2 Wt and BY-2 *KCH1* during the cultivation period clearly showed that premitotic nuclear migration is delayed as a result of *KCH1* overexpression.

A further biochemical analysis should contribute to a better understanding of the putative molecular function of OsKCH1. The binding strength of the protein to both types of cytoskeletal elements was assessed via quantitative analysis of the specific binding kinetics. The obtained dissociation constants showed that OsKCH1 has an unusually low affinity to microtubules but a high affinity to actin filaments. In addition, OsKCH1 was found to assemble into dimers and tetramers both *in vivo* and *in vitro*. As a consequence, OsKCH1 might contain several domains that are free to interact simultaneously with microtubules and microfilaments. In fact, *in vitro* bundling assays demonstrated that OsKCH1 is capable to generate functional links, either between filaments of one kind, or between both microtubules and actin microfilaments. The characteristics of OsKCH1 as a molecular motor were finally investigated via *in vivo* trackings, which revealed that the protein possesses certain dynamic properties.

DISCUSSION

Many processes during cell growth and development rely on a tight coordination of microtubules and microfilaments. In animals and fungi, a number of proteins have already been identified that mediate such interactions between the different types of cytoskeletal elements (Rodriguez et al., 2003). In plants, the situation has remained unclear. However, the recently identified plant kinesins with calponin-homology domain (KCHs) have been linked with a putative role in microtubule-microfilament interaction (Tamura et al., 1999; Preuss et al., 2004).

This study reports the identification of a new KCH from rice, OsKCH1. The protein is analyzed with regard to this presumed bifunctionality. Furthermore, the putative biological role of OsKCH1 is investigated.

In the following sections, the findings will first be discussed with respect to a general role of KCHs as bifunctional linkers between actin filaments and microtubules. A second part focuses on the specific role of OsKCH1 in the coordination of actin filaments and microtubules during nuclear positioning.

1 KCHs are plant-specific and evolutionary conserved

The family of kinesin-14 is highly expanded in angiosperms and contains several members that differ in domain organization greatly from their fungal and animal counterparts, such as the kinesins with calponin-homology domain (KCHs).

The thorough search of genome and protein databases has identified members of the KCH subgroup of the kinesin-14 family in all investigated land plants, including the moss *Physcomitrella patens*, which were absent in animals, fungi and algae. This is consistent with findings from a previously performed analysis of kinesins in photosynthetic organisms by Richardson et al. (2006), and indicates that the KCH subgroup might have evolved specifically during the development of higher plants.

Interestingly, other plant kinesin-14 family members, such as AtKatA or Zwichel (Marcus et al., 2002; Oppenheimer et al., 1997; Reddy et al., 1996), clustered in the phylogenetic analysis together with kinesins from animal and fungi rather than with their neighboring plant kinesin-14 family members from the KCH subgroup. Thus, the plant KCHs seem to form a phylogenetically distinct subgroup within the kinesin-14 family with possibly distinct characteristics and functions.

The evolution of such exceptional types of kinesins in plants has presumably originated in gene duplication and subsequent functional diversification by inclusion of additional and unusual domains. It might take account to the fact that plants have evolved several plant-specific features, including for example unique microtubule arrays such as the PPB and the phragmoplast as well as the organization of microtubules without centrosomes (Reddy and Day, 2001). In addition, flowering plants lack dyneins as well as dynactin-complex proteins (Lawrence et al., 2001; Miki et al., 2005; Wickstead and Gull, 2007), and the functions performed by these proteins in

animals, including the establishment of spindle poles and the movement of nuclei and chromosomes (Koonce, 2000; Sharp et al., 2000), must be covered differently. Hence, it is possible that the expansion of kinesins in plants including the development of the KCH subgroup accounts for the need for plant-specific as well as retrograde-directed motors in angiosperms.

2 OsKCH1 is a bifunctional protein

The rice KCH member OsKCH1 is a close homologue to the previously identified cotton GhKCH1 (Preuss et al., 2004). As typical for KCHs, it contains an N-terminal calponin-homology (CH) domain, known as actin-binding motif, and a centrally located microtubule-binding motor core. It thus represents a putative bifunctional protein, presumably able to interact with both types of cytoskeletal elements. The ability of the cotton KCH member GhKCH1 to bind to actin and microtubules was already assessed in developing cotton fibers (Preuss et al., 2004). However, it remained unclear whether the presumed bifunctionality represents a conserved function among the KCHs, or is rather limited to the specialized cell system cotton fiber. In this work, the rice KCH family member OsKCH1 was investigated for its binding to both microtubules and microfilaments using a combination of *in vivo* colocalization studies in different cell types, pharmacological treatments, and *in vitro* binding studies with recombinantly expressed proteins. The findings are discussed in the context of KCHs and other proteins as putative linkers of microtubules and actin microfilaments during plant cell growth and development.

2.1 OsKCH1 associates with actin and microtubules *in vivo* and *in vitro*

The localization of OsKCH1 was studied in rice coleoptiles as a model system for non-cycling cells and in tobacco BY-2 as a model for cycling cells. In both systems, OsKCH1 was localized in the cell cortex and along filamentous structures in the cell center and surrounding the nucleus. Coexpression studies showed a colocalization of OsKCH1 with markers for microtubules and actin microfilaments in different parts of the cell, respectively. In the cell cortex, a clear colocalization with transversely oriented microtubules was found, whereas in the cell center OsKCH1 colocalized to a higher extent with actin microfilaments. In rice coleoptiles, OsKCH1 was predominantly found on longitudinally oriented microfilaments and often the signals accumulated on presumed crossings between transversely oriented microtubules and the longitudinally oriented filamentous structures. In tobacco BY-2 cells, by contrast, OsKCH1 mainly localized to radial actin filaments, reaching from the nucleus to the periphery. These results are consistent with previously published data on the localization pattern of the cotton KCH homologue GhKCH1 (Preuss et al., 2004), which was found to be associated with cortical microtubules and with actin cables in cotton fibers.

Our results show that the observed interaction of GhKCH1 with both types of cytoskeletal elements *in vivo* represents a general feature of KCH proteins that can be found in cycling as well

as in elongating cells, and is not restricted to the highly specialized cotton fiber cell system. The observed association of OsKCH1 with both microtubules and longitudinally oriented actin filaments might point to a role of the protein in cytoskeletal coordination, possibly regulating the orientation of microtubules and actin microfilaments with respect to each other. OsKCH1 is localized along cortical microtubules – and the *in silico* analysis of the neck-linker region predicts that the protein is a minus-end directed motor. This is consistent with a model, where OsKCH1 is involved in the organization of actin microfilaments relative to the minus-end of cortical microtubules. Conversely, microtubule minus-ends might be oriented through OsKCH1 with respect to the longitudinally arranged actin filaments.

OsKCH1 was found on actin filaments surrounding the nucleus in both investigated cell types, however clearly more pronounced in the cycling BY-2 cells, sometimes resulting in a tight perinuclear network structure. This indicates that the localization of OsKCH1 to the nuclear region might be more important and hence more prominent in cycling as compared to non-cycling cells. In a following section (discussion, chapter 3), this issue will be further discussed along with the putative biological roles of OsKCH1.

In vitro binding assays with recombinantly expressed OsKCH1 and both microtubules and actin microfilaments further underlined the finding of protein bifunctionality and showed that the binding of the protein to both types of cytoskeletal elements is clearly domain-dependent. Thus, the N-terminal part of OsKCH1, including the CH domain and the first two coiled-coil stretches, was found to convey the specific interaction with actin microfilaments while the central protein fragment, comprising the motor core, seems to be required for microtubule-binding.

In summary, these results provide evidence that the presumed link between microtubules and actin microfilaments is a general function of KCHs, both in cycling and non-cycling cells. Thus, KCHs are unique plant kinesins, able to interact with both actin microfilaments and microtubules. Knowledge of the close interaction of both major components of the plant cytoskeleton during various processes of plant cell growth and developments has emerged during the past years (for review see Collings, 2008). The molecular basis of this interaction is, however, still far from being resolved. The bifunctional KCH proteins could, hence, represent important components in this process.

2.2 In addition to KCHs a variety of other players are involved in cytoskeletal coordination in plants

Many processes in cell growth and development require a tight temporal and spatial coordination of the two types of cytoskeletal elements. Fundamental cellular processes, known to integrate the functions of actin filaments and microtubules in plants, are intracellular transport (Cai and Cresti, 2009), the formation of the mitotic and cytokinetic apparatus (Kost and Chua, 2002; Nick, 2008), and the control of cell axis and directional cell expansion (Smith and Oppenheimer, 2005; Nick, 2008).

As already discussed above, KCH proteins possess characteristic molecular properties that make them ideal candidates for dynamic bifunctional mediation between both types of cytoskeletal elements. Such controllable, dynamic interaction could contribute to the spatial organization of a dynamic microtubular cytoskeleton relative to a distinct actin lattice (Nick, 2008). Lately, evidence has accumulated for several other plant proteins to be similarly involved in microtubule-microfilament interaction, either by simultaneously binding to both types of cytoskeletal elements, or by forming complexes of monofunctional proteins. The recently identified microtubule-associated protein SB401 from *Solanum berthaultii*, for example, has been shown to bind to and bundle both actin filaments and microtubules *in vitro* and to colocalize with cortical microtubules in pollen tubes (Huang et al., 2007). However, homologous of SB401 have only been found in *Solanaceae* so far, and are exclusively expressed in anthers. A different example is given by formins, a diverse family of proteins conserved among animals and plants. Formins contain characteristic formin homology (FH) domains known to mediate interactions with monomeric and filamentous actin (for review see Deeks et al., 2002; Goode and Eck, 2007). Several of their members were recently found to not only bind to actin filaments, but also to confer direct association with microtubules and membranes (Bartolini et al., 2008; Deeks et al., unpublished results). In the cell cortex of yeast and mammalian cells, formins have as well been implicated in the control of the organization of microtubular arrays by interaction with microtubule plus-end tracking proteins (Wen et al., 2004; Martin et al., 2005). If similar associations might be formed with plant homologues of microtubule plus-end interacting proteins such as EB1 (Chan et al., 2003) and CLASP (Ambrose et al., 2007) remains to be elucidated. Interestingly, microtubule and actin-binding has as well be shown for a number of proteins that seem, on the first glance, not to be related to the cytoskeleton. One example in this context is Phospholipase D, which belongs to a superfamily of plasma membrane associated signaling enzymes (Gardiner et al., 2001; Dhonukshe et al., 2003; Kusner et al., 2003; Ho et al., 2009). In these cases, the interaction might rather implicate regulatory instead of structural functions.

In conclusion, the interaction and coordination of the microtubule and actin cytoskeletons during growth and development of plant cells seem to involve a variety of different proteins and protein complexes, putatively acting at different cellular levels and time-points. Many of these proteins, including the family of KCHs, are unique to plants, indicating that cytoskeletal coordination in plant cells seems to differ clearly from the situation in animals where dyneins, dynactin complexes, myosins and ERM proteins have been identified as main components. The further elucidation of the distinct roles, specificities and regulations of the candidate proteins within plant cells will be an interesting goal of future research. The KCHs represent in this context proteins of special interest, due to their characteristic molecular properties. The following chapter will further discuss putative biological roles of this interesting class of molecular motors.

3 OsKCH1 influences cell division, cell elongation and premitotic nuclear migration

As already discussed above, KCHs are highly conserved in structure and function within higher plants (results section 1; Tamura et al., 1999; Preuss et al., 2004; Xu et al., 2009), and their ability to bind to microtubules and microfilaments makes them interesting candidates for bifunctional mediation between both cytoskeletal elements (results section 2; Preuss et al., 2004; Xu et al., 2009). Coordination and cross-talk between microtubules and microfilaments is necessary for many processes during plant growth and development such as the control of cell elongation and tissue expansion (for review see Collings, 2008; Petrášek and Schwarzerová, 2009). The cellular roles of KCH proteins in microtubule-actin interaction are, however, still far from understood. Xu et al. (2009) have suggested that GhKCH2 might play a role in cotton fiber elongation through cross-linking of microtubules and microfilaments, but no further evidence has been provided. Therefore, this work addressed the potential biological role of the rice KCH member OsKCH1. Gene expression of *OsKCH1* was analyzed and showed tissue and developmental regulation. Rice *kch1 Tos17* knock-out mutants as well as a *KCH* overexpression line generated in tobacco BY-2 cells were furthermore investigated for specific phenotypes. In both systems, cell elongation was altered antagonistically as result of knock-down and overexpression, together with a concomitant change in cell number. Additionally, microscopic studies showed dynamic repartitioning of OsKCH1 during the cell cycle and demonstrated that *KCH* overexpression delays nuclear positioning and mitosis in BY-2. The findings are discussed with regard to a putative role of KCHs as linkers between actin filaments and microtubules during nuclear positioning.

3.1 Changes in OsKCH1 expression levels alter cell division and elongation

The potential biological role of OsKCH1 was in a first step addressed via gene expression studies, which revealed that the transcription of *OsKCH1* is regulated in a tissue and development specific way. High transcript abundances were found in young and developing tissues, pointing towards a possible involvement of the protein in cell division and development. For other members of KCH, similar variations of protein expression in different developmental stages have been reported. Preuss et al. (2004), for example, show that the GhKCH1 protein in cotton fibers was predominantly abundant at 10 to 17 days post anthesis (DPA), whereas the levels strongly decreased at time-points later than 21 DPA. Furthermore, Tamura et al. (1999) could detect the *Arabidopsis* KatD protein only in total protein extract of flowers and not in any other organ including leaflets, stems, roots, or siliques. The other KCH family members from *Arabidopsis* are similarly expressed at varying levels during plant development, as a search in the gene expression database Genevestigator demonstrates (www.genevestigator.com).

A morphological investigation revealed that rice *kch1 Tos17* insertion mutants are impaired with respect to cell elongation in coleoptiles. The average cell length in coleoptiles was clearly

reduced in the mutants. Additionally, in contrast to the wild type, the apical cells were still not fully expanded when the primary leaves emerged. This indicates reduced and delayed elongation growth, producing generally shorter cells. In the lower third of mutant coleoptiles, cell length reached only about 60 % of the length observed in wildtypes. During subsequent development, however, no additional prominent phenotypes were identified, similar to the situation in *Arabidopsis*, where no significant phenotypes of null-mutations in *AtKatD* had been observed (Preuss et al., 2004).

Richardson et al. (2006) already conducted a thorough phylogenetic analysis of kinesins in different photosynthetic organisms and detected 7 copies of *KCH* in *Arabidopsis thaliana*, assumingly emerged through gene duplication during plant evolution. Our database search similarly found 7 copies of *KCH* in the genome of *Oryza sativa*. Thus, it cannot be excluded that functional redundancy exists among KCHs. This hypothesis is further underlined by the observed and above discussed development- and tissue-dependent regulations of *KCH* gene expressions in rice, cotton and *Arabidopsis*. A phylogenetic analysis, including KCHs from the grass model plant *Oryza sativa*, the Rosids *Arabidopsis thaliana*, *Populus trichocarpa*, *Vitis vinifera*, *Ricinus communis* and the moss *Physcomitrella patens*, shows that the proteins cluster into 4 different clades (Fig. 20). Each clade contains at least one copy of *KCH* from all species, with exception of the *KCHs* from *Physcomitrella* that solely form a branch, indicating a possible higher evolutionary divergence of these proteins. *OsKCH1* clusters into the most expanded branch, together with two other closely related rice *KCH* family members, such that functional redundancy is to be expected.

Antagonistically to the observed coleoptile phenotype in rice *kch1* mutants, BY-2 cells overexpressing *OsKCH1* were clearly more elongated than the non-transformed BY-2 wildtype (Wt) cells and a cell line overexpressing *free GFP*. A potential role in cell expansion has already been proposed for *KCH* members from cotton. GhKCH1, for example was mainly expressed during rapid cell elongation of the fiber (Preuss et al., 2004) – a process that specifically depends on the presence of a parallel array of cortical microtubules (Kim and Triplett, 2001). GhKCH2 was similarly proposed to be associated in fiber elongation through cross-linking of microtubules and microfilaments (Xu et al., 2009). Our observations of knock-out and overexpression phenotypes for *OsKCH1* confirm that this protein is involved in cell elongation. Inhibitor studies have demonstrated that actin filaments and microtubules interact closely during cell growth and elongation for various plant and cell systems including cotton fibers (Seagull, 1990), *Arabidopsis* roots (Baskin and Bivens, 1995; Collings et al., 2006), and seedlings of maize and rice (Giani et al., 1998; Wang and Nick, 1998; Blancaflor, 2000). The *KCH1* proteins interact with both cytoskeletal elements and are therefore good molecular candidates for this interaction. Our observations would be consistent with a model, in which *KCH1* is required for efficient cell elongation by stabilizing transverse arrays of microtubules. Loss-of-function should then result in reduced cell length (which was observed in the coleoptiles of the *Tos17* mutants, Fig. 19), whereas elevated abundance of *KCH1* should result in increased cell length (as observed in the BY-2 *OsKCH1* overexpressor, Fig. 21).

However, the reality might be more complex than this simple working hypothesis. The observed changes in cell length were always accompanied by antagonistic changes in cell number. In the *kch1* insertion mutants cell length was strongly reduced, but this was almost compensated by a concomitant increase in cell number (Fig. 19). Conversely, in the BY-2 *OsKCH1* overexpressor, the increased cell length was accompanied by a reduced mitotic index during the first days of the culture cycle (Fig. 22). Therefore, our observations are equally compatible with a model, where the primary target of *KCH1* is not cell expansion, but cell division. This is further underlined by the fact that the highest expression of *OsKCH1* was found in young roots, young leaves, young flowers, and flowers post pollination – in other words, in tissues endowed with meristematic activity. In adult leaves, that still expand throughout their life time, *OsKCH1* transcripts were almost absent. When interpreting the relatively high expression of *OsKCH1* in coleoptiles (where no cell division is observed following germination), one has to bear in mind that the coleoptile is the embryonic organ with the highest mitotic activity continuing till the very onset of dormancy (Nick et al., 1994).

At first glance, the observed antagonism between cell elongation and cell division might appear trivial: Cells are obviously larger when they have undergone a lower number of divisions. Nevertheless, this trivial model ignores the fact that the regulation of cell division and cell expansion clearly differs – as found in both *Arabidopsis* seedlings (Chen et al., 2001; Perfus-Barbeoch et al., 2004) and tobacco cells (Chen et al., 2001; Campanoni and Nick, 2005). Whereas auxin stimulates cell expansion via the receptor ABP1 and independently of G-protein signaling, cell division is controlled by an auxin receptor that differs with respect to ligand specificity and triggers G-protein dependent signaling (Ullah et al., 2001; Campanoni and Nick, 2005). How is the regulation of cell division and cell expansion via the different signaling networks integrated within the cells, and which role does *OsKCH1* have within these signaling networks? These questions remain to be elucidated in further research.

3.2 *OsKCH1* influences nuclear positioning

If cell division is a primary target for *KCH1*, it should be possible to observe directly that *KCH1* colocalizes with mitotic structures, and that overexpression of *KCH1* alters these structures or the process of division. An investigation of mitosis in the BY-2 *KCH1* overexpressor, however, showed that spindle morphology was identical to non-transformed wildtype cells. This suggests that mitosis in general was not structurally disturbed by the overexpression. Nevertheless, the rate of mitosis during the first days of the culture cycle was clearly reduced in BY-2 *KCH1*, pointing towards a delayed onset of mitosis.

A microscopic analysis of the localization of GFP *OsKCH1* in tobacco BY-2 revealed a dynamic repartitioning of the protein during the cell cycle (Fig. 23, 24 and 33). In interphasic and premitotic cells, a punctate *OsKCH1* signal was clearly aligned with filaments that tethered the nucleus to the periphery. In addition, the signals accumulated at the sites, where these filaments emanate from the nuclear rim and where they merged into the cell cortex. Interestingly, at the

onset of mitosis, OsKCH1 retracted from the nucleus and the division plane such that it did not colocalize with mitotic microtubule structures. Following division, OsKCH1 then reassembled during cytokinesis around the newly formed daughter nuclei and repopulated the filaments that joined the nuclei to the periphery and the newly formed cross wall. This dynamic relocation pattern does not support a direct role of KCH1 in mitosis in the strict sense, but rather indicates a relation with the position of the nucleus.

In plant cells that prepare for division, a migration of the nucleus occurs towards the site where the prospective cell plate will form (for review see Nick, 2008). Such migration in tobacco BY-2 cells was found to be highly sensitive to inhibitors of microtubules and microfilaments (Katsuta and Shibaoka, 1988; Katsuta et al., 1990), indicating a tight interplay between both types of cytoskeletal elements. Katsuta et al. (1990) proposed that the premitotic network of microtubules might serve as a scaffold for the positioning of actin filaments that establish and maintain the position of the nucleus and the mitotic apparatus. As already discussed above, KCHs are able to bind to both microtubules and microfilaments in different organisms and cell types (see discussion, section 2). OsKCH1 (Fig. 30) and its cotton homologue GhKCH2 (Xu et al., 2009) were moreover found to cross-link actin and microtubules *in vitro*. OsKCH1 further predominantly localized at contact points between actin filaments and microtubules *in vivo* (Fig. 11 d). Most interestingly, BY-2 cells overexpressing OsKCH1 showed clearly delayed premitotic movement of the nucleus into the cell center (Fig. 26). As already discussed above, this correlates with diminished mitotic activity during the culture cycle and elevated cell expansion. In addition, these findings are accompanied by accumulation of GFP-tagged KCH1 along perinuclear filaments that surround the nucleus as long as the nuclear envelope is contiguous. As soon as the nuclear envelope disintegrates, these signals, however, repartition.

The most straightforward models to explain these observations would assume that KCH1 proteins participate in the control of premitotic nuclear positioning. Fig. 33 shows two principal models that illustrate how KCH1 might contribute to nuclear movement and are not mutually exclusive. Microtubules and actin filaments might transmit forces that are generated by KCH1 at the perinuclear contact sites to the cortex such that the nucleus is either pulled or pushed, or both. Alternatively, KCH1 might simply anchor the perinuclear network at the cell cortex and move the nucleus by mutual sliding of actin filaments and microtubules in the cortical cytoplasm. The fact that overexpression of *KCH1* delays premitotic nuclear movement as well as mitotic activity, whereas inhibition of its activity by a *Tos17* insertion leads to increased cell number, might furthermore indicate that *KCH1*-dependent nuclear movement is part of a cellular checkpoint that releases M-phase only after the nucleus has reached its correct position in the cell center.

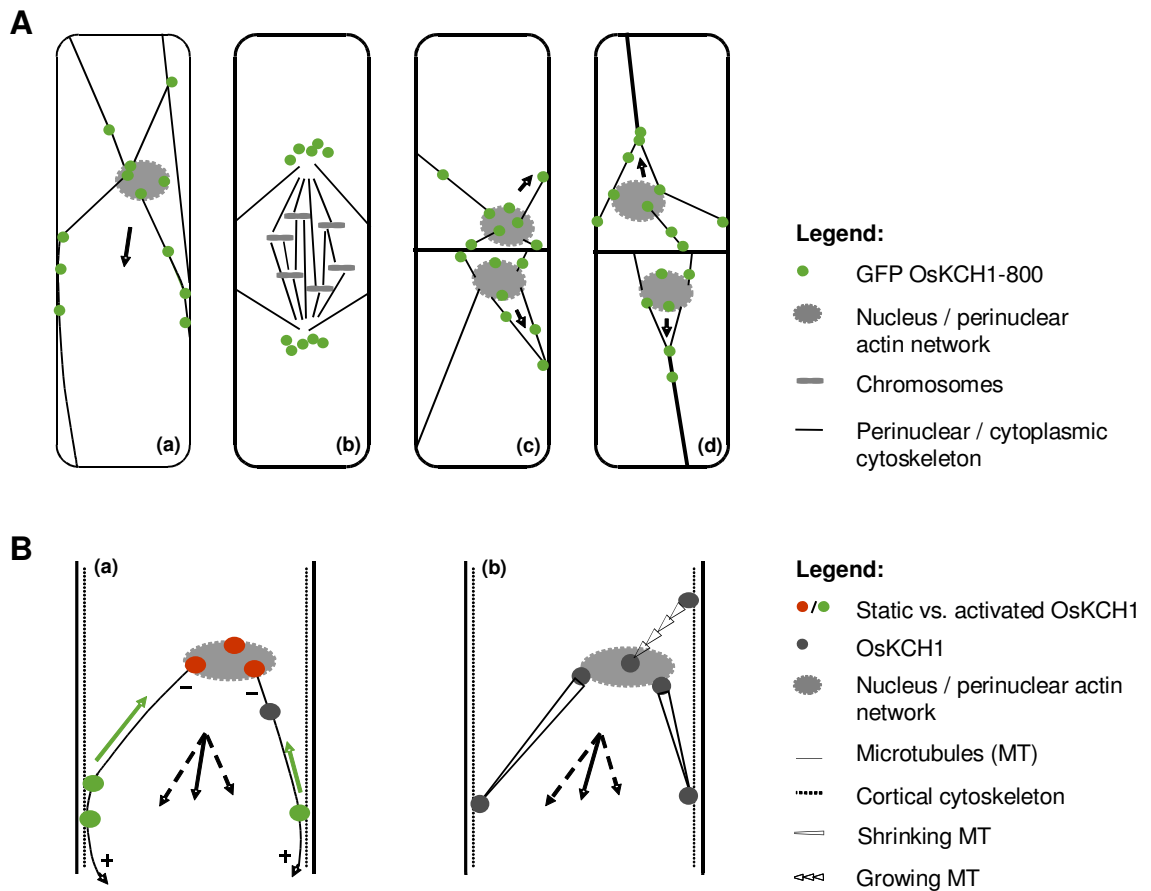


Fig. 33: Localization of *OsKCH1* during the cell cycle and working models for the function in nuclear positioning

[A] Dynamic redistribution of GFP *OsKCH1* during the cell cycle. In interphasic and premitotic cells (a), *OsKCH1* signals colocalized with a cytoskeletal network that tethers the nucleus to the periphery. Punctate signals accumulated at the sites, where the filaments reached the nuclear envelope or connected to the cell cortex. During mitosis (b), *OsKCH1* retracted from nucleus and division plane and did not colocalize with mitotic microtubule structures. During cytokinesis, *OsKCH1* signals were repartitioned and subsequently mainly found surrounding the newly formed nuclei, again along the cytoskeletal network that tethered these nuclei to the periphery or connected the nuclei with the cell poles. Arrows indicate the observed directions of nuclear movement. [B] Schematic models for the function of *OsKCH1* in nuclear positioning. A ‘sliding model’ (a) is based on two different populations of *OsKCH1*. Static *OsKCH1* proteins anchor the minus-end of radial microtubules at the nuclear envelope, possibly via interaction with the perinuclear actin network. The plus-ends of the microtubules are captured at the cortex by protein complexes involving activated *OsKCH1* motors that move towards microtubule minus-ends (red arrow), but are anchored such that they generate a sliding force (arrow heads) which finally acts on the nucleus. Black arrows depict the force vectors that produce a resulting force (plain arrow) pointing in the observed directions of nuclear movement. A ‘pulling/pushing model’ (b) relies rather on microtubule dynamics. Microtubules are captured by anchor protein complexes involving *OsKCH1* on both the nuclear envelope and the cell cortex. Depending on the accessory protein complexes, microtubule dynamics are differentially regulated, resulting either in growth or shrinkage. Black arrows again depict the force vectors.

3.3 KCHs could represent functional homologues of dyneins in nuclear positioning

Nuclear positioning has already been studied in *S. cerevisiae*, *S. pombe*, filamentous fungi, and a variety of animal cells and tissues. The systems that orient and move nuclei were found to be moderately conserved among the different systems and involve dynein and dynactin as key players (Morris, 2003; Yamamoto and Hiraoka, 2003).

Extensive studies on nuclear positioning in budding yeast have revealed that the migration of the nucleus into the bud is driven by two basic, partially overlapping mechanisms that involve the minus-end directed microtubule motor dynein (Adames and Cooper, 2000; Yamamoto and Hiraoka, 2003). In a first step, inactive dynein is recruited together with dynactin and several microtubule plus-end directed proteins into protein complexes at the distal ends of astral microtubules. These complexes then mediate the attachment of the microtubules to the cell cortex and the actin cytoskeleton within the bud and the mother cell. Subsequently, movement force is generated on the nucleus through a controlled induction of microtubule depolymerization that involves concerted antagonistic actions of the microtubule-destabilizing dynein/dynactin-complexes and the microtubule-stabilizing kinesin motor Kip2. In parallel, by anchoring to the cell cortex, dynein motors become activated and in turn move on the microtubule towards the minus-end. This generates cortical sliding of astral microtubules and, in consequence, as well drives nuclear migration. The combination of repulsive and attractive forces, generated by microtubule polymerization and depolymerization events on one hand, and dynein-mediated sliding of microtubules along the cell cortex on the other hand, renders nuclear migration in the budding yeast a fine-tunable process. The described mechanism is highly conserved and similarly found in *S. pombe* and filamentous fungi (reviewed by Yamamoto and Hiraoka, 2003). A high degree of similarity to the fungal system is furthermore found for nuclear positioning in animal cells (Morris et al., 2003).

By contrast, in higher plants, which lack dyneins and its associated proteins (Lawrence et al., 2001), the mechanisms for moving nuclei must involve a variety of fundamentally different players. Interestingly, this process seems to not only involve microtubules, but as well actin filaments (Katsuta and Shibaoka, 1988; Katsuta et al., 1990; Chytilova et al., 2000; Ketelaar et al., 2002). Might – as proposed by Katsuta et al. (1990) – the premitotic network of microtubules serve as a scaffold for the positioning of actin filaments that establish and maintain the position of the nucleus and the mitotic apparatus? Due to their characteristic molecular properties, KCH proteins represent interesting candidates for bifunctional linkers in this context. The cellular phenotypes establishing upon overexpression or knock-down of *OsKCH1* further point towards an involvement of the protein in this process. Our knowledge of the molecular details remains, however, incomplete. Could KCH proteins be the functional homologues of dyneins as cortical anchors with minus-end directed motor activity? For further elucidation of the structural binding characteristics as well as the motor-dependent properties of *OsKCH1*, additional biochemical analysis were performed, and the results are discussed in the following chapter.

4 OsKCH1 is a dynamic structural linker of the cytoskeleton

Due to their molecular properties, KCHs are interesting candidates for bifunctional mediation between both cytoskeletal elements in plants (results section 2; Preuss et al., 2004; Xu et al., 2009). Coordination and cross-talk between microtubules and microfilaments is necessary for many processes during plant cell growth and development. A tight spatiotemporal coordination is especially required for the control of cell division and elongation (for review see Collings, 2008; Petrášek and Schwarzerová, 2009). The previous chapter has already discussed a putative involvement of OsKCH1 in this context. Two different, but not mutually exclusive models were proposed that describe possible roles of OsKCH1 during nuclear positioning – a process that precedes mitosis in plants, but is so far only sparsely understood. As already described in detail in chapter 3.3, the movement of nuclei within a cell is a highly conserved process in animal and fungi and involves several groups of proteins (reviewed by Morris, 2003; Yamamoto and Hiraoka, 2003). Microtubule plus-end associated proteins together with cortical anchor proteins typically act as structural linkers and attach the astral microtubules to the cell cortex. Microtubule minus-end directed dynein motors, together with dynactin complexes, are rather involved in the generation of force that acts on the nucleus, either indirectly by promoting microtubule depolymerization, or directly by sliding of astral microtubules along the cell cortex. Higher plants, however, lack dyneins (Lawrence et al., 2001). Hence, nuclear positioning must involve a variety of fundamentally different players. As illustrated in the model in Fig. 33, the bifunctional OsKCH1 protein represents an interesting candidate in this context. The molecular details remain, however, unclear. Thus, a further characterization of the biochemical properties is necessary to obtain a better understanding of the possible involvement of KCH proteins in nuclear movement.

In the course of this work the binding behavior of OsKCH1 to both microtubules and actin filaments was therefore further investigated and quantified. An assessment of the specific binding kinetics showed that OsKCH1 associates with a high affinity to actin filaments and, to lower extend, also to microtubules. Interestingly, OsKCH1 was found to form dimers and tetramers, and this oligomerization seemed to be a prerequisite to confer binding to actin and to induce filament-bundling as well as microtubule-microfilament cross-linking. Unlike several internal motor proteins from different kinesin families, OsKCH1 did not show microtubule depolymerization activity *in vitro*. Kinetic analysis of OsKCH1 *in vivo*, however, could detect a slow movement of OsKCH1 in the cell cortex of tobacco BY-2 cells. These findings point towards a role of OsKCH1 as a dynamic structural linker protein of microtubules and microfilaments and are discussed in respect to a putative role of OsKCH1 during nuclear positioning.

4.1 KCH family members are unusual in their cytoskeletal binding affinities

As already discussed in detail in a previous chapter (discussion section 2), OsKCH1 is a bifunctional protein and able to bind to actin filaments and microtubules *in vitro* and *in vivo*. In order to obtain a better understanding of the putative binding preferences of the protein to both types of cytoskeletal elements, the specific binding kinetics were assessed. The strength of a protein interaction is typically described by the equilibrium dissociation constant K_d . The specific K_d values for the interaction of OsKCH1 with either actin microfilaments or microtubules were thus assessed *in vitro* via concentration-dependent cosedimentation assays.

Interestingly, recombinantly expressed KCH1 showed quite high affinity for actin filaments in these cosedimentation assays. This is reflected by the small dissociation constant ($K_d = 1.76 \mu\text{M}$; Fig. 27) of the complex formed between actin filaments and the recombinantly expressed truncation KCH1-cc1, encoding the N-terminus of OsKCH1 including the CH-domain and the first coiled-coil stretch. A previous study by Xu et al. (2009) similarly showed a high binding affinity of the N-terminal part of the cotton KCH member GhKCH2 to actin filaments ($K_d = 0.42 \mu\text{M}$) and thus further supports our observations. Interestingly, we obtained slightly different K_d values for the interactions of the nearly full-length KCH1-cc3 and the truncated protein KCH1-cc1 with actin filaments ($K_{d\text{cc3}} = 4.80 \mu\text{M}$ versus $K_{d\text{cc1}} = 1.76 \mu\text{M}$). Hence, the presence of additional domains within the protein, such as the motor domain, obviously influences the protein's overall affinity to actin – possibly due to steric effects.

In contrast to the observed tight association of KCH1 with actin filaments, clearly lower affinities were found in cosedimentation assays of recombinantly expressed KCH1 with microtubules. The nearly full-length construct KCH1-cc3 bound to microtubules with a K_d value of $7.74 \mu\text{M}$. The association of the truncated protein KCH1-mot – containing only the central protein part including the motor domain – with microtubules showed a characteristic K_d value of $6.77 \mu\text{M}$ (Fig. 27). The observation that the K_d values for both the full-length and the truncated protein did not differ substantially, indicates that the binding of OsKCH1 to microtubules depends specifically on the motor domain, and is not influenced by the presence of other domains within the protein, such as the CH domain. In a previous study, Xu et al. (2007) already investigated the microtubule-binding behavior of the cotton KCH member GhKCH2. A specific K_d value of $7.69 \mu\text{M}$ was found for the interaction of the motor domain of GhKCH2 ($M_{396-734}$) with microtubules. The affinities of OsKCH1 and GhKCH2 to microtubules were thus in a similar range, underlining the tight functional conservation among KCH members from different species.

Interestingly, the obtained dissociation constants for the KCH members were about 10-15 fold higher than the K_d values obtained for other well-characterized kinesins. The plus-end directed conventional kinesin motor KHC, for example, has a microtubule dissociation constant of $0.4 \mu\text{M}$ (Huang and Hackney, 1994), and the minus-end directed *Drosophila* kinesin-14 family member Ncd has a K_d of $0.7 \mu\text{M}$ (Lockhart et al., 1995). In comparison to these kinesins, the affinities of both OsKCH1 and GhKCH2 for microtubules are thus rather low, indicating clear

differences in the binding characteristics of KCH proteins not only with regard to plus-end directed kinesins, but as well to other members of the kinesin-14 family. Intriguingly, unlike most kinesins, dynein motors possess quite low intrinsic affinities to microtubules. As shown in recent studies, the characteristic K_d values determined for several dynein constructs from mouse and *Dictyostelium* ranged between 2.2 and 12 μM (Gibbons et al., 2005; Imamura et al., 2007).

The overall binding of a number of kinesins and other MAPs to microtubules, however, has been shown to depend not only on their intrinsic affinities, but as well on protein modifications and the interaction with additional regulatory components. Phosphorylation of the motor domain of *Drosophila* kinesin-13, for example, was found to increase its affinity for microtubules (Mennella et al., 2009). Other studies showed that posttranslational modifications of kinesin-associated proteins as well affected the microtubule-binding characteristics of the motors (McIlvain et al., 1994). In addition to this direct regulations, the activity of kinesins can further be modulated indirectly, such as by modifications of the microtubule population. Only recently, for example, the *Aspergillus nidulans* kinesin UncA was found to associate preferentially with detyrosinated microtubules (Zekert and Fischer, 2009). Similar to kinesins, the affinity of dyneins for microtubules, as well as their motor activity, has been shown to underly tight regulation (Kardon and Vale, 2009).

The binding of OsKCH1 with microtubules and microfilaments thus might not only be determined by the intrinsic affinity constants, but could be subject to additional regulations. Posttranslational modifications and an additional association with other complex partners, hence, could lead to a certain amount of fine-tuning of the interactions – for example as a result of altering cellular requirements. In order to elucidate if this might be the case for the association of KCH proteins with microtubules and microfilaments, further biochemical studies will be necessary.

4.2 OsKCH1 oligomers bind and bundle actin and microtubules

The previous chapters already displayed the ability of OsKCH1 to bind to both microtubules and actin filaments (discussion sections 2 and 4.1). Detailed quantitative biochemical analysis has especially revealed the tight association of the protein with actin filaments. This is however a most intriguing finding, as KCHs contain only a single CH domain whereas actin-binding typically requires two CH domains in tandem (Gimona and Mital, 1998; Gimona et al., 2002). In accordance with our results on the specific association with recombinantly expressed full-length and truncated OsKCH1 (Fig. 16 and 27), previously published data by Preuss et al. (2004) and Xu et al. (2009) reported the cosedimentation of the N-terminal portions of the KCH members GhKCH1 and GhKCH2 with actin microfilaments. How could this conserved binding of KCH members to actin be explained?

Interestingly, the protein calponin, which itself as well only contains one single CH domain, is an actin-binding protein and has an additional actin-binding site mapped to a region between the CH domain and the C-terminus of the protein (Gimona and Mital, 1998). It might thus be possible that a certain portion in the N-terminal part of KCHs, but outside the CH domain, is addi-

tionally required for the binding. Alternatively, a protein complex that contains more than one CH domain could be generated through protein oligomerization. Dimerization and tetramerization is a widely known structural features of kinesins (Miki et al., 2005) and generally occurs via long coiled-coils stalks.

As shown by *in silico* analysis, OsKCH1 harbors three putative coiled-coil regions, two upstream and one downstream of the motor core, which might be involved in protein oligomerization. The observation that only protein truncations which contain at least one coiled-coil in addition to the CH domain, such as KCH1-cc1, KCH1-cc2 and KCH1-cc3, showed efficient binding to actin in the cosedimentation assays, further supports this hypothesis. A shorter truncation KCH1-sh, encoding only the CH domain, did only show weak association with actin filaments. A similar observation was made by Preuss et al. (2004) with respect to the binding of GhKCH1 to actin filaments. While a truncated GhKCH1 protein encoding both the CH domain and the first coiled-coil stretch cosedimented with actin, this was not observed for a shorter variant that only included the CH domain.

These results clearly point towards an oligomerization of KCH proteins. Therefore, a combination of Bimolecular Fluorescence Complementation (BiFC) assays and size-exclusion chromatography (SEC) with recombinantly expressed protein were used to test for protein oligomerization both *in vivo* and *in vitro*. The BiFC assays clearly showed a reconstitution of split-YFP signals in rice and BY-2, indicating the formation of complexes *in cellula* presumably due to dimerization of KCH1 via the coiled-coils (Fig. 28). In accordance with the BiFC results, SEC gelfiltration of recombinantly expressed OsKCH1-mot, containing the coiled-coil domains and the motor core, showed the oligomerization of the protein *in vitro* (Fig. 29). Thus, OsKCH1 might bind to actin microfilaments in a homodimeric or tetrameric complex, such that more than one CH domain would be available at a time to confer binding.

An oligomeric complex of OsKCH1 would not only contain several CH domains to confer binding to actin, but at the same time would be free to interact with microtubules. Hence, the question arises whether OsKCH1 is capable to generate functional linkages between either filaments of one kind, as well as between both microtubules and actin microfilaments. Fluorescence microscopy of various mixtures of microtubules, actin filaments, and recombinantly expressed variants of OsKCH1 clearly showed bundling of both microtubules and actin filaments (Fig. 30). In accordance with the above discussed results on the oligomerization of OsKCH1, the filament-bundling ability was tightly associated with the presence of coiled-coil domains within the molecule. Thus, the nearly full-length KCH1-cc3, containing all three coiled-coil domains, induced strong actin- as well as microtubule-bundling throughout the suspensions, while for the shorter construct bundling was either only observed to a smaller extend or not at all. This finding clearly underlines the importance of the coiled-coil regions and presumably of protein oligomerization for mediation of filament bundling.

KCH1-cc3 did, however, not only efficiently bundle either microtubules or actin filaments, but did as well cross-link and co-align both types of cytoskeletal elements. For the shorter truncations, that either contained only the CH domain or the motor core, similar co-alignment of both

types of cytoskeletal elements was not observed, further supporting the domain-specificity of binding.

Taken together, these results underline the ability of OsKCH1 to bind to microtubules and actin, and to act as bifunctional mediators between both types of cytoskeletal elements. The binding is most likely to involve protein oligomerization, generating a protein complex that contains several functional domains which are able to confer similar binding to microtubules and actin at a time. The observation that OsKCH1 indeed was able to confer cross-linking and co-alignment of both cytoskeletal elements further points towards a putative role of the protein as a linker in the structural coordination process of the actin and microtubule networks within the cell.

4.3 KCHs contribute to a dynamic cytoskeletal reorganization

Due to their bifunctional molecular properties, KCHs are interesting candidates for spatiotemporal coordination of microtubules and actin filaments (results section 2; Preuss et al., 2004; Xu et al., 2009). The cellular phenotypes that establish upon overexpression or knock-down of OsKCH1 point towards an involvement of the protein in premitotic nuclear positioning and thus an indirect influence on the control of cell division and elongation (see results, section 3). The mechanisms for the movement of nuclei in plants interestingly involve not only microtubules but as well actin filaments (Katsuta and Shibaoka, 1988; Katsuta et al., 1990; Chytilova et al., 2000; Ketelaar et al., 2002). The coordination of this process would require mediators between both types of cytoskeletal elements – such as KCH proteins. The previous chapter already presented two general models that describe a possible contribution of OsKCH1 to nuclear movement (Fig. 33). In both cases, the bifunctional protein OsKCH1 would anchor the perinuclear network at the cell cortex. Movement force would subsequently either be generated by mutual motor-dependent sliding of actin filaments and microtubules in the cortical cytoplasm, or by cytoskeletal dynamics that result in pushing or pulling of the nucleus. Additional biochemical analysis have already underlined the filament cross-linking properties of OsKCH1 (Fig. 30) and thus the presumed role of KCH proteins as mediators between the premitotic network of microtubules and the actin filaments that establish and maintain the position of the nucleus.

Our knowledge of the molecular properties of OsKCH1 has, however, remained incomplete. In fungal and animal systems the process of nuclear migration involves several key players that not only perform structural functions by mediating the attachment of astral microtubules to the cell cortex, but as well generate motor-dependent movement force or modulate cytoskeletal dynamics. Key components in this context are the minus-end directed dynein motors, dynein/dynactin complexes and microtubule-destabilizing kinesins (Adames and Cooper, 2000; Morris, 2003; Yamamoto and Hiraoka, 2003). Higher plants, however, lack homologues of these key components (Lawrence et al., 2001). In consequence, the process of nuclear positioning in plants must involve a variety of fundamentally different players.

Phylogenetic analysis has shown that KCH proteins belong to the kinesin-14 subfamily. This family is vastly expanded in plants and contains motors that confer – unlike most other kinesins – minus-end directed motility along microtubules. A detailed analysis of the domain structure of OsKCH1 has interestingly revealed that the neck-linker, which is known to confer minus-end directed motility for many kinesin-14 family members, is conserved in KCH proteins. Could KCH proteins possibly as well confer directed microtubule-based motility and thus represent putative functional homologues to dyneins or dynein/dynactin complexes from animal and fungal systems? Or might KCHs rather be involved in the regulation of cytoskeletal dynamics? The fact that KCHs possess centrally located motor cores, which are quite similar to the domain structures of proteins from the kinesin-8 and kinesin-13 family, would further point towards the second possibility. Members of these families are typically involved in microtubule-destabilization instead of conferring directed motility.

The characteristic properties of OsKCH1 as a molecular motor protein were thus further analysed. The recombinantly expressed OsKCH1-mot was investigated for microtubule-destabilizing activity in microtubule depolymerization assays. Under the respective *in vitro* conditions no microtubule-destabilizing activity was detected (Fig. 31). However, it can not be excluded that OsKCH1 shows microtubule-destabilizing activity *in vivo* – maybe in concerted interaction with other complex binding partners, or upon posttranslational modification. For further clarification of this point, *in vivo* investigations as well as the identification of putative binding partners or regulatory components will be necessary.

While no destabilizing activity could be attributed to recombinant KCH1, the *in vivo* tracking of fluorescent KCH1 in the cell cortex clearly revealed motility. Time-lapse microscopy and subsequent kinetic analysis showed movement of fluorescent stubs of KCH1 with an average speed of 13 nm/sec. Motility was, however, not observed simultaneously for all fluorescent dots but only for parts of the population – indicating that the intracellular activity of the protein might undergo a certain amount of regulation. The observed dynamics of OsKCH1 are in accordance with previous results that reported ATPase activity for the cotton KCH member GhKCH2 (Xu et al., 2006). The ability of a kinesin to hydrolyze ATP is typically closely connected with the conformational change that leads to stepwise movement of the motors along microtubules.

Interestingly, the obtained velocities for OsKCH1 were about 10-30 fold lower than the velocities estimated for other well-characterized kinesins. The plus-end directed conventional kinesin motor KHC, for example, moves with a typical speed of 0.78 $\mu\text{m}/\text{sec}$ along to microtubules in mammalian cells during vesicle transport (Cai et al., 2007). *In vitro* assays furthermore showed that the *Drosophila* kinesin-14 member Ncd moves with an average velocity of 0.15 $\mu\text{m}/\text{sec}$ towards microtubule minus-ends (Chandra et al., 1993). The kinesin-14 family KCBP from *Arabidopsis* was the first plant kinesin investigated for microtubule-based motility. It showed mean velocities of 0.16 $\mu\text{m}/\text{sec}$ *in vitro*, quite similar to *Drosophila* Ncd (Song et al., 1997). In comparison to these kinesins, the velocity observed for the movement of OsKCH1 *in vivo* is rather low. This indicates possible differences in the movement characteristics of KCH proteins not only from plus-end directed motors, but as well from other members of the kinesin-14 family such as Ncd and KCBP.

However, the movement velocities of several kinesins were shown to be highly dependent on the specific loads. Higher movement velocities, thus, typically occur in combination with low force requirements – for example as result of small cargoes (Coppin et al., 1997; Valentine and Block, 2009; Zheng et al., 2009). A load-dependency of the movement velocity was not only observed for kinesins but as well for other molecular motors. The plant myosin XI, for example, is involved in the low-force transport of small vesicles along actin filaments in plant cells and shows an about 10-fold higher velocity as the mammalian muscle myosin-II (Tominaga et al., 2003). The velocities measured for dynein-dependent movement as well varied in a quite broad range. While investigations of the vesicle transport velocities of chicken dynein have revealed typical values of about 0.6-0.8 $\mu\text{m}/\text{sec}$ (Schroer and Sheetz, 1991), the average speed of the dynein/dynactin complex required for nuclear movement in *S. cerevisiae* was recently reported to be only about 77 nm/sec (Kardon et al., 2009).

In summary, the molecular properties of the different classes of molecular motors are regulated by a variety of factors that include the specific cargo, the interaction with other complex binding partners, as well as specific protein modifications. Dynamic behavior of OsKCH1 was so far only observed *in vivo*. A future detailed analysis of the protein motility *in vitro* will be required to obtain a better understanding of its specific movement characteristics. Nevertheless, we can already conclude that the KCH members OsKCH1 and GhKCH2 possesses distinct dynamic properties. Thus, KCHs are not only effective bifunctional linkers of microtubules and microfilaments, but can as well contribute to their dynamic reorganization.

CONCLUSION

Tight spatiotemporal coordination of microtubules and microfilaments is necessary for many processes during plant cell growth and development. In animals and fungi a number of proteins have been identified that mediate such interactions (Rodriguez et al., 2003). In plants, however, the situation has remained unclear. The recently identified kinesins with calponin-homology domain (KCHs) possess a characteristic domain structure that includes both actin and microtubule binding motifs (Preuss et al., 2004; Tamura et al., 1999). KCHs form a phylogenetically distinct and highly conserved subgroup within the plant kinesin-14 family. The cotton family member GhKCH1 has already been linked with a putative role in microtubule-microfilament interaction in developing cotton fibers (Preuss et al., 2004). It remained, however, unclear, if this presumed bifunctionality represents a conserved function among the KCHs, or was rather limited to the highly specialized nature of the cotton fiber cell system.

This study reports the identification of a new KCH from rice, OsKCH1, and demonstrates its association with microtubules and actin microfilaments in different cell systems *in vivo*. OsKCH1 furthermore binds in a domain-dependent way to microtubules and actin microfilaments *in vitro*. In summary, these results provide evidence that the presumed association with microtubules and actin microfilaments is a general function of KCHs, which is found both in cycling and non-cycling cells, as well as *in vitro*. Thus, KCHs constitute a unique class of plant kinesins. They are highly conserved in structure and function and represent interesting candidates for bifunctional mediation between both cytoskeletal elements during diverse processes in plant cell growth and development.

In order to gain insight in the biological roles of KCH proteins, the specific cellular function of the rice KCH member OsKCH1 was investigated. Rice *kch1 Tos17* knock-out mutants, as well as a *KCH* overexpression line generated in tobacco BY-2 cells, showed specific cellular phenotypes. In both systems, cell elongation was altered antagonistically and was accompanied by concomitant changes in cell number. In addition, the gene expression pattern of *OsKCH1* showed clear developmental regulation, with highest transcript abundances in dividing tissues. Microscopic studies revealed dynamic repartitioning of the protein during the cell cycle. Furthermore, OsKCH1 was predominantly localized on filaments that tether the nucleus to the periphery in interphasic and premitotic cells – pointing towards a relation of OsKCH1 with the positioning of the nucleus. In fact, additional quantitative investigations supported this hypothesis. Thus, the observed reduced mitosis in BY-2 cells that overexpress *OsKCH1* were assigned to a delay in premitotic nuclear migration towards the cell center. This shows the involvement of KCHs in the regulation of nuclear positioning and, as a consequence, in the progression of mitosis. As premitotic nuclear migration in plant cells relies on a tight interplay between microtubules and microfilaments, the bifunctional KCH proteins are indeed interesting candidates for the mediation and the control of this process.

The molecular mechanisms that orient and move nuclei in other organisms, such as yeast, filamentous fungi and animal cells, are fairly conserved. As key players, they involve dynein, dynactin and other proteins that accumulate at the plus-ends of astral microtubules and mediate

interaction with the cell cortex (Morris, 2003; Yamamoto and Hiraoka, 2003). Both repulsive and attractive forces are generated by a combination of microtubule polymerization and depolymerization events, complemented by dynein-mediated sliding of microtubules along the cell cortex (Adames and Cooper, 2000). As dyneins and its associated proteins lack in plants (Lawrence et al., 2001), the mechanisms for nuclear movement must involve fundamentally different players that are able to interact with both premitotic microtubules and actin filaments. Could KCH proteins be these missing links that anchor – as functional homologues of dyneins – motor activity to the cortex? Based on the mechanisms of nuclear positioning in fungal and animal systems, the present work has developed two principal but not mutually exclusive models that illustrate how KCH1 might contribute to nuclear movement in plant cells. Following these models, the bifunctional protein OsKCH1 would anchor the perinuclear network to the cell cortex. Subsequently, movement force would either be generated by motor-dependent sliding of actin filaments and microtubules in the cortical cytoplasm, or by cytoskeletal dynamics that result in pushing or pulling of the nucleus.

These models were further supported by the results of additional biochemical investigations. A combination of BiFC assays *in vivo* and SEC with recombinantly expressed proteins *in vitro* showed that OsKCH1 is able to assemble into dimers and tetramers. This oligomerization of OsKCH1 was found to be a prerequisite for conferring an efficient binding to cytoskeletal elements. Hence, the oligomeric OsKCH1 can be envisaged as a bifunctional protein. It contains several domains which are simultaneously free to interact with both microtubules and actin filaments. *In vitro* bundling assays, in fact, confirmed the ability of OsKCH1 to generate functional interactions between both cytoskeletal elements. *In vivo* trackings of the intracellular protein dynamics finally indicate that OsKCH1 is not only a structural linker of microtubules and microfilaments but as well possesses dynamic properties.

OUTLOOK

The present thesis could show that OsKCH1, a member of the unconventional and plant-specific KCH subgroup of kinesins, is able to act as a bifunctional linker of microtubules and actin. Furthermore, the results of this work indicate an involvement of OsKCH1 in the structural and dynamic coordination of both types of cytoskeletal elements during the nuclear positioning process. These findings lead to several interesting questions referring to the intrinsic properties of OsKCH1 as a molecular motor, the interaction of OsKCH1 with other proteins as well as binding partners, and the involvement of OsKCH1 in regulatory circuits during cell development. Future work might therefore focus on the following two aspects.

1 Intrinsic motor properties of OsKCH1

This thesis has presented two basic models that describe putative contributions of KCH1 to nuclear movement in plant cells. In these models, the movement force that acts on the nucleus would either be generated by motor-dependent sliding of actin filaments and microtubules in the cortical cytoplasm, or by cytoskeletal dynamics that result in pushing or pulling of the nucleus. First investigations have indicated that OsKCH1 indeed possesses characteristic and tunable motor properties. However, to obtain a better understanding of the specific role of the protein during nuclear positioning, a more detailed knowledge of these intrinsic properties would be necessary.

Well established methods to analyze the characteristics of molecular motors include gliding assays and ATPase measurements. *In vitro* gliding assays with recombinantly expressed chimeric OsKCH1 that contain elongated coiled-coil stalks could help to provide insights on the movement directionality of the protein along microtubules. In addition, the specific movement-coupled ATP turn-over of recombinant OsKCH1 could be assessed *in vitro* using ATPase assays.

2 Regulatory components of OsKCH1

The interaction of OsKCH1 with both cytoskeletal elements, as well as the characteristic motor properties, might not only be determined by the intrinsic affinity constants and the ATPase activity, but might be subject to additional regulations. Post-translational modifications and the association with other binding partners could lead to a certain amount of fine-tuning of the interactions – for example as a result of altering cellular requirements.

In vitro tests, such as gliding and ATPase assays, as well as the measurements of binding affinities, are useful tools to assess the influence of external factors on the characteristic motor properties. The activity of many kinesins is, for example, induced by the presence of microtubules, other binding partners, or specific conditions. Could the characteristic molecular properties of OsKCH1 possibly underlie similar regulations? And which effects might have post-translational modifications of the protein itself or its cytoskeletal targets, such as for example (de)tyrosina-

tion of microtubules? An application of varying actin or microtubule concentrations, cofactors, or specific buffer and pH-conditions in the different *in vitro* assays and an assessment of possible alterations in the activity of OsKCH1, could provide answers to this important question.

In order to obtain a better understanding of the cellular regulations that might be connected to KCH proteins, future research could aim to identify a broad range of putative binding and interaction partners via protein complex immunoprecipitation. To gain additional knowledge on the regulatory circuits that modulate the activity of this fascinating and unconventional class of molecular motors, gene expression studies might be performed to investigate possible regulations in the expression of *OsKCH1* in response to various external and internal stimuli, such as gravitropism, light, and plant hormones.

REFERENCES

- Adames, N.R., and Cooper, J.A.** (2000). Microtubule interactions with the cell cortex causing nuclear movements in *Saccharomyces cerevisiae*. *J Cell Biol* **149**, 863-874.
- Ambrose, J.C., Shoji, T., Kotzer, A.M., Pighin, J.A., and Wasteneys, G.O.** (2007). The Arabidopsis CLASP gene encodes a microtubule-associated protein involved in cell expansion and division. *Plant Cell* **19**, 2763-2775.
- An, G.** (1985). High Efficiency Transformation of Cultured Tobacco Cells. *Plant Physiol* **79**, 568-570.
- Bannigan, A., and Baskin, T.I.** (2005). Directional cell expansion--turning toward actin. *Curr Opin Plant Biol* **8**, 619-624.
- Barkai, N., and Leibler, S.** (1997). Robustness in simple biochemical networks. *Nature* **387**, 913-917.
- Bartolini, F., Moseley, J.B., Schmoranzler, J., Cassimeris, L., Goode, B.L., and Gundersen, G.G.** (2008). The formin mDia2 stabilizes microtubules independently of its actin nucleation activity. *J Cell Biol* **181**, 523-536.
- Baskin, T.I., and Bivens, N.J.** (1995). Stimulation of radial expansion in Arabidopsis roots by inhibitors of actomyosin and vesicle secretion but not by various inhibitors of metabolism. *Planta* **197**, 514-521.
- Berken, A.** (2006). ROPs in the spotlight of plant signal transduction. *Cellular and Molecular Life Sciences* **63**, 2446-2459.
- Blancaflor, E.B.** (2000). Cortical actin filaments potentially interact with cortical microtubules in regulating polarity of cell expansion in primary roots of maize (*Zea mays* L.). *J Plant Growth Regul* **19**, 406-414.
- Blanchoin, L., and Staiger, C.J.** (2008). Plant formins: Diverse isoforms and unique molecular mechanism. *Biochim Biophys Acta*.
- Bradford, M.** (1976). A rapid and sensitive method for the quantitation of microgram quantities of protein utilizing the principle of protein-dye binding. *Anal Biochem.* **72**, 248-254.
- Burk, D.H., Liu, B., Zhong, R., Morrison, W.H., and Ye, Z.H.** (2001). A katanin-like protein regulates normal cell wall biosynthesis and cell elongation. *Plant Cell* **13**, 807-827.
- Cai, D., Verhey, K.J., and Meyhofer, E.** (2007). Tracking single Kinesin molecules in the cytoplasm of mammalian cells. *Biophys J* **92**, 4137-4144.
- Cai, G., and Cresti, M.** (2009). Organelle motility in the pollen tube: a tale of 20 years. *J Exp Bot* **60**, 495-508.
- Campanoni, P., and Nick, P.** (2005). Auxin-dependent cell division and cell elongation. 1-Naphthaleneacetic acid and 2,4-dichlorophenoxyacetic acid activate different pathways. *Plant Physiol* **137**, 939-948.

- Cao, T.T., Chang, W., Masters, S.E., and Mooseker, M.S.** (2004). Myosin-Va binds to and mechanochemically couples microtubules to actin filaments. *Mol Biol Cell* **15**, 151-161.
- Cardenas, L., Lovy-Wheeler, A., Kunkel, J.G., and Hepler, P.K.** (2008). Pollen tube growth oscillations and intracellular calcium levels are reversibly modulated by actin polymerization. *Plant Physiol* **146**, 1611-1621.
- Case, R.B., Pierce, D.W., Hom-Booher, N., Hart, C.L., and Vale, R.D.** (1997). The directional preference of kinesin motors is specified by an element outside of the motor catalytic domain. *Cell* **90**, 959-966.
- Chan, J., Calder, G.M., Doonan, J.H., and Lloyd, C.W.** (2003). EB1 reveals mobile microtubule nucleation sites in Arabidopsis. *Nat Cell Biol* **5**, 967-971.
- Chandra, R., Salmon, E.D., Erickson, H.P., Lockhart, A., and Endow, S.A.** (1993). Structural and functional domains of the Drosophila ncd microtubule motor protein. *J Biol Chem* **268**, 9005-9013.
- Chen, C., Marcus, A., Li, W., Hu, Y., Calzada, J.P., Grossniklaus, U., Cyr, R.J., and Ma, H.** (2002). The Arabidopsis ATK1 gene is required for spindle morphogenesis in male meiosis. *Development* **129**, 2401-2409.
- Chen, J.G., Shimomura, S., Sitbon, F., Sandberg, G., and Jones, A.M.** (2001). The role of auxin-binding protein 1 in the expansion of tobacco leaf cells. *Plant J* **28**, 607-617.
- Chu, B., Kerr, G., and Carter, J.** (1993). Stabilizing microtubules with taxol increases microfilament stability during freezing of rye root tips. *Plant, Cell and Environment* **16**, 883-889.
- Chytilova, E., Macas, J., Sliwinska, E., Rafelski, S.M., Lambert, G.M., and Galbraith, D.W.** (2000). Nuclear dynamics in Arabidopsis thaliana. *Mol Biol Cell* **11**, 2733-2741.
- Cleary, A.L., Gunning, B.E.S., Wasteneys, G.O., and Hepler, P.K.** (1992). Microtubule and F-actin dynamics at the division site in living Tradescantia stamen hair cells. *J Cell Sci* **103**, 977-988.
- Collings, D., and Wasteneys, G.** (2005). Actin microfilament and microtubule distribution patterns in the expanding root of Arabidopsis thaliana. *Canadian Journal of Botany* **83**, 579-590.
- Collings, D.A.** (2008). Crossed-Wires: Interactions and Cross-Talk Between the Microtubule and Microfilament Networks in Plants. In *Plant Microtubules*, P. Nick, ed (Berlin / Heidelberg: Springer Verlag), pp. 47-79.
- Collings, D.A., Asada, T., Allen, N.S., and Shibaoka, H.** (1998). Plasma membrane-associated actin in bright yellow 2 tobacco cells. Evidence for interaction with microtubules. *Plant Physiol* **118**, 917-928.
- Collings, D.A., Lill, A.W., Himmelspach, R., and Wasteneys, G.O.** (2006). Hypersensitivity to cytoskeletal antagonists demonstrates microtubule-microfilament cross-talk in the control of root elongation in Arabidopsis thaliana. *New Phytol* **170**, 275-290.

- Cooper, G., and Hausman, R.** (2003). *The Cell: A molecular approach*. (Sinauer Associates).
- Coppin, C.M., Pierce, D.W., Hsu, L., and Vale, R.D.** (1997). The load dependence of kinesin's mechanical cycle. *Proc Natl Acad Sci U S A* **94**, 8539-8544.
- Cross, R.A.** (2004). The kinetic mechanism of kinesin. *Trends Biochem Sci* **29**, 301-309.
- Dagenbach, E.M., and Endow, S.A.** (2004). A new kinesin tree. *J Cell Sci* **117**, 3-7.
- Deeks, M.J., Hussey, P.J., and Davies, B.** (2002). Formins: intermediates in signal-transduction cascades that affect cytoskeletal reorganization. *Trends Plant Sci* **7**, 492-498.
- Dehmelt, L., Smart, F.M., Ozer, R.S., and Halpain, S.** (2003). The role of microtubule-associated protein 2c in the reorganization of microtubules and lamellipodia during neurite initiation. *J Neurosci* **23**, 9479-9490.
- Desai, A., and Mitchison, T.J.** (1997). Microtubule polymerization dynamics. *Annu Rev Cell Dev Biol* **13**, 83-117.
- Dhonukshe, P., Laxalt, A.M., Goedhart, J., Gadella, T.W., and Munnik, T.** (2003). Phospholipase d activation correlates with microtubule reorganization in living plant cells. *Plant Cell* **15**, 2666-2679.
- DiBella, L.M., and King, S.M.** (2001). Dynein motors of the *Chlamydomonas* flagellum. *Int Rev Cytol* **210**, 227-268.
- Ding, B., Turgeon, R., and Parthasarathy, M.V.** (1991a). Microfilament organization and distribution in freeze substituted tobacco plant tissues. *Protoplasma* **165**, 96-105.
- Ding, B., Turgeon, R., and Parthasarathy, M.V.** (1991b). Microfilaments in the preprophase band of freeze substituted tobacco root cells. *Protoplasma* **165**, 209-211.
- Eleftheriou, E.P., and Palevitz, B.A.** (1992). The effect of cytochalasin D on preprophase band organization in root tip cells of *Allium*. *J Cell Sci* **103**, 989-998.
- Endle, M.C., Stoppin, V., Lambert, A.M., and Schmit, A.C.** (1998). The growing cell plate of higher plants is a site of both actin assembly and vinculin-like antigen recruitment. *Eur J Cell Biol* **77**, 10-18.
- Endow, S.A.** (1999). Determinants of molecular motor directionality. *Nat Cell Biol* **1**, E163-167.
- Endow, S.A., and Waligora, K.W.** (1998). Determinants of kinesin motor polarity. *Science* **281**, 1200-1202.
- Endow, S.A., and Barker, D.S.** (2003). Processive and nonprocessive models of kinesin movement. *Annu Rev Physiol* **65**, 161-175.
- Eun, S.O., and Lee, Y.** (1997). Actin Filaments of Guard Cells Are Reorganized in Response to Light and Abscisic Acid. *Plant Physiol.* **115**, 1491-1498.
- Finer, J., Vain, P., Jones, M., and McMullen, M.** (1992). Development of the particle inflow gun for DNA delivery to plant cells. *Plant Cell Reports* **11**, 323-328.

- Franke, W.W., Herth, W., VanDerWoude, W.J., and Morr , D.J.** (1972). Tubular and filamentous structures in pollen tubes: Possible involvement as guide elements in protoplasmic streaming and vectorial migration of secretory vesicles. *Planta* **105**, 317-341.
- Gardiner, J.C., Harper, J.D., Weerakoon, N.D., Collings, D.A., Ritchie, S., Gilroy, S., Cyr, R.J., and Marc, J.** (2001). A 90-kD phospholipase D from tobacco binds to microtubules and the plasma membrane. *Plant Cell* **13**, 2143-2158.
- Giani, S., Qin, X., Faoro, F., and Breviario, D.** (1998). In rice, Oryzalin and abscisic acid differentially affect tubulin mRNA and protein levels. *Planta* **205**, 334-341.
- Gibbons, I.R., Garbarino, J.E., Tan, C.E., Reck-Peterson, S.L., Vale, R.D., and Carter, A.P.** (2005). The affinity of the dynein microtubule-binding domain is modulated by the conformation of its coiled-coil stalk. *J Biol Chem* **280**, 23960-23965.
- Giddings, T.H., and Staehelin, L.A.** (1991). Microtubule-mediated control of microfibril deposition; a reexamination of the hypothesis. (Academic Press).
- Gimona, M., and Mital, R.** (1998). The single CH domain of calponin is neither sufficient nor necessary for F-actin binding. *J Cell Sci* **111** (Pt **13**), 1813-1821.
- Gimona, M., Djinovic-Carugo, K., Kranewitter, W.J., and Winder, S.J.** (2002). Functional plasticity of CH domains. *FEBS Lett* **513**, 98-106.
- Gittes, F., Mickey, B., Nettleton, J., and Howard, J.** (1993). Flexural rigidity of microtubules and actin filaments measured from thermal fluctuations in shape. *J Cell Biol* **120**, 923-934.
- Goode, B.L., and Eck, M.J.** (2007). Mechanism and function of formins in the control of actin assembly. *Annu Rev Biochem* **76**, 593-627.
- Goodrich, J.A., and Kugel, J.F.** (2007). *Binding and Kinetics for Molecular Biologists*. (Cold Spring Harbor, N.Y. : Cold Spring Harbor Laboratory Press).
- Gossot, O., and Geitmann, A.** (2007). Pollen tube growth: coping with mechanical obstacles involves the cytoskeleton. *Planta* **226**, 405-416.
- Grabski, S., and Schindler, M.** (1996). Auxins and Cytokinins as Antipodal Modulators of Elasticity within the Actin Network of Plant Cells. *Plant Physiol* **110**, 965-970.
- Grabski, S., Arnoys, E., Busch, B., and Schindler, M.** (1998). Regulation of Actin Tension in Plant Cells by Kinases and Phosphatases. *Plant Physiol.* **116**, 279-290.
- Guindon, S., Lethiec, F., Duroux, P., and Gascuel, O.** (2005). PHYML Online--a web server for fast maximum likelihood-based phylogenetic inference. *Nucleic Acids Res* **33**, W557-559.
- Gutjahr, C., Riemann, M., Muller, A., Duchting, P., Weiler, E.W., and Nick, P.** (2005). Cholodny-Went revisited: a role for jasmonate in gravitropism of rice coleoptiles. *Planta* **222**, 575-585.

- Hepler, P.K., Vidali, L., and Cheung, A.Y.** (2001). Polarized cell growth in higher plants. *Annu Rev Cell Dev Biol* **17**, 159-187.
- Higaki, T., Sano, T., and Hasezawa, S.** (2007). Actin microfilament dynamics and actin side-binding proteins in plants. *Curr Opin Plant Biol* **10**, 549-556.
- Higuchi, H., and Endow, S.A.** (2002). Directionality and processivity of molecular motors. *Curr Opin Cell Biol* **14**, 50-57.
- Hirokawa, N., Noda, Y., Tanaka, Y., and Niwa, S.** (2009). Kinesin superfamily motor proteins and intracellular transport. *Nat Rev Mol Cell Biol* **10**, 682-696.
- Ho, A.Y.Y., Day, D.A., Brown, M.H., and Marc, J.** (2009). Arabidopsis phospholipase D as an initiator of cytoskeleton-mediated signalling to fundamental cellular processes. *Functional Plant Biology* **36**, 190-198
- Holweg, C., Susslin, C., and Nick, P.** (2004). Capturing in vivo dynamics of the actin cytoskeleton stimulated by auxin or light. *Plant Cell Physiol* **45**, 855-863.
- Hook, P., and Vallee, R.B.** (2006). The dynein family at a glance. *J Cell Sci* **119**, 4369-4371.
- Howard, J.** (2001). *Mechanics of Motor Proteins and the Cytoskeleton* (Sinauer Associates Inc.).
- Howard, J., and Hyman, A.A.** (2007). Microtubule polymerases and depolymerases. *Curr Opin Cell Biol* **19**, 31-35.
- Howard, J., Hudspeth, A.J., and Vale, R.D.** (1989). Movement of microtubules by single kinesin molecules. *Nature* **342**, 154-158.
- Hu, C.D., and Kerppola, T.K.** (2003). Simultaneous visualization of multiple protein interactions in living cells using multicolor fluorescence complementation analysis. *Nat Biotechnol* **21**, 539-545.
- Hu, C.D., Grinberg, A.V., and Kerppola, T.K.** (2005). Visualization of protein interactions in living cells using bimolecular fluorescence complementation (BiFC) analysis. *Curr Protoc Protein Sci* **Chapter 19**, Unit 19 10.
- Huang, S., Jin, L., Du, J., Li, H., Zhao, Q., Ou, G., Ao, G., and Yuan, M.** (2007). SB401, a pollen-specific protein from *Solanum berthaultii*, binds to and bundles microtubules and F-actin. *Plant J* **51**, 406-418.
- Huang, T.G., and Hackney, D.D.** (1994). *Drosophila* kinesin minimal motor domain expressed in *Escherichia coli*. Purification and kinetic characterization. *J Biol Chem* **269**, 16493-16501.
- Hunter, A.W., Caplow, M., Coy, D.L., Hancock, W.O., Diez, S., Wordeman, L., and Howard, J.** (2003). The kinesin-related protein MCAK is a microtubule depolymerase that forms an ATP-hydrolyzing complex at microtubule ends. *Mol Cell* **11**, 445-457.

- Hussey, P.J., Ketelaar, T., and Deeks, M.J.** (2006). Control of the actin cytoskeleton in plant cell growth. *Annu Rev Plant Biol* **57**, 109-125.
- Imamula, K., Kon, T., Ohkura, R., and Sutoh, K.** (2007). The coordination of cyclic microtubule association/dissociation and tail swing of cytoplasmic dynein. *Proc Natl Acad Sci U S A* **104**, 16134-16139.
- Ingber, D.E.** (1998). The architecture of life. *Sci Am* **278**, 48-57.
- Ingber, D.E.** (2003a). Tensegrity I. Cell structure and hierarchical systems biology. *J Cell Sci* **116**, 1157-1173.
- Ingber, D.E.** (2003b). Tensegrity II. How structural networks influence cellular information processing networks. *J Cell Sci* **116**, 1397-1408.
- Insall, R.H., and Machesky, L.M.** (2009). Actin dynamics at the leading edge: from simple machinery to complex networks. *Dev Cell* **17**, 310-322.
- Irvine, G.B.** (2001). Determination of molecular size by size-exclusion chromatography (gel filtration). *Curr Protoc Cell Biol* **5**, Chapter 5.5.
- Ishii, Y., Nishiyama, M., and Yanagida, T.** (2004). Mechano-chemical coupling of molecular motors revealed by single molecule measurements. *Curr Protein Pept Sci* **5**, 81-87.
- Iwai, S., Ishiji, A., Mabuchi, I., and Sutoh, K.** (2004). A novel actin-bundling kinesin-related protein from *Dictyostelium discoideum*. *J Biol Chem* **279**, 4696-4704.
- Jaffe, M.J.** (1973). Thigmomorphogenesis: The response of plant growth and development to mechanical stimulation. *Planta* **114**, 143-157.
- Jedd, G., and Chua, N.H.** (2002). Visualization of peroxisomes in living plant cells reveals acto-myosin-dependent cytoplasmic streaming and peroxisome budding. *Plant Cell Physiol* **43**, 384-392.
- Jurgens, G.** (2005). Cytokinesis in higher plants. *Annu Rev Plant Biol* **56**, 281-299.
- Kakimoto, T., and Shibaoka, H.** (1987). A New Method for Preservation of Actin Filaments in Higher Plant Cells. *Plant Cell Physiol.* **28**, 1581-1585.
- Kardon, J.R., and Vale, R.D.** (2009). Regulators of the cytoplasmic dynein motor. *Nat Rev Mol Cell Biol* **10**, 854-865.
- Kardon, J.R., Reck-Peterson, S.L., and Vale, R.D.** (2009). Regulation of the processivity and intracellular localization of *Saccharomyces cerevisiae* dynein by dynactin. *Proc Natl Acad Sci U S A* **106**, 5669-5674.
- Karimi, M., Inze, D., and Depicker, A.** (2002). GATEWAY vectors for *Agrobacterium*-mediated plant transformation. *Trends Plant Sci* **7**, 193-195.
- Karimi, M., De Meyer, B., and Hilson, P.** (2005). Modular cloning in plant cells. *Trends Plant Sci* **10**, 103-105.

- Katsuta, J., and Shibaoka, H.** (1988). The Roles of the Cytoskeleton and the Cell Wall in Nuclear Positioning in Tobacco BY-2 Cells. *Plant Cell Physiol.* **29**, 403-413.
- Katsuta, J., Hashiguchi, Y., and Shibaoka, H.** (1990). The Role of the Cytoskeleton in Positioning of the Nucleus in Premitotic Tobacco BY-2 Cells. *J Cell Sci* **95**, 413-422.
- Ketelaar, T., Faivre-Moskalenko, C., Esseling, J.J., de Ruijter, N.C., Grierson, C.S., Dogterom, M., and Emons, A.M.** (2002). Positioning of nuclei in Arabidopsis root hairs: an actin-regulated process of tip growth. *Plant Cell* **14**, 2941-2955.
- Kim, H.J., and Triplett, B.A.** (2001). Cotton fiber growth in planta and in vitro. Models for plant cell elongation and cell wall biogenesis. *Plant Physiol* **127**, 1361-1366.
- Kircher, S., Wellmer, F., Nick, P., Rugner, A., Schafer, E., and Harter, K.** (1999). Nuclear import of the parsley bZIP transcription factor CPRF2 is regulated by phytochrome photoreceptors. *J Cell Biol* **144**, 201-211.
- Klein, M.G., Shi, W., Ramagopal, U., Tseng, Y., Wirtz, D., Kovar, D.R., Staiger, C.J., and Almo, S.C.** (2004). Structure of the actin crosslinking core of fimbrin. *Structure* **12**, 999-1013.
- Klotz, J.** (2008). Ein Kinesin auf Abwegen: Das pflanzenspezifische OsKCH1 als dynamische Verbindung zwischen Mikrotubuli und Aktinfilamenten; Diplomarbeit (University of Karlsruhe, Institut of Botany I).
- Kobayashi, H., Fukuda, H., and Shibaoka, H.** (1988). Interrelation between the spatial disposition of actin filaments and microtubules during the differentiation of tracheary elements in cultured *Zinnia* cells. *Protoplasma* **143**, 29-37.
- Koonce, M.P.** (2000). Dictyostelium, a model organism for microtubule-based transport. *Protist* **151**, 17-25.
- Koonce, M.P., and Samsó, M.** (1996). Overexpression of cytoplasmic dynein's globular head causes a collapse of the interphase microtubule network in Dictyostelium. *Mol Biol Cell* **7**, 935-948.
- Korenbaum, E., and Rivero, F.** (2002). Calponin homology domains at a glance. *J Cell Sci* **115**, 3543-3545.
- Korn, E.D., Carlier, M.F., and Pantaloni, D.** (1987). Actin polymerization and ATP hydrolysis. *Science* **238**, 638-644.
- Kost, B., and Chua, N.H.** (2002). The plant cytoskeleton: vacuoles and cell walls make the difference. *Cell* **108**, 9-12.
- Kost, B., Bao, Y.Q., and Chua, N.H.** (2002). Cytoskeleton and plant organogenesis. *Philos Trans R Soc Lond B Biol Sci* **357**, 777-789.
- Krendel, M., and Mooseker, M.S.** (2005). Myosins: Tails (and Heads) of Functional Diversity. *Physiology* **20**, 239-251.

- Kull, F.J., Vale, R.D., and Fletterick, R.J.** (1998). The case for a common ancestor: kinesin and myosin motor proteins and G proteins. *Journal of Muscle Research and Cell Motility* **19**, 877-886.
- Kusner, D.J., Barton, J.A., Qin, C., Wang, X., and Iyer, S.S.** (2003). Evolutionary conservation of physical and functional interactions between phospholipase D and actin. *Arch Biochem Biophys* **412**, 231-241.
- Laemmli, U.K.** (1970). Cleavage of Structural Proteins during the Assembly of the Head of Bacteriophage T4. *Nature* **227**, 680-685.
- Lawrence, C.J., Morris, N.R., Meagher, R.B., and Dawe, R.K.** (2001). Dyneins have run their course in plant lineage. *Traffic* **2**, 362-363.
- Lawrence, C.J., Dawe, R.K., Christie, K.R., Cleveland, D.W., Dawson, S.C., Endow, S.A., Goldstein, L.S., Goodson, H.V., Hirokawa, N., Howard, J., Malmberg, R.L., McIntosh, J.R., Miki, H., Mitchison, T.J., Okada, Y., Reddy, A.S., Saxton, W.M., Schliwa, M., Scholey, J.M., Vale, R.D., Walczak, C.E., and Wordeman, L.** (2004). A standardized kinesin nomenclature. *J Cell Biol* **167**, 19-22.
- Lee, J.R., Shin, H., Ko, J., Choi, J., Lee, H., and Kim, E.** (2003). Characterization of the movement of the kinesin motor KIF1A in living cultured neurons. *J Biol Chem* **278**, 2624-2629.
- Lee, Y.R., and Liu, B.** (2004). Cytoskeletal motors in Arabidopsis. Sixty-one kinesins and seventeen myosins. *Plant Physiol* **136**, 3877-3883.
- Letunic, I., and Bork, P.** (2007). Interactive Tree Of Life (iTOL): an online tool for phylogenetic tree display and annotation. *Bioinformatics* **23**, 127-128.
- Leung, C.L., Sun, D., Zheng, M., Knowles, D.R., and Liem, R.K.** (1999). Microtubule actin cross-linking factor (MACF): a hybrid of dystonin and dystrophin that can interact with the actin and microtubule cytoskeletons. *J Cell Biol* **147**, 1275-1286.
- Lillie, S.H., and Brown, S.S.** (1992). Suppression of a myosin defect by a kinesin-related gene. *Nature* **356**, 358-361.
- Liu, B.Q., Jin, L., Zhu, L., Li, J., Huang, S., and Yuan, M.** (2009). Phosphorylation of microtubule-associated protein SB401 from *Solanum berthaultii* regulates its effect on microtubules. *J Integr Plant Biol* **51**, 235-242.
- Lockhart, A., Crevel, I.M., and Cross, R.A.** (1995). Kinesin and ncd bind through a single head to microtubules and compete for a shared MT binding site. *J Mol Biol* **249**, 763-771.
- Lodish, H., Berk, A., Kaiser, C., Krieger, M., Scott, M., Bretscher, A., Ploegh, H., and Matsudaira, P.** (2007). *Molecular Cell Biology*. (W. H. Freeman).
- Lupas, A.** (1996). Prediction and analysis of coiled-coil structures. *Methods Enzymol* **266**, 513-525.

- Lupas, A., Van Dyke, M., and Stock, J.** (1991). Predicting coiled coils from protein sequences. *Science* **252**, 1162-1164.
- Maisch, J., and Nick, P.** (2007). Actin is involved in auxin-dependent patterning. *Plant Physiol* **143**, 1695-1704.
- Maisch, J., Fiserova, J., Fischer, L., and Nick, P.** (2009). Tobacco Arp3 is localized to actin-nucleating sites in vivo. *J Exp Bot*.
- Mandelkow, E., and Mandelkow, E.M.** (1989). Microtubular structure and tubulin polymerization. *Curr Opin Cell Biol* **1**, 5-9.
- Mandelkow, E.M., and Mandelkow, E.** (1985). Unstained microtubules studied by cryo-electron microscopy. Substructure, supertwist and disassembly. *J Mol Biol.* **181**, 123-135.
- Marc, J., Granger, C.L., Brincat, J., Fisher, D.D., Kao, T., McCubbin, A.G., and Cyr, R.J.** (1998). A GFP-MAP4 reporter gene for visualizing cortical microtubule rearrangements in living epidermal cells. *Plant Cell* **10**, 1927-1940.
- Marcus, A.I., Li, W., Ma, H., and Cyr, R.J.** (2003). A kinesin mutant with an atypical bipolar spindle undergoes normal mitosis. *Mol Biol Cell* **14**, 1717-1726.
- Marcus, A.I., Ambrose, J.C., Blickley, L., Hancock, W.O., and Cyr, R.J.** (2002). Arabidopsis thaliana protein, ATK1, is a minus-end directed kinesin that exhibits non-processive movement. *Cell Motil Cytoskeleton* **52**, 144-150.
- Martin, S.G., McDonald, W.H., Yates, J.R., 3rd, and Chang, F.** (2005). Tea4p links microtubule plus ends with the formin for3p in the establishment of cell polarity. *Dev Cell* **8**, 479-491.
- McIlvain, J.M., Jr., Burkhardt, J.K., Hamm-Alvarez, S., Argon, Y., and Sheetz, M.P.** (1994). Regulation of kinesin activity by phosphorylation of kinesin-associated proteins. *J Biol Chem* **269**, 19176-19182.
- Meagher, R., and Fechheimer, M.** (2009). The Arabidopsis Cytoskeletal Genome. In *The Arabidopsis Book (The American Society of Plant Biologists)*, pp. 1-26.
- Meagher, R.B., McKinney, E.C., and Kandasamy, M.K.** (1999). Isovariant dynamics expand and buffer the responses of complex systems: the diverse plant actin gene family. *Plant Cell* **11**, 995-1006.
- Mennella, V., Tan, D.Y., Buster, D.W., Asenjo, A.B., Rath, U., Ma, A., Sosa, H.J., and Sharp, D.J.** (2009). Motor domain phosphorylation and regulation of the Drosophila kinesin 13, KLP10A. *J Cell Biol* **186**, 481-490.
- Miki, H., Okada, Y., and Hirokawa, N.** (2005). Analysis of the kinesin superfamily: insights into structure and function. *Trends Cell Biol* **15**, 467-476.
- Mineyuki, Y., and Palevitz, B.A.** (1990). Relationship between preprophase band organization, F-actin and the division site in Allium: Fluorescence and morphometric studies on cytochalasin-treated cells. *J Cell Sci* **97**, 283-295.

- Mineyuki, Y., and Gunning, B.E.S.** (1990). A role for preprophase bands of microtubules in maturation of new cell walls, and a general proposal on the function of preprophase band sites in cell division in higher plants. *J Cell Sci* **97**, 527-537.
- Miyao, A., Tanaka, K., Murata, K., Sawaki, H., Takeda, S., Abe, K., Shinozuka, Y., Onosato, K., and Hirochika, H.** (2003). Target site specificity of the Tos17 retrotransposon shows a preference for insertion within genes and against insertion in retrotransposon-rich regions of the genome. *Plant Cell* **15**, 1771-1780.
- Morris, N.R.** (2003). Nuclear positioning: the means is at the ends. *Curr Opin Cell Biol* **15**, 54-59.
- Nagata, T., Nemoto, Y., and Hasezawa, S.** (1992). Tobacco BY-2 cell line as the "HeLa" cell in the cell biology of higher plants. *International Review of Cytology* **132**, 1-30.
- Nebenfuhr, A., Frohlick, J.A., and Staehelin, L.A.** (2000). Redistribution of Golgi stacks and other organelles during mitosis and cytokinesis in plant cells. *Plant Physiol* **124**, 135-151.
- Ni, C.Z., Wang, H.Q., Xu, T., Qu, Z., Liu, G.Q.** (2005). AtKP1, a kinesin-like protein, mainly localizes to mitochondria in *Arabidopsis thaliana*. *Cell Research* **15**, 725-733
- Nick, P.** (2008). Control of Cell Axis. In *Plant Microtubules*, P. Nick, ed (Berlin / Heidelberg: Springer Verlag), pp. 23-46.
- Nick, P.** (2010). Mechanics of the cytoskeleton. In *Mechanointegration of plant cells and plants*, edited by P. Wojtaszek (in preparation)
- Nick, P., Heuing, A., and Ehmann, B.** (2000). Plant chaperonins: a role in microtubule-dependent wall formation? *Protoplasma* **211**, 234-244.
- Olyslaegers, G., and Verbelen, J.P.** (1998). Improved staining of F-actin and co-localization of mitochondria in plant cells. *Journal of Microscopy* **192**, 73-77.
- Oppenheimer, D.G., Pollock, M.A., Vacik, J., Szymanski, D.B., Ericson, B., Feldmann, K., and Marks, M.D.** (1997). Essential role of a kinesin-like protein in *Arabidopsis* trichome morphogenesis. *Proc Natl Acad Sci U S A* **94**, 6261-6266.
- Otegui, M.S., Mastrorarde, D.N., Kang, B.H., Bednarek, S.Y., and Staehelin, L.A.** (2001). Three-dimensional analysis of syncytial-type cell plates during endosperm cellularization visualized by high resolution electron tomography. *Plant Cell* **13**, 2033-2051.
- Ovechkina, Y., Wagenbach, M., and Wordeman, L.** (2002). K-loop insertion restores microtubule depolymerizing activity of a "neckless" MCAK mutant. *J Cell Biol* **159**, 557-562.
- Peloquin, J., Komarova, Y., and Borisy, G.** (2005). Conjugation of fluorophores to tubulin. *Nat Methods* **2**, 299-303.
- Perfus-Barbeoch, L., Jones, A.M., and Assmann, S.M.** (2004). Plant heterotrimeric G protein function: insights from *Arabidopsis* and rice mutants. *Curr Opin Plant Biol* **7**, 719-731.

- Petrasek, J., and Schwarzerova, K.** (2009). Actin and microtubule cytoskeleton interactions. *Curr Opin Plant Biol* **12**, 728-734.
- Preuss, M.L., Delmer, D.P., and Liu, B.** (2003). The cotton kinesin-like calmodulin-binding protein associates with cortical microtubules in cotton fibers. *Plant Physiol* **132**, 154-160.
- Preuss, M.L., Kovar, D.R., Lee, Y.R., Staiger, C.J., Delmer, D.P., and Liu, B.** (2004). A plant-specific kinesin binds to actin microfilaments and interacts with cortical microtubules in cotton fibers. *Plant Physiol* **136**, 3945-3955.
- Rayment, I.** (1996). Kinesin and myosin: molecular motors with similar engines. *Structure* **4**, 501-504.
- Reddy, A.S., and Day, I.S.** (2001). Kinesins in the Arabidopsis genome: a comparative analysis among eukaryotes. *BMC Genomics* **2**, 2.
- Reddy, A.S., Safadi, F., Narasimhulu, S.B., Golovkin, M., and Hu, X.** (1996). A novel plant calmodulin-binding protein with a kinesin heavy chain motor domain. *J Biol Chem* **271**, 7052-7060.
- Reddy, A.S., Day, I.S., Narasimhulu, S.B., Safadi, F., Reddy, V.S., Golovkin, M., and Harnly, M.J.** (2002). Isolation and characterization of a novel calmodulin-binding protein from potato. *J Biol Chem* **277**, 4206-4214.
- Richardson, D., Simmons, M., and Reddy, A.** (2006). Comprehensive comparative analysis of kinesins in photosynthetic eukaryotes. *BMC Genomics* **7**, 18.
- Riemann, M., Riemann, M., and Takano, M.** (2008). Rice JASMONATE RESISTANT 1 is involved in phytochrome and jasmonate signalling. *Plant Cell Environ* **31**, 783-792.
- Ritchie, M.D., Geeves, M.A., Woodward, S.K., and Manstein, D.J.** (1993). Kinetic characterization of a cytoplasmic myosin motor domain expressed in *Dictyostelium discoideum*. *Proc Natl Acad Sci U S A* **90**, 8619-8623.
- Rodriguez, O.C., Schaefer, A.W., Mandato, C.A., Forscher, P., Bement, W.M., and Waterman-Storer, C.M.** (2003). Conserved microtubule-actin interactions in cell movement and morphogenesis. *Nat Cell Biol* **5**, 599-609.
- Rosenbaum, J.L., and Witman, G.B.** (2002). Intraflagellar transport. *Nat Rev Mol Cell Biol* **3**, 813-825.
- Sambrook, J., and Russell, D.W.** (2001). *Molecular cloning : a laboratory manual* / Joseph Sambrook, David W. Russell. (Cold Spring Harbor, N.Y. : Cold Spring Harbor Laboratory Press).
- Sanger, F., Nicklen, S., and Coulson, A.R.** (1977). DNA sequencing with chain-terminating inhibitors. *Proc Natl Acad Sci U S A* **74**, 5463-5467.
- Schliwa, M.** (2003). Kinesin: walking or limping? *Nat Cell Biol* **5**, 1043-1044.

- Schmit, A.C.** (2002). Acentrosomal microtubule nucleation in higher plants. *Int Rev Cytol* **220**, 257-289.
- Schmit, A.C., and Lambert, A.M.** (1988). Plant actin filament and microtubule interactions during anaphase--telophase transition: effects of antagonist drugs. *Biol Cell* **64**, 309-319.
- Schroer, T.A., and Sheetz, M.P.** (1991). Two activators of microtubule-based vesicle transport. *J Cell Biol* **115**, 1309-1318.
- Seagull, R.** (1990). The effects of microtubule and microfilament disrupting agents on cytoskeletal arrays and wall deposition in developing cotton fibers. *Protoplasma* **159**, 44-59.
- Sharp, D.J., Rogers, G.C., and Scholey, J.M.** (2000). Cytoplasmic dynein is required for poleward chromosome movement during mitosis in *Drosophila* embryos. *Nat Cell Biol* **2**, 922-930.
- Smith, L.G., and Oppenheimer, D.G.** (2005). Spatial control of cell expansion by the plant cytoskeleton. *Annu Rev Cell Dev Biol* **21**, 271-295.
- Smith, L.G., Gerttula, S.M., Han, S., and Levy, J.** (2001). Tangled1: a microtubule binding protein required for the spatial control of cytokinesis in maize. *J Cell Biol* **152**, 231-236.
- Song, H., Golovkin, M., Reddy, A.S., and Endow, S.A.** (1997). In vitro motility of AtKCBP, a calmodulin-binding kinesin protein of *Arabidopsis*. *Proc Natl Acad Sci U S A* **94**, 322-327.
- Srivastava, J., and Barber, D.** (2008). Actin Co-Sedimentation Assay; for the Analysis of Protein Binding to F-Actin. *JoVE* **13**.
- Staehein, L.A., and Hepler, P.K.** (1996). Cytokinesis in higher plants. *Cell* **84**, 821-824.
- Staiger, C.J., and Lloyd, C.W.** (1991). The plant cytoskeleton. *Curr Opin Cell Biol* **3**, 33-42.
- Steeves, T., and Sussex, I.** (1989). *Patterns in Plant Development*. (Cambridge, UK: Cambridge University Press).
- Stolpe, T., Susslin, C., Marrocco, K., Nick, P., Kretsch, T., and Kircher, S.** (2005). In planta analysis of protein-protein interactions related to light signaling by bimolecular fluorescence complementation. *Protoplasma* **226**, 137-146.
- Svoboda, K., Schmidt, C.F., Schnapp, B.J., and Block, S.M.** (1993). Direct observation of kinesin stepping by optical trapping interferometry. *Nature* **365**, 721-727.
- Tamura, K., Nakatani, K., Mitsui, H., Ohashi, Y., and Takahashi, H.** (1999). Characterization of katD, a kinesin-like protein gene specifically expressed in floral tissues of *Arabidopsis thaliana*. *Gene* **230**, 23-32.
- Tominaga, M., Morita, K., Sonobe, S., Yokota, E., and Shimmen, T.** (1997). Microtubules regulate the organization of actin filaments at the cortical region in root hair cells of *Hydrocharis*. *Protoplasma* **199**, 83-92.

- Tominaga, M., Kojima, H., Yokota, E., Orii, H., Nakamori, R., Katayama, E., Anson, M., Shimmen, T., and Oiwa, K.** (2003). Higher plant myosin XI moves processively on actin with 35 nm steps at high velocity. *Embo J* **22**, 1263-1272.
- Towbin, H., Staehelin, T., and Gordon, J.** (1979). Electrophoretic transfer of proteins from polyacrylamide gels to nitrocellulose sheets: procedure and some applications. *Proceedings of the National Academy of Sciences of the United States of America* **76**, 4350-4354.
- Traas, J.A., Doonan, J.H., Rawlins, D.J., Shaw, P.J., Watts, J., and Lloyd, C.W.** (1987). An actin network is present in the cytoplasm throughout the cell cycle of carrot cells and associates with the dividing nucleus. *J Cell Biol* **105**, 387-395.
- Ullah, H., Chen, J.G., Young, J.C., Im, K.H., Sussman, M.R., and Jones, A.M.** (2001). Modulation of cell proliferation by heterotrimeric G protein in Arabidopsis. *Science* **292**, 2066-2069.
- Umeki, N., Mitsui, T., Umezu, N., Kondo, K., and Maruta, S.** (2006). Preparation and characterization of a novel rice plant-specific kinesin. *J Biochem* **139**, 645-654.
- Uppalapati, M., Huang, Y.-M., Shastry, S., Jackson, T., and Hancock, W.** (2009). *Microtubule Motors in Microfluidics*. (Norwood: ARTECH HOUSE).
- Uribe, R., and Jay, D.** (2009). A review of actin binding proteins: new perspectives. *Molecular Biology Reports* **36**, 121-125.
- Vale, R.D., Reese, T.S., and Sheetz, M.P.** (1985). Identification of a novel force-generating protein, kinesin, involved in microtubule-based motility. *Cell* **42**, 39-50.
- Valentine, M.T., and Block, S.M.** (2009). Force and premature binding of ADP can regulate the processivity of individual Eg5 dimers. *Biophys J* **97**, 1671-1677.
- Valster, A.H., Pierson, E.S., Valenta, R., Hepler, P.K., and Emons, A.** (1997). Probing the Plant Actin Cytoskeleton during Cytokinesis and Interphase by Profilin Microinjection. *Plant Cell* **9**, 1815-1824.
- VanBuren, P., Begin, K., and Warshaw, D.M.** (1998). Fluorescent phalloidin enables visualization of actin without effects on myosin's actin filament sliding velocity and hydrolytic properties in vitro. *J Mol Cell Cardiol* **30**, 2777-2783.
- Vetter, I.R., and Wittinghofer, A.** (2001). The guanine nucleotide-binding switch in three dimensions. *Science* **294**, 1299-1304.
- Vidali, L., van Gisbergen, P.A., Guerin, C., Franco, P., Li, M., Burkart, G.M., Augustine, R.C., Blanchoin, L., and Bezanilla, M.** (2009). Rapid formin-mediated actin-filament elongation is essential for polarized plant cell growth. *Proc Natl Acad Sci U S A* **106**, 13341-13346.
- Wachsstock, D.H., Schwartz, W.H., and Pollard, T.D.** (1993). Affinity of alpha-actinin for actin determines the structure and mechanical properties of actin filament gels. *Biophys J* **65**, 205-214.

- Wade, R.H., and Kozielski, F.** (2000). Structural links to kinesin directionality and movement. *Nat Struct Biol* **7**, 456-460.
- Waller, F., and Nick, P.** (1997). Response of actin microfilaments during phytochrome-controlled growth of maize seedlings. *Protoplasma* **200**, 154-162.
- Wang, Q.Y., and Nick, P.** (1998). The auxin response of actin is altered in the rice mutant Yin-Yang. *Protoplasma* **204**, 22-33.
- Wasteneys, G.O., and Galway, M.E.** (2003). Remodeling the cytoskeleton for growth and form: an overview with some new views. *Annu Rev Plant Biol* **54**, 691-722.
- Wen, Y., Eng, C.H., Schmoranzler, J., Cabrera-Poch, N., Morris, E.J., Chen, M., Wallar, B.J., Alberts, A.S., and Gundersen, G.G.** (2004). EB1 and APC bind to mDia to stabilize microtubules downstream of Rho and promote cell migration. *Nat Cell Biol* **6**, 820-830.
- Whittington, A.T., Vugrek, O., Wei, K.J., Hasenbein, N.G., Sugimoto, K., Rashbrooke, M.C., and Wasteneys, G.O.** (2001). MOR1 is essential for organizing cortical microtubules in plants. *Nature* **411**, 610-613.
- Wickstead, B., and Gull, K.** (2007). Dyneins across eukaryotes: a comparative genomic analysis. *Traffic* **8**, 1708-1721.
- Winkler, R.G., and Feldmann, K.A.** (1998). PCR-based identification of T-DNA insertion mutants. *Methods Mol Biol* **82**, 129-136.
- Woehlke, G., and Schliwa, M.** (2000). Directional motility of kinesin motor proteins. *Biochim Biophys Acta* **1496**, 117-127.
- Wordeman, L.** (2005). Microtubule-depolymerizing kinesins. *Curr Opin Cell Biol* **17**, 82-88.
- Xu, T., Sun, X., Jiang, S., Ren, D., and Liu, G.** (2007). Cotton GhKCH2, a plant-specific kinesin, is low-affinitive and nucleotide-independent as binding to microtubule. *J Biochem Mol Biol* **40**, 723-730.
- Xu, T., Qu, Z., Yang, X., Qin, X., Xiong, J., Wang, Y., Ren, D., and Liu, G.** (2009). A cotton kinesin GhKCH2 interacts with both microtubules and microfilaments. *Biochem J* **421**, 171-180.
- Yamamoto, A., and Hiraoka, Y.** (2003). Cytoplasmic dynein in fungi: insights from nuclear migration. *J Cell Sci* **116**, 4501-4512.
- Yildiz, A., and Selvin, P.R.** (2005). Kinesin: walking, crawling or sliding along? *Trends Cell Biol* **15**, 112-120.
- Zekert, N., and Fischer, R.** (2009). The *Aspergillus nidulans* kinesin-3 UncA motor moves vesicles along a subpopulation of microtubules. *Mol Biol Cell* **20**, 673-684.
- Zheng, W., Fan, D., Feng, M., and Wang, Z.** (2009). The intrinsic load-resisting capacity of kinesin. *Phys Biol* **6**, 36002.
- Zimmermann, W.** (1965). *Die Telomtheorie*. (Stuttgart: G. Fischer).

APPENDIX

1 Overview of KCHs in different plants

Species	Swiss-Prot/TrEMBL Accession	Other designation	KCH subgroup	Literature
<i>Oryza sativa</i> ssp. <i>japonica</i>	Q0IMS9	OsKCH1	IV	This work
	Q10MN5		IV	
	A3CDK9		IV	
	B9FFM0		III	
	B9EUM5		II	
	B9FL70		I	
	Q5JKW1		I	
<i>Arabidopsis thaliana</i>	O81635	AtKatD	IV	Tamura et al., 1999 Ni et al., 2005
	Q84W97	AtKP1	IV	
	O22260		IV	
	O80491		IV	
	Q8W1Y3		III	
	Q9SS42		II	
	Q9FHD2		I	
<i>Gossypium hirsutum</i>	Q5MNV6	GhKCH1	IV	Preuss et al., 2004 Xu et al., 2009
	A4GU96	GhKCH2	IV	
<i>Vitis vinifera</i>	A5BG13		IV	
	A5C0F0		IV	
	A7Q9E6		III	
	A5APK4		II	
	A5BH78		I	
<i>Physcomitrella patens</i>	A9SJ46		n.c.	
	A9SDI6		n.c.	
	A9SPL2		n.c.	
<i>Populus trichocarpa</i>	B9I798		IV	
	B9GSE0		IV	
	B9GH20		III	
	B9H9K3		II	
	B9GWJ1		I	
<i>Ricinus communis</i>	B9SAW6		IV	
	B9RFF9		IV	
	B9T1P9		III	
	B9T5B8		II	
	B9RCC3		I	

Tab. 16: Members of the KCH subfamily in different plants

The table gives an overview of all KCHs that have been identified in the sequenced plants by database search, together with their respective Swiss-Prot/TrEMBL accessions, and, if present, the corresponding literature references and the trivial names of the proteins. The classification of KCHs into the different subgroups follows the phylogenetic tree given in Fig. 20. Subgroup IV corresponds to the clade marked in blue in the tree, subgroup III to the clade marked in yellow, subgroup II to the clade marked in green and subgroup I to the clade marked in red. The KCHs from *Physcomitrella* do not cluster into any of the clades, but form a solitary branch and are therefore not classified (n.c.).

2 Sequence information

2.1 Coding sequence of OsKCH1

```

1  ATGATGGCCG CGGCGGTCTGA GGAGGAGGAG ATGGTGGAGA GGATGCACGG GTGGGCGAGG GACATGGACG TGGCGTCACG CAGGGCCGAG GAGGAAGCAA
101 TGAGACGGTA TGATGCGGCA AGTTGGTTGC GAAGCACGGT TGGGGTAGTG TGTGCAAGAG ACCTGCCAGA TGAACCGTCT GAGGAGGAAT TCCGGCTTGG
201 GCTGAGAAAT GGGATTGTTT TTTGCAATGC ACTGAATAAG ATCCAGCCTG GTGCCATACC TAAGTTGTA CAAGCCAGT CAGATGCTGC TGGCCCCACG
301 GATGGCTCAG CTCTGTGTGC ATATCAGTAC TTTGAGAATC TGCGGAACCT CCTTGTGTTT GTAGAAGATT TAAGGCTTCC TACATTTGAG GTGTCCGATT
401 TAGAAAAGGG TGGCAAGGT GTTCGGGTTG TGGATTGTGT TCTTGCTTTG AAGTCATTCA GTGAAAGTAA TAAACAGGG AGACAAGCTT CGTGTAAATA
501 TGGCGGCCTT TCAAACCTT TGACAGCCAG AAGTATTTT ATACTCAAGA ATACTGATGC TTTTATGAAT AAGATAATGA AAGGCCTACT AGCAGAGGCA
601 ATCCAGAGTG AATTTTCAGA GGGGCAAGC ATAGTTACTG ATTTTCTTAT AGAGTCTAAT GAGATGACTA CTTCAGACTC CCTTAGCATT CTTTTCGCTA
701 AAGTTCCTTT AGATAAGAAA CCAGAGGAAG TCCCATTGAT TGTGTAGTCG ATCCTAAGCA AAGTTATTCA GGAATATGAG CATCGAATTG CAATCCAGAA
801 CAAGATGGAT GAGGAGGAG AAAATCTCTT GAATATCACG GAACAGGTCA ACCATGATGT TGTAAATGGT GATGGTGAAG TTAACAGTT CCAACTAGAG
901 GCACAGACAA ATTTTGTGTT GCAACAAAAA CAGATCCAGG AATTGAAGGG TGCTCTTTCT TTTGTCAAGT CTGCCATGGA ACAACTGAGA TTACAGTACT
1001 CTGAAGAATT TGCTAAACTT GGGAAACATT TCTACACTCT CTCCAATGCG GCTTCCAGCT ACCATAAAGT TCTTGAGGAA AACCAGCAAT TATACAACCA
1101 AATACAGGAC CTTAAAGGAA ATATTAGAGT ATACTGTCTGA GTGAGGCCTT TCCTACCTGG ACATAGAAGT TTATCAAGCA GTGTTGCTGA CACGGAAGAA
1201 AGAACATCA CAATAATCAC TCCCACAAAA FATGGGAAAG ATGGGTGCAA ATCATTCACT TTTAACAGGG TCTTTGGTCC AGCATCTACT CAAGAAGAGG
1301 TCTTTTCAGA CATGCAGCCT TTGATCCGTT CAGTCTTGA TGGTTTCAAT GCTGCATAT TTGCATATGG CCAAACTGGA TCAGGAAGA CTTTACCATT
1401 GAGTGGACCG AAAGTTTGA CAGAGGAAAG CCTCGTGTGT AACTATAGAG CACTAAATGA CTTATTTAAT ATTAAGCAC AGAGAAAGGG GACAATCGAT
1501 TATGAAATTT CTGTGCAGAT GATTGAGATC TACAATGAGC AAGTGAGGGA TCTCCTCAG GATGGTGAAG ACAGGAGATT AGAATAAGA AATACTCCAC
1601 AGAAGGGCT TGCTGTTCCG GATGCAAGCA TAGTTCCTGT CACATCTACG GCGGATGTTG TTGAATTGAT GAATCAAGGC CAGAAGAATC GTGCAGTGGG
1701 TTCACAGCC ATCAACGATC GAAGTAGCCG CTCTCATAGC TGCTGTCTCG TTCATGTCCA AGGAAAATAT TTAACATCTG GGGCAATGTT GAGAGGTTGC
1801 ATGCATCTTG TGGATCTAGC TGGTAGTGAA AGAGTTGATA AGTCTGAGGT TGTAGGAGAC AGGCTGAAGG AAGCACAGTA CATAAACAAG TCACTTTCAG
1901 CATTAGGAGA TGTGATTGCA TCTCTTGAC AGAAAAATTC GCATGTCCCT TACCGAAACA GCAAGCTTAC CCAGCTTTTG CAAGATTCTC TAGGAGGACA
2001 AGCAAAAACG CTGATGTTTG TTCACGTAAG CCCGGAACCTA GATGCTGTCG GTGAGACAAAT AAGCACATTG AAATTTGCTG AAAGGGTTGC TTCAGTTGAG
2101 CTTGTGCAG CAAAAGCAA CAAAGAAGGC AGTGAGGTTA GAGAGCTCAA AGAACAGATT GCTACCCTCA AGGCGGCATT GGCTAAAAAG GAAGGAGAAC
2201 CAGAAAACAT TCAAAGCACA CAGTCAAGCC CTGACATGTA TAGAATTAAA AGAGGCAATG CAATACCTGC CTTCCCTAAA AATAGACAGC CAATGGAAGA
2301 AGTTGGAAC TTAGAGGTCC GGAACAATGC CACTCCAATG CAAAAGAAGG CCAGCTTTCA ATTTCTGGT GTCTCAGTG AGAACAACTC ATCCGACTTG
2401 GCTGAAAATT GCAATGGCAT TCAGAAGACC GATAGAATGG CTGTGCGTAA TAATCAATTT GAGAATGGAA ATTCATTCT AGAGCTGGAG CCTGGCGCAA
2501 CTCAGCTTCC AACATTTTTT TACCAAAGAT ATGATCCCGA CAAGCAAAGG CGTAGGGCTG AACCAGTAGA AACTGATGAC TCAGATAGT TTGATGTCTC
2601 TACTAGCTCG CCTTCCGACC AAGAAATGTT GTTGCCACC AGTGGCTCA AAGCTGATGG TATTGCCAGC AGAGGTGCCT TTATTATAAA GAAACCTCAA
2701 ACAAGAATA CAAAATTTAC AGCAACGAAG ATTTCAAATC TTGCAATGAA GTCGCCAATG TCAGAGAAAA GGCTGCAAAC CCCAATCAG AACAGCAAGC
2801 AGCTACCTTT CAGCACTACG GGTGGAAGAA GAACCTGAAA TGGCAAATT AACACTCCA AATAA

```

2.2 Sequence of the BY-2 PCR amplification product

The detection of KCH cDNA levels in tobacco BY-2 was performed using a set of degenerated primers (NF 73/74). In order to verify the identity of the sequence amplified from tobacco BY-2 cells, the PCR product was sequenced (GATC, Konstanz, Germany).

The sequencing yielded the following sequence information:

```

1   AGCAATTTGC CACGGTAGAA CTTAGTGCTA CTCGTGTAAG CAAGGATAGT GTAGATGTGA AAGAGCTGAA AGAACAGGTT CTGAATGCTC TCANTATTTA
101 TCATTCTTCT CAATTCTTAT TTATTCTTCT GAAAACTTTG AACTATTATT ACAGATTGCT ACCCTCAAGG

```

The sequence was aligned with *KCH* sequence data from rice and *Arabidopsis* (see Fig. 34). A high identity was detected, indicating that the set of degenerated primers indeed amplifies a *KCH* sequence from tobacco. The primer pair thus was suitable to measure the *KCH* level in the BY-2 *KCH* overexpression cell line.

OsKCH1 (2220)	CGTAAGCCCGSAACTAGATGCTGTCGGTGAACAATANGCAATTGAAATTGGCTGAAAGGTTCTTCAGTTGGCTTGGTGCAGCAAAAACAACAA
AtKatD (2138)	CATAAATCCAGAACTGACACTCTCGGAGAACTATTNGTATCTGAAAGITTCGTCGACCGAGTGGGGAGTGTGGCTAGCCGCTGCTCGTCTGAACAAA
BY-2 Seq	-----CGAATTTCCAGGCTAGAACTTATGGCTACTCGTCTAAACAAG
Consensus	C TAAG CC GAAC GA CT TCGG GA AC AT AG AC TGAA TTTGCTGAACGAGTTGC AC GTTGAAGCTTGGTGTGCTGCTCGTGAACAAA
OsKCH1 (2320)	GAGTCAAGTGAAGCTTAGAGAGCTCAAAGAACAGATTGCTA-CCCTCAAGGCGCATTG-----GCTAAAAG-GATGGGAACAGAAACATTCAAA
AtKatD (2238)	GATAATCTCGAGCTTAGAGAGCTTAAAGAGCAGATTGCTA-ATCTTAAGATGGCTCTAGTGAAGAAAGGAAATGGTAATGATGTACA-ACCAACAGCTAT
BY-2 Seq	GATAGTGTAGATGTGAAGAGCTGAAAGAACAGGTTCTGATGCTTCANTATTATCATC--TTCTCAATCTTATTATCTTCTGAAACTGTGA
Consensus	GATAGC AGAGGTTAAAGAGCT AAAGAACAGATTGCTA CTCAAG TGGCT T T CT AAATG TAATGAT CA AAAAAGCTT AA
OsKCH1 (2411)	-GCCAAGTCAAG--CCCTGACATCTT-
AtKatD (2336)	ACCAATCAACGTGAGAGAATATCGAGAGCA
BY-2 Seq	--CTATTATTACAGAT-TGCTACCCTCAAGG
Consensus	CAATCA TC AGA CTA C TGAAG

Fig. 34: Alignment of the identified BY-2 sequence with reference data

Alignment of the DNA sequences of the *KCH* members from rice *OsKCH1* and *Arabidopsis AtKatD* with the sequence amplified from tobacco BY-2 cells using the set of degenerated primers NF 73/74. Blue indicates identities in two of the three sequences, yellow in all three sequences.

CURRICULUM VITAE

Persönliche Daten

Name	Nicole Frey
Geburtsdatum	12.03.1982 in Darmstadt
Nationalität	deutsch
Kontakt	Werderstr. 68 76137 Karlsruhe frey_nicole@gmx.de 0173-9895343

Ausbildung

seit 04/2007	Promotionsstudium Karlsruher Institut für Technologie (KIT)
10/2004 – 12/2006	Studium Biochemistry and Molecular Biology Universität Bremen Abschluss: Master of Science
09/2003 – 03/2004	Auslandsstudium Biotechnologie Université Montpellier I, Frankreich
08/2001 – 09/2004	Studium Molekulare Biotechnologie Ruprecht-Karls Universität, Heidelberg Abschluss: Bachelor of Science
08/1992 – 07/2001	Edith-Stein Schule (Gymnasium), Darmstadt Abschluss: Allgemeine Hochschulreife

Wissenschaftliche Tätigkeiten

seit 04/2007	Wissenschaftliche Mitarbeiterin (Doktorandin) Karlsruher Institut für Technologie (KIT) Institut für Botanik I, AG Prof. Nick
01/2007 – 04/2007	Wissenschaftliche Mitarbeiterin Ruprecht-Karls Universität, Heidelberg Institut für Pflanzenwissenschaften, AG Prof. Robinson
04/2006 – 11/2006	Masterarbeit BASF Plant Science, Ludwigshafen Fungal Resistance Research Titel der Arbeit: <i>Comparative analysis of defence responses against biotrophic and necrotrophic fungi in Arabidopsis thaliana</i>

07/2005 – 09/2005	Auslandspraktikum Griffith University, Brisbane, Australien Institute for Glycomics, AG Prof. Kelm
02/2005 – 04/2005	Industriepraktikum BASF AG, Ludwigshafen Fungicide Research
05/2004 – 07/2004	Bachelorarbeit Ruprecht-Karls Universität Heidelberg Institut für Biophysikalische Chemie, AG Prof. Spatz Titel der Arbeit: <i>Motility assays with microtubules on gold-nanostructured surfaces</i>
08/2003 – 09/2003	Industriepraktikum VivaCell Biotechnology GmbH, Freiburg

Stipendien

04/2002 – 10/2006	Studienförderung durch das Evangelische Studienwerk e.V.
09/2003 – 03/2004	Auslandsstipendium durch das EU-Programm ERASMUS

Publikationen

- Frey, N., Klotz, J., Nick, P. (in preparation)
A kinesin with calponin-homology domain is involved in premitotic nuclear migration
- Eggenberger, K., Frey, N., Zienicke, B., Siebenbrock, J., Schunck, T., Fischer, R., Bräse, S., Birtalan, E., Nann, T., Nick, P. (2010)
Use of nanoparticles to study and manipulate plant cells
Advanced Biomaterials (in press)
- Frey, N., Klotz, J., Nick, P. (2009)
Dynamic bridges – a calponin-domain kinesin from rice links actin filaments and microtubules in both cycling and non-cycling cells
Plant Cell Physiology 50 (8), p. 1493-1506.
- Frey, N., and Nick, P. (2008)
Identification, localization and expression of rice OsKCH1, a novel plant-specific kinesin
EJCB 87, Supplement 1, p. 21.